This is to certify that the

dissertation entitled

Mutational and fluorescence studies on the VP16 transcriptional activation domain

presented by

Fan Shen

has been accepted towards fulfillment
of the requirements for

Ph.D. degree in Biochemistry

Major professor

Date 8/18/95

MUTATIONAL AND FLUORESCENCE STUDIES OF THE VP16 TRANSCRIPTIONAL ACTIVATION DOMAIN

By

Fan Shen

A DISSERTATION

Submitted to
Michigan State University
in partial fulfillment of the requirements
for the degree of

DOCTOR OF PHILOSOPHY

Department of Biochemistry

1995

ABSTRACT

MUTATIONAL AND FLUORESCENCE STUDIES OF THE VP16 TRANSCRIPTIONAL ACTIVATION DOMAIN

By

Fan Shen

The herpes simplex virus virion protein VP16 is a potent transcriptional activator of viral immediate early genes. Its activation domain is a prototype acidic activation domain. In the present work, oligonucleotide-directed mutational analysis and fluorescence spectroscopy analysis were used to study the structural features of this domain and its activation mechanism.

The amino acid character required at the critical position 442 of the VP16 activation domain was examined by saturation mutational analysis. This study explicitly demonstrated the importance of an aromatic or bulky hydrophobic residue at this position for the function of its activation domain. Similar results have since been reported for other activation domains.

Time-resolved and steady-state fluorescence approaches were applied to directly characterize the structural features of the VP16 activation domain. Unique intrinsic fluorescent probes were obtained by replacing Phe residues with Trp at positions 442 or 473 of VP16. Emission spectra, decay-associated spectra, dynamic quenching analyses and anisotropy decay measurements

together indicate that these Trp residues are solvent exposed and are highly mobile, suggesting that this isolated activation domain is unstructured.

Biochemical analyses have shown that the VP16 activation domain can bind to various components of the basal transcriptional machinery to activate transcription. To examine the interactions between VP16 and two of its potential targets, TBP and TFIIB using fluorescence spectroscopy techniques, tryptophan analogs were incorporated at positions 442 or 473 of VP16. Binding constants between TBP and VP16 activation domain were calculated from steady-state anisotropy analyses. Anisotropy decay experiments indicated that TBP induced a more ordered structure in both subdomains of VP16 while TFIIB only induced a slight change for VP16 labeled at 473. TBP (but not TFIIB) caused a spectral shift of VP16 labeled at either position, indicating a change to a more hydrophobic environment. Quenching analyses also demonstrated that TBP reduced solvent accessibility of both residues while TFIIB only effected the fluorophore at 473. These results support models of TBP as a target protein for transcriptional activators and suggest that ordered structure in the VP16 activation domain is induced upon interaction with target proteins.

To My Grandparents and Parents

ACKNOWLEDGMENTS

I am truly grateful to my advisor Dr. Steven Triezenberg for his guidance, encouragement, and support in the past five years. Steve has shown me in many ways how to be a good and decent scientist and I believe my experience as Steve's student will be very beneficial for my future career. Past and present members of Triezenberg lab, namely Lee Alexander, Andrea Cress, Doug Cress, Peter Horn, Rath Pichyangkura, Jaya Reddy, Jeff Regier, John Stebbins and Susan Sullivan have given me many suggestions and helps over the years. Their friendship have made life so much warmer even in the coldest Michigan winters. The happiness and the frustrations we shared will all be treasures in my heart. I also appreciate my committee members, Dr. Zachary Burton, Dr. Thomas Deits, Dr. Jerry Dodgson, Dr. Rawle Hollingsworth and Dr. Loren Snyder for their advice and encouragement along the way.

I am very thankful to our collaborators Dr. Jay Knutson, Denise Porter at NIH and Dr. Preston Hensley at SmithKline Beecham for teaching me fluorescence spectroscopy and for their significant contributions to this project. Without the many long nights we worked together in the fluorescence lab at NIH, I would not have reached this point.

Finally, I wish to thank my grandparents and parents for their inspirations, their unconditional love, and their total faith in me. I am also very grateful for my best friend, Xiang Lu, for his love, understanding, patience and support over the years.

TABLE OF CONTENTS

LIST OF TABLES

PAGE

CHAPTER II

CHAPTER III

CHAPTER IV

LIST OF FIGURES

PAGE

CHAPTER I

CHAPTER II

CHAPTER III

CHAPTER IV

LIST OF ABBREVIATIONS

5HW	5-hydroxy-tryptophan
7AW	7-aza-tryptophan
aa	amino acid
AAD	acidic activation domain
AAH	amphipathic alpha-helix
AdMLP	major late promoter of adenovirus
ATP	adenosine triphosphate
bp	base pair
CD	circular dichroism
CTD	carboxyl terminal domain of the largest subunit of RNAP II
DAS	decay associated spectra
ε_{280nm}	extinction coefficient at 280 nm
FTIR	Fourier-transform infrared
IPTG	isopropyl-β-D-thiolgalactopyranoside
HEPES	N-2-hydroxyethylpiperiazine-N'-2-ethanesulfonic acid

HSV-1	herpes simplex virus type-1
IE	immediate early
kDa	kilodaltons
NMR	nuclear magnetic resonance
NOE	nuclear overhauser effect
OD	optical density
RNAP II	RNA polymerase II
RAP	RNA polymerase associated proteins
SCB	standard column buffer
SDS-PAGE	sodium dodecyl sulfate-polyacrylamide gel electrophorysis
TAF_{II}	TBP Associated Factor of RNA Polymerase II transcription
TBP	TATA-box binding protein
TFII	transcription factor of RNA polymerase II
VP16	virion protein 16

Sigle letter abbreviations for the amino acids: A, Ala; C, Cys; D, Asp; E, Glu; F, Phe; G, Gly; H, His; I, Ile; K, Lys; L, Leu; M, Met; N, Asn; P, Pro; Q, Gln; R, Arg; S, Ser; T, Thr; V, Val; W, Trp; and Y, Tyr.

CHAPTER I

INTRODUCTION

SECTION 1 EUKARYOTIC TRANSCRIPTION ACTIVATION

The regulation of transcription is a key point of genetic regulation in eukaryotic cells. It plays a fundamental role in a wide variety of biological process such as cell growth, tissue differentiation, organ development and cell response to extracellular signals. Thus transcriptional regulation is a subject of active and intense investigation. The fascination with transcription also arises from another perspective. The complexity of the transcriptional apparatus, the large number of distinct transcription factors, and the combinatorial mode in which they regulate gene expression raise many intellectually challenging mechanistic questions.

In eukaryotic cells, gene promoters typically have a core promoter element, which is specifically recognized by a DNA binding factor and provides a nucleation site for transcription initiation complex formation. Protein-encoding genes are transcribed by RNA polymerase II (RNAP II). To initiate promoter-specific transcription, RNAP II requires a number of general transcription factors (Zawel and Reinberg, 1993; Conaway and Conaway, 1993). Seven general transcription factors have been identified and the genes encoding most of the factors have been cloned. These factors are termed TFIIA, B, D, E, F, H, and J (TFII stands for transcription factor of RNAP II). These factors are essential for initiation and are sufficient to direct a basal level of transcription from many core promoters. Most RNAP II promoters contain another class of elements, the gene specific regulatory sequence, to which the transcriptional regulatory proteins

bind and mediate their action (Johnson and McKnight, 1989). These regulatory proteins are not required for transcription initiation, but instead they affect the level of transcription. Transcriptional activators increase the output of transcription while repressors decrease it.

RNA Polymerase II (RNAP II)

Purified RNAP II alone is capable of template-dependent synthesis of RNA, but it is not capable of specific initiation at promoters (Sawadogo and Sèntenac, 1990). Recent genetic studies demonstrated the role of the largest subunit of RNAP II in transcription start site selection, indicating that RNAP II is not passive in specific transcription initiation (Berroteran et al., 1994).

RNAP II is a conserved multisubunit complex among eukaryotes (Young, 1991). RNAP II is generally composed of 10 to 12 subunits. Subunit sequences from different species share 40% - 50% identity at the amino acid level. Yeast RNAP II has been most intensively studied. The three essential largest subunits of yeast RNAP II are related to the prokaryotic core RNA polymerase subunits and are responsible for RNA catalysis. Three other essential subunits are also found in RNAP I and III which transcribe ribosomal RNA and small RNA, respectively. These three subunits could contribute to the coordinate regulation of rRNA, mRNA and tRNA synthesis or nuclear localization. The remaining small subunits maybe involved in fine tuning of the transcription apparatus.

The most unique feature of RNAP II is that its largest subunit has a unique carboxyl-terminal domain (CTD) which is absent in prokaryotic RNAP, RNAP I and RNAP III (Corden, 1990). This CTD comprises tandem repeats of consensus heptapeptide sequences, Pro-Thr-Ser-Pro-Ser-Tyr-Ser. There is no structural data for CTD yet, however this domain seems not likely to form a globular structure.

Based on the regular spacing of proline residues and the tendency for these residues to form turn conformation, this domain is predicted to adopt a novel secondary structure consisting a series of consecutive turns, stretching out from the RNAP II core. CTD is essential for cell growth in vivo while the requirement for CTD in vitro is controversial, and may depend on the promoter used (Allison et al., 1988; Bartolomei et al., 1988; Zehring et al., 1988; Thompson et al., 1989; Zehring et al., 1988; Serizawa et al., 1993).

The largest subunit of RNAP II can be resolved into three major forms in SDS-PAGE, namely, the IIo, IIa and IIb form (Cadena and Dahmus, 1987). These forms differ only in the state of the CTD. The IIo form contains a highly phosphorylated CTD while the CTD of the IIa form is non-phosphorylated. The IIb form lacks the CTD, and is probably a proteolytic artifact of purification. The phosphorylation state of the CTD has been followed through the transcription cycle. The non-phosphorylated form IIa was found stably associated with the assembling initiation complex while the phosphorylated form IIo was associated with the active elongation complex (Laybourn and Dahmus, 1990; Lu et al., 1991). Further, the nonphosphorylated form IIa, but not the phosphorylated form IIo, specifically associated with the TATA-binding protein (TBP) (Usheva et al., 1992). These results lead to the attractive model in which phosphorylation of the CTD may be a means to uncouple the RNAP II from the preinitiation complex and trigger the onset of transcription (Peterson and Tjian, 1992). The discovery of general factor TFIIH as the CTD kinase strengthens the importance of CTD phosphorylation in transcription initiation (Feaver et al., 1991; Fischer et al., 1992; Lu et al., 1992).

Kornberg and colleagues reported the three dimensional structure of yeast RNAP II at 16 Å resolution studied by electron crystallographic analysis (Darst et al., 1991). The most prominent feature of the structure is that it has a 25 Å

channel which is similar to the E. coli RNAP channel that is thought to be the DNA-binding channel. A finger of protein density projecting from the molecule is speculated to represent the CTD. Using this technique, other forms of RNAP II (such as RNAP II associated with DNA and RNA in paused elongation complexes or RNAP II lacking CTD) could also be studied. These studies should provide structural basis for functional studies of transcriptional regulation.

Basal Transcription Factors

Transcription factor IID is a multiprotein complex critical for RNAP II transcription. It consists the core protein TBP (TATA box binding protein) and multiple TBP associated factors (TAFs) (Gill and Tjian, 1992; Goodrich and Tjian, 1994). In addition to this TBP-TAF_{II} (TAFs for RNAP II) complex in RNAP II transcription, there are three other compositionally distinct TBP-TAF complexes involved in RNAP I and RNAP III transcription. SL1 is the TBP-TAF complex required for RNAP I transcription (Comai et al., 1992), and TFIIIB and SNAPc are two different TBP-TAF complexes involved in RNAP III transcription (Lobo et al., 1992; Kassavetis et al., 1992; Taggart et al., 1992; White and Jackson, 1992; Sadowski et al., 1993). Distinct sets of TAFs in these TBP-TAF complexes provide the promoter selectivity at which the given complex functions.

Promoters for RNAP II often contains a TATA box, located a short distance upstream of the transcription start site (25-30 bp in higher eukaryotes; 40-120 bp in yeast). TATA box is recognized by TBP, the only general transcription factor which has a sequence-specific DNA-binding activity. TBP is capable of nucleating a functional RNAP II pre-initiation complex in vitro. TBP is also important for initiation from another class of RNAP II promoter, the TATA-less promoter (Weis and Reinberg, 1993). The cDNA encoding yeast TBP

was the first cloned gene for general transcription factors (Hahn et al., 1989; Horikoshi et al., 1989). This led to the isolation of cDNA clones encoding homologous TBP proteins from a variety of species, including *Arabidopsis*, *Drosophila*, mouse and human (Gasch et al., 1990; Hoey et al., 1990; Tamura et al., 1991; Kao et al., 1990; Peterson et al., 1990). Cloned TBPs range in size from 22 kDa (*Arabidopsis*), 27 kDa (yeast TBP) to 38 kDa (human). The carboxyl-terminal domain of 180 amino acids of all TBPs are highly conserved and it is the functional core of TBP. This domain is sufficient to bind to the TATA sequence and it can interact with general transcription factors TFIIA and TFIIB to form the promoter bound DAB complex (Buratowski et al., 1989; Maldonado et al., 1990). It is competent for basal transcription in vitro as well as sufficient to support normal growth in yeast and for response to transcriptional activators in vivo (Lieberman et al., 1991; Poon et al., 1991; Cormack et al., 1991; Gill and Tjian, 1991). The amino-terminal region of TBPs from different species vary greatly in size and sequences and its function is unclear. Surprisingly, the minor difference in the conserved C-terminal domain rather than the divergent N-terminal domain contributes to species difference (Cormack et al., 1991; Gill and Tjian, 1991). In addition to its central role in nucleating the preinitiation complex, TBP has been proposed as a major target protein for transcriptional activators.

Atomic resolution crystal structures of TBP and the TBP-TATA complex have been solved (Nikolov et al., 1992; Chasman et al., 1993; Kim et al., 1993a; Kim et al., 1993b). TBP resembles a "molecular saddle" made up of two roughly symmetrical halves. TBP binds in the minor grove of DNA via a curved eight-stranded antiparallel β-sheet of the inner surface of the saddle. Binding of TBP to TATA induced a significant distortion in the DNA which permits a closer association of the preinitiation complex than on linear DNA . It may also serve to align the upstream regulatory proteins to the basal transcription machinery. The

outer surface of the protein are accessible for interactions with other transcription factors.

Many of the TAF_{II}s in the TFIID complex have been cloned: all eight TAF_{II}s in *Drosophila* (dTAF_{II} 250, 150, 110, 80, 60, 40, 30α and 30β), three out of seven TAF_{II}s (hTAF_{II}230, 70 and 55) in human and two out of nine in yeast (yTAF_{II}145 and 90) (Goodrich and Tjian, 1994; Chiang and Roeder, 1995; Reese et al., 1994). Multivalent TAF_{II}-TAF_{II} interactions and TAF_{II}-TBP interactions have been demonstrated and may account for the stability of the TFIID complex. These TAF_{II}s may also interact with other general transcription factors to facilitate assembly or stability of the preinitiation complex (Goodrich et al., 1993; Lieberman and Berk, 1994). Moreover, several specific TAF_{II}-activator interactions have been reported and suggest the TAF_{II}s may function as coactivators (Hoey et al., 1993; Goodrich et al., 1993).

Transcription factor IIA in yeast is composed of two subunits of 32 kDa and 13 kDa (Ranish et al., 1992). Human and *Drosophila* TFIIA are both made up of three subunits of 37 kDa (α), 19 kDa (β) and 13 kDa (γ) (Yokomori et al., 1993; DeJong and Roeder, 1993; Yokomori et al., 1994; Ozer et al., 1994; Sun et al., 1994). The α and β subunits of mammalian TFIIA are generated by protein-processing from a single-polypeptide precursor and they share sequence similarity with the large subunit of yeast TFIIA, while the γ subunit is homology to the small subunit of yeast TFIIA. TFIIA is capable of stimulating the basal transcription. It may function so by facilitating the recruitment of TBP or TFIID to the template. It binds TBP with high affinity as well as directly interacts with TAFs in the TFIID complex. Alternatively, TFIIA may function so by physically removing negative components present in the crude TFIID fraction (Zawel and Reinberg, 1995). TFIIA can also stimulate activated transcription (DeJong and

Roeder, 1993; Ma et al., 1993; Yokomori et al., 1993; Yokommori et al., 1994; Ozer et al., 1994; Sun et al., 1994).

Transcription factor IIB is a 38 kDa singular polypeptide in yeast, a 34 kDa in *Drosophila*, and a 33 kDa protein in human (Pino et al., 1992; Ha et al., 1991). Structural motifs such as a putative amphipathic α-helix, a potential Zn finger, and direct sequence repeats are well conserved. TFIIB plays an important role in transcription as it function as the "bridging" factor between promoter-bound TBP and the RNAP II/TFIIF (Buratowski and Zhou, 1993; Barberis et al., 1993; Ha et al., 1993). Several functional domains in TFIIB have been mapped. The C-terminal domain of TFIIB is sufficient to interact with the promoter-bound TBP and form the complex containing TFIID and TFIIB on promoter region (DB complex), while the N-terminal domain directly interacts with RNAP II and the TFIIF small subunit and recruits them to the promoter to build up the preinitiation complex. TFIIB and RNAP II functionally interact to select the transcription start site. This was initially suggested by genetic studies in which a yeast TFIIB mutant and RNAP II largest subunit mutant shifted the transcription start site of several genes (Pinto et al., 1992; Berroteran et al., 1994). The finding that exchanging TFIIB/RNAP II pair of the *S. cereviasiae* and *S. pombe* transcription machinery results in shifts of the start site further strengthens the role of TFIIB in start site selection (Li et al., 1994). TFIIB has also been proposed as one of the major target proteins of transcriptional activators (Maldonado and Reinberg, 1995).

Transcription factor IIF of mammalian species consists two subunits of 30 and 74 kDa (i. e., RAP30 and RAP74, RAP stands for RNAP II associating factor). The cDNAs encoding both subunits were isolated (Sopta et al., 1989; Finkelstein et al., 1992). RAP30 binds to RNAP II directly and prevents it from binding nonspecifically to DNA (Killeen and Greenblatt, 1992). RAP30, together with

RNAP II, can bind to the promoter sequences containing TBP, TFIIA and TFIIB (Flores et al., 1991). In this manner, RAP30 may function analogously to σ^{70}, a bacterial factor which increases the association of bacterial core polymerase with promoter, to facilitate the association of RNAP II with promoter region (Sopta et al., 1989). The role of TFIIF in different stages of transcription cycle were further dissected (Chang et al., 1993; Chang, 1995). RAP30 is required for accurate initiation while RAP74 is not. Instead, RAP74 is critical for the transition from initiation complex to the productive elongation complex. RAP74 is capable of stabilizing short transcripts, which may explain the requirement of this factor in promoter escape, in which the initiating RNAP II is converted into an elongation-competent form (Goodrich and Tjian, 1994). Yeast TFIIF consists three subunits of 105 kDa, 54 kDa and 30 kDa (Henry et al., 1995). The two large subunits are equivalent of mammalian RAP74 and RAP30. The third subunit associates less tightly with RNAP II and is not essential for cell viability. Interestingly, this subunit is $yTAF_{II}30$ and is present in the holo-RNAP II (see below), suggesting a role of TFIIF in transcriptional activation.

Transcription factor IIE in human is a heterotetramer composed of two α subunits (56 kDa) and two β subunits (34 kDa) (Peterson et al., 1991; Ohkuma et al., 1991). TFIIE is essential for basal transcription. In a study to define the role of TFIIE, the interactions of TFIIE with all of the components of the basal transcription machinery were systematically examined (Maxson et al., 1994). TFIIE binds selectively to the nonphosphorylated form of RNAP II and to both subunits of TFIIF as well as to TFIID. Importantly, TFIIE selectively recruits the intact TFIIH and also stimulates the CTD kinase activity of TFIIH (Ohkuma and Roeder, 1994). Together, these results support the model in which TFIIE is involved in the step of promoter clearance in transcription cycle (Goodrich and

Tjian, 1994). TFIIE has also been suggested to play an important role in coupling transcription to DNA excision repair (Drapkin and Reinberg, 1994).

Transcription factor IIH is a multiprotein complex consisting of nine proteins ranging in size from 34 to 89 kDa and is involved in multiple cellular processes (Drapkin and Reinberg, 1994; Maldonado and Reinberg, 1995). It is the only general transcription factor which exhibits enzymatic activities, including a DNA-dependent ATPase, an ATP-dependent helicase and a kinase specific for the CTD of the largest subunit of RNAP II. TFIIH has been suggested to serve important roles in transcription, including CTD-phosphorylation, open-complex formation and promoter clearance. The CTD kinase resides with MO15/Cdk7, a cyclin-dependent kinase (Feaver et al., 1994; Roy et al., 1994). Cyclin H, the regulatory partner of MO15/Cdk7, is also found in the TFIIH complex (Serizawa et al., 1995). The presence of cell-cycle regulators in TFIIH raised an intriguing possibility that TFIIH may regulate the transcription activity for specific cellular genes. Link between TFIIH and another cellular process, nucleotide excision repair (NER), was first suggested by the identifications of several subunits of TFIIH (p89, p80 and SSL1) as the proteins (i.e., ERCC2 and ERCC3) involved in NER and further established by the dependence of TFIIH in reconstituted NER system (Schaeffer et al., 1993; Drapkin et al., 1994; Humbert et al., 1994; Mu et al., 1995). ERCC3 has an ATPase/helicase activity and is essential for transcription. The involvement of TFIIH in NER may facilitate the coupling of active genes to the repair machinery at DNA lesions.

Transcriptional Activators And VP16

Transcriptional activators are the class of regulatory proteins which associate with gene-specific regulatory elements and stimulate transcription,

achieving the specific expression pattern of such genes. Following the cloning of many activator proteins, deletion analysis and "domain-swap" experiments have shown that activators have a modular structure in which distinct separable domains of the protein mediate particular functions (Mitchell and Tjian, 1989; Pabo and Sauer, 1992). One domain is responsible for the DNA binding specificity, and one or several discrete domains are necessary for transcriptional activation. There are several well-established families of DNA-binding proteins, including the helix-turn-helix protein (such as the λ Cro protein, Lac repressor, Trp repressor), the homeodomain proteins (such as Oct-1, Oct-2 and the *Drosophila* Antp and engrailed protein), zinc finger proteins (such as Sp1 and GAL4), the steroid receptor (such as the gluococorticoid receptor, estrogen receptor), leucine zipper proteins (such as C/EBP, GCN4, c-Jun and c-Fos), the helix-loop-helix proteins (such as the MyoD and c-Myc) and the β-sheet motif containing protein (such as Arc repressor protein). DNA-binding domain of these proteins form highly ordered 3-dimensional structures. The activity of DNA binding domain can be regulated by several mechanisms (Wagner and Green, 1994). Enzymatic regulation of DNA binding activity includes phosphorylation and oxidation. Viral proteins (such as adenovirus E1a) as well as cellular proteins (such as high mobility group protein) have been shown to regulate the DNA binding activity of some transcription factors. Transcription factors from related (such as heterodimer c-Jun/ATF-2) or even from different family (such as c-Jun and glucocorticoid receptor) can interact with each other to modulate DNA binding activity, therefore regulating the gene expression.

In contrast to the rich structural information of the DNA-binding domain of the transcriptional activators, no three dimensional structure has yet been reported for any activation domain (AD). Limited secondary structure analyses of several acidic activation domains (AADs) suggest that the activation domain

alone is poorly structured and it may assume specific conformation upon interaction with its in vivo target proteins (O'Hare and Williams, 1992; Donaldson and Capone, 1992; Van Hoy et al., 1993; Schmitz et al., 1994; Dahlman-Wright et al., 1995; Shen et al., 1995a; Shen et al., 1995b).

Activation domains have been conventionally classified into acidic (such as herpesvirus protein VP16, and yeast proteins GAL4 and GCN4), glutamine-rich (such as Sp1, Oct-1, Oct-2 and Jun) and proline-rich activators (such as CTF/NF1) simply based on unusual abundance of particular amino acids within such domains (Mitchell and Tjian, 1989). In fact, such classification could be misleading. Instead, recent mutational analyses revealed that most activation domains are equally or more sensitive to mutations in bulky hydrophobic residues than to mutations of the most abundant residues (Triezenberg, 1995). The importance of a pattern of bulky hydrophobic residues have been seen in the AADs of the herpesvirus protein VP16, the foamyvirus protein Bel-1, the mammalian protein p53 and RelA, the yeast protein GAL4 and GCN4 and the glutamine-rich activation domain of Sp1 and Oct-1 (Cress and Triezenberg, 1991; Regier et al., 1993; Blair et al., 1994a; Lin et al., 1994; Blair et al., 1994b; Leuther et al., 1993; Drysdale et al., 1995; Gill et al., 1994; Tanaka and Herr, 1994).

Another common feature of activation domains is that an activator often contains multiple smaller activation subdomains (Triezenberg, 1995). This has been seen in activation domains of herpesvirus protein VP16, Epstein-Barr virus activators Rta and ZEBRA, mammalian proteins c-Rel, c-Fos and c-Jun, Sp1 and Oct-2, and yeast proteins GAL4 and GCN4 (Regier et al., 1993; Seipel et al., 1994; Hardwick et al., 1992; Chi and Carey, 1993; Blair et al., 1994b; Sutherland et al., 1992; Pascal and Tjian, 1991; Tanaka and Herr, 1994; Ma and Ptashne, 1987; Hope and Struhl, 1986). These smaller subdomains act synergistically to activate transcription.

The virion protein VP16 (also called αTIF, ICP25, Vmw65) of herpes simplex type-1 virus (HSV-1) is a potent transcriptional activator (Sadowski et al., 1988). HSV-1 is a widespread human pathogen (Wagner, 1990). It possesses a large double-stranded DNA genome encoding approximately 70 genes which are transcribed by host RNAP II. During lytic HSV-1 infection viral genes are temporally expressed in three coordinately regulated classes known as immediate-early (IE), delayed early (DE), and late (L) genes. Roughly 500-1000 molecules of VP16 are assembled in the virion and deposited into the host cell upon infection, where VP16 specifically and potently activates viral IE gene expression (Spector et al., 1990).

The gene encoding VP16 has been cloned and sequenced from several strains of HSV-1 (Pellett et al., 1985; Dalrymple et al., 1985). The polypeptide is composed of 490 aa residues as deduced from the DNA sequence. Functional domains within VP16 were defined by testing the transcriptional activity of a series of VP16 deletion mutants (Triezenberg et al., 1988a). The N-terminal 400 aa residues of VP16 comprise the IE gene specificity domain, while the transcriptional activation function is conferred by the C-terminal 80 aa residues.

VP16 does not have a high affinity for DNA (Marsden et al., 1987), but rather is tethered to the cis-element TAATGARAT (R=purine) of IE genes by binding to the host octamer-binding protein Oct-1, which directly binds to the TAATGARAT sequence (Kristie and Roizman, 1984; Stern et al., 1989). The enhancers of each of the five HSV IE gene contain one or more copies of this cis element. For example, there are three TAATGARAT sequence located at sites 360, 270 and 110 bp from the mRNA cap site of the IE gene encoding ICP4 (infected protein 4) (Triezenberg et al., 1988b). To effectively associate with Oct-1, VP16 binds an auxiliary protein termed host cell factor (HCF) (Katan et al., 1990; Xiao and Capone, 1990; Kristie and Sharp, 1993). HCF comprises a series of

related polypeptides that range in size from 110 kDa to 300 kDa, all of which are encoded by a single gene (Wilson et al., 1993).

The activation domain of VP16 is one of the most potent activation domains yet identified (Sadowski et al., 1989). It is rich in acidic amino acids; twenty one acidic residues are found in the 78 aa activation domain. It contains two activation subdomains, namely, the N-subdomain (410-456 aa) and the C-subdomain (453-490 aa) (Triezenberg et al., 1988b; Regier et al., 1993). Each of the subdomain has approximately one half of the activity of the full-length activation domain. As one of the most potent activation domains identified, the VP16 activation domain is an important model for the study of transcription activation in eukaryotes and is the subject of this thesis study.

The mechanisms of transcriptional activation has been the focus of intense investigation and many possible functional roles of activators have been suggested (Tjian and Maniatis, 1994; Triezenberg, 1995). Some aspects of the activation mechanisms will be described below in the context of different stages of transcription.

RNA Polymerase II Transcription And Activators

Transcription is a multi-step process, involving (1) template activation; (2) preinitiation complex assembly; (3) open complex formation; (4) promoter clearance; (5) elongation; (6) termination; (7) recycling of general transcription factors and RNAP II. Theoretically, activators could function at any step to increase the efficiency of transcription.

(1)Template Activation

In eukaryotic cells, gene expression is regulated in the context of the native chromatin template. Major components of chromatin, including nucleosome cores (DNA wrapped around an octamer of four different histone proteins) and histone H1 protein (which binds to the linker DNA between nucleosome cores), present barriers blocking access of the basal transcription machinery to the promoter region and the binding of upstream regulatory proteins (Paranjape et al., 1994; Lewin, 1994). Kadonaga and colleagues defined this state in which gene exists as a transcriptionally repressed chromatin structure (i. e., compacted and inaccessible to transcription factors) as the inactive ground state (Paranjape et al., 1994). They also defined two other states of gene activity. Through a process termed antirepression, the state of gene activity changes to the derepressed state in which the chromatin-mediated repression of transcription is relieved and template becomes accessible to transcription factors. In this state, the chromatin structure become decondensed and unfolded, the core histones may be modified, the nucleosome structure may be reconfigured and nucleosome positioning may be altered, and the histone H1 protein may be depleted. Through another process termed "true activation", gene activity reaches the activated state in which transcriptional activators increase the intrinsic transcription rate.

Recent genetic and biochemical studies have identified a multiprotein complex termed the SWI-SNF complex which remodels the chromatin structure and facilitates the binding of both TBP to TATA sequence and activators to the upstream regulatory sequences (Peterson and Tamkun, 1995; Kwon et al., 1994; Imbalzano et al., 1994). This SWI-SNF complex possesses DNA-dependent ATPase activity and its stimulation of transcription requires ATP hydrolysis to

provide energy. This complex is conserved among eukaryotes and has been regarded as a "global activator" of transcription.

Transcriptional activators are directly involved in the reconfiguration of the chromatin structure to antirepress the inhibition of chromatin, and the activation domains may be crucial in these processes. The yeast PHO system provides one example that a change in nucleosome organization is involved in gene activation (reported in Lewin, 1995). The transcription activator PHO4 induces the disruption of four precisely positioned nucleosome at the PHO5 promoter upon phosphate starvation. This nucleosome disruption is activation domain-dependent, and the VP16 activation domain can substitute for that of PHO4. For another example, Kingston and colleagues demonstrated that GAL4 derivatives containing an acidic activation domain such as the VP16 activation domain alleviated repression of promoters during nucleosome assembly (Workman et al., 1991). Majors and colleagues demonstrated that GAL4 disrupted a repressing nucleosome during activation of *GAL1* transcription in vivo and the ability of nucleosome disruption correlated to the strength of the activation domain (Axelrod et al., 1993). In addition to counteracting the repression of nucleosome cores, transcriptional activators such as Sp1 and GAL4-VP16 (a chimeric transcriptional activator composed of the DNA-binding domain of GAL4 and the activation domain of VP16) also release histone H1-mediated inhibition of transcription (Croston et al., 1991). Together, these experiments suggest that chromatin reconfiguration occurs, at least in part, by the protein-protein interactions that involve the same region of the activation domain that make protein-protein contacts in the "true activation" process.

(2) Preinitiation Complex Assembly

After the chromatin structure of the gene which will be transcribed is reorganized to the active configuration, the RNAP II transcription machinery can nucleate on the promoter and form the preinitiation complex. RNAP II promoters can be classified into two classes based on whether they possess a TATA sequence located a short distance upstream of the transcription start site: TATA-containing and TATA-less promoters (Zawel and Reinberg, 1995). TATA-less promoters typically have an Initiator sequence (Inr) encompassing the start site. Some TATA-containing promoters also contain the Inr element. For TATA-containing promoters, the first step in the assembly of the initiation complex is the binding of TFIID complex to the TATA element. TATA binding specificity is conferred by the TBP subunit of TFIID. For the TATA-less promoters, Inr nucleates the preinitiation complex formation either through interactions between Inr and Inr-binding proteins, or between Inr and TAFs in the TFIID complex, or between Inr and RNAP II. TFIID is also required for the nucleation of this class of promoters and is brought to the promoter at very early stage of preinitiation complex assembly. There are two models describe the events after the initial nucleation step in the preinitiation complex formation process, namely, the stepwise assembly model and the holoenzyme model.

a. Stepwise Assembly Model

The traditional view of the preinitiation complex formation is proposed largely based on kinetic assays, native gel electrophoresis and nuclease protection assay (Buratowski et al., 1989; Zawel and Reinberg, 1995). In this step-wise model, general transcription factors and RNAP II are brought to the promoter region through protein-DNA and protein-protein interactions in a highly ordered fashion. The initial template committed complex (formed

between TFIID binding to the promoter) provides the binding sites for TFIIB, resulting in the formation of the DB complex. TFIIA may facilitates this complex formation by either stabilizing it or ensuring the productive conformation (Hahn, 1993). TFIIB in the DB or DAB complex serves as a molecular bridge for the following delivery of RNAP II by TFIIF to form the DABPolF complex. Subsequently, TFIIE, TFIIH and TFIIJ join to the DABPolF complex to form the complete preinitiation complex.

b. Holoenzyme Model

Recent studies suggest a different point of view on the assembly of preinitiation complex formation (Kim et al., 1994a; Koleske and Young, 1995). Young and colleagues identified a pre-assembled complex, an RNA polymerase holoenzyme, in yeast (Thompson et al., 1993; Koleske and Young, 1994) during their attempt to purify the SRB proteins. SRB proteins (suppresser of RNA polymerase B) were previously identified through genetic screen for mutations that suppress the RNAP II largest subunit CTD mutants. This holoenzyme discovered by Young's lab contains the RNAP II, a subset of general transcription factors (i.e., TFIIB, TFIIF, and TFIIH), and all nine SRB proteins. Kornberg and colleagues purified a subcomplex of yeast holoenzyme which contains RNAP II, TFIIF, SRB proteins, GAL11 and SUG1 (Kim et al., 1994). The CTD of RNAP II may provides the interaction sites for multiple SRB proteins and basal transcription factors to form the holoenzyme. The holoenzyme is highly stable in the absence of DNA, and can efficiently initiate transcription when the missing general transcription factors are supplemented. CTD, SRB2, and SRB5 are all capable of interacting with TBP directly (Young, 1991; Koleske et al., 1992; Thompson et al., 1993). The interaction of the holoenzyme with template-bound TFIID may thus be stabilized by these multiple interactions. Together, these

results suggest that the pre-assembled holoenzyme is recruited to the TFIID-bound promoter in one step to form the preinitiation complex. Thompson and Young (1995) recently demonstrated important evidence to support this model. The feature that distinguishes the holoenzyme from other forms of RNAP II is the tight association with SRB proteins. The effects of temperature-sensitive mutations in SRB genes on RNAP II transcription were tested and mRNA synthesis was found to be rapidly decreased at the restrictive temperature. Considering that all of the SRB proteins in the cell are in the holoenzyme form, Young and colleagues propose that SRB proteins are a general requirement for RNAP II transcription in vivo and the holoenzyme is the form of RNAP II recruited to most promoters of the cell.

These two models regarding preinitiation complex formation are not mutually exclusive. Using purified factors, direct interactions between many components of the basal transcription machinery have been shown, including TFIIF and RNAP II, TFIIB and RNAP II, TFIIF and TFIIB, TFIIF and TFIIE, TFIIF and TFIIH, TFIIE and TFIIH. Therefore, it is possible that these basal components and RNAP II form a stable holoenzyme in the context of the cell and this pre-assembled complex as a whole is the complex recruited at the promoter. On the other hand, the holoenzyme contains only a fraction of the RNAP II in a cellular extract and this fraction may not be enough to transcribe all the gene. Further, the existence of two kinds of holoenzyme (i.e., identified by Young's lab and by Kornberg's lab) with somewhat different compositions suggests the possibility that there are many more different forms of RNAP II in the cell. The simplest form is the RNAP II only. Moreover, even the holoenzyme which contains the most components does not contain all the general transcription factors and the remaining factors must enter the preinitiation complex in another

step. Therefore, even in the case of recruitment of holoenzyme, the preinitiation complex assembly may still be a multi-step process.

Different promoters have different structures and are associated with different regulatory proteins and respond to different signals to fulfill different biological functions. One should not be surprised by the existence of variations of transcription mechanisms. It is possible that on some promoters the preinitiation complex assembles in a stepwise fashion, while on some other promoters RNAP II binds in the holoenzyme form. More interestingly, recent studies suggest that not all promoters require the full set of general transcription factors in vitro (Tyree et al., 1993; Parvin and Sharp, 1993; Usheva and Shenk, 1994). As an example, the negatively supercoiled immunoglobulin heavy chain (IgH) promoter can be transcribed to high level in the presence of only TBP and TFIIB in vitro (Parvin and Sharp, 1993).

c. Activators And Preinitiation Complex Assembly

Activators are believed to play important roles in the preinitiation complex assembly process. Activators bind to the upstream regulatory sequence and assist the assembly of the preinitiation complex through interactions with the components of the transcription machinery. The intervening DNA are proposed to loop out to permit the interactions. Direct interactions have been detected between activators and several components of the basal transcription machinery (Hori and Carey, 1994; Triezenberg, 1995; Zawel and Reinberg, 1995).

(a) Activators And Stepwise Assembly Model

According to the stepwise assembly model, activators can function during any step of the assembly pathway. In principle, every step in the pathway can be reversible and can be rate-limiting. Activators presumably can increase the equilibrium association constant for any one of the steps by targeting any of the

component in the transcription machinery, driving the assembly process forward (Kingston and Green, 1994).

Activators And TBP

Much evidence has implicated TBP as the molecular target of activators. Considering TBP (the core protein of TFIID) binding is the first step in establishing transcription initiation, this is an appealing model. The association of TBP with the promoter has been shown to be slow in vitro (Schmidt et al., 1989). Kinetic analysis of yeast TBP and TATA sequence association using gel retardation and DNase I protection assay demonstrated that the slow step of binding is concentration dependent (Hoopes et al., 1992). These results suggest that the concentration of TBP in vivo may limit the rate of initiation complex formation. Recently, Struhl and colleagues measured transcription from promoter with mutated TATA sequence in combination of a specificity altered TBP in the absence and presence of acidic activator GCN4 in yeast (Klein and Struhl, 1994). Results from this study suggest that the accessibility of TBP to the promoter is rate limiting in vivo and activation domains increase the recruitment of TBP to promoters in vivo. Their subsequent experiments further demonstrated that the recruitment of TBP to promoter is a rate-limiting step in vivo (Chatterjee and Struhl, 1995). When TBP is brought to the promoter by a heterologous DNA binding domain (LexA) in the form of chimeric LexA-TBP, it efficiently activates transcription from a promoter containing a LexA operator upstream of a TATA sequence. A Genetic screen in yeast for TBP mutants defective in activated transcription resulted in identification of a class of mutants severely impaired in TATA box binding, also suggesting that activators may enhance the formation or stability of TBP-TATA complex at certain genes in vivo (Arndt et al., 1995).

Using affinity resins containing the immobilized VP16 activation domain, a direct and specific interaction between TBP and an activation domain was demonstrated (Stringer et al., 1990; Ingles et al., 1991). An extensive collection of VP16 activation domain mutants were tested in this binding assay and a good correlation between the transcriptional activities of these mutants assayed in vivo and their affinities for TBP were observed (Ingles et al., 1991). The specific interaction between TBP and VP16 was the first directly demonstrated interaction between any general transcription factor and any activation domain. The methodology utilized since then have been widely applied to identify the target proteins of various activation domains. Other strategies have also been used to demonstrate interactions between activators and basal transcription factors, including coimmunoprecipitation, Far-Western blot (protein-protein blot), DNase protection, gel-retardation, sedimentation centrifugation, and photo-crosslinking. As a result of the extensive attempt to identify target proteins, many other activation domains have been found to bind TBP in vitro, including viral activator E1A, Zta, Tat, Tax1, IE2, cellular protein E2F-1, p53, PU.1, Sp1, Oct-1, Oct-2 , c-Rel, c-Fos and yeast protein GAL4 (Lee et al., 1991; Lieberman and Berk, 1991; Kashanchi et al., 1994; Caron et al., 1993; Hagemeier et al., 1992; Emili and Ingles, 1995; Truant et al., 1993; Hagemeier et al., 1993; Emili et al., 1994; Zwilling et al., 1994; Xu et al., 1993; Metz et al., 1994; Melcher and Johnston, 1995). Although TBP exists as part of the TFIID complex in vivo , the spatial positioning between TBP and TAF_{II}s is not clear. Not every TAF_{II} is directly associated with TBP, thus TBP may still have accessible surface to interact with activators (Gill and Tjian, 1994). TBP mutants which are competent in basal level transcription but defective in activated transcription have been identified (Kim et al., 1994b; Tansey et al., 1994). Some of the mutants are deficient in binding to activation domains, demonstrating that TBP is one of the

target proteins. One particular point mutant (L114K) of yeast TBP is defective in both activated transcription and binding to VP16 AAD (Kim et al., 1994b). Interestingly, this TBP mutant reduces its binding affinity to the GAL4 AAD to the same degree as to the VP16 AAD (Melcher and Johnston, 1995). This result suggests that these two AADs contact the same surface of TBP. Various activator mutants which are defective in transcription activation have also been tested in the binding assays. Correlation between transcriptional activity of these activators and their binding ability to TBP have been generally observed. The demonstrated binding specificity between activation domains and TBP reassures that TBP is a reasonable target of activators. Furthermore, direct interactions between activators and TBP are also suggested by some in vivo experiments (Xu et al., 1993; Metz et al., 1994).

In addition to directly increasing the recruitment of TBP to promoters, activators may function through TBP by some other mechanisms. In one study, p53 was found to promote the formation of a more stable p53-TBP-promoter complex (Chen et al., 1993). In another study, the activation domain of E1A was found to disrupt the interaction between TBP and its inhibitor protein Dr1, reversing Dr1-mediated inhibition (Kraus et al., 1994).

Activators And TAF_{II}

Several lines of evidence suggests that TAF_{II}s which associate with TBP in the TFIID complex are also the targets of activators. First, TBP is not sufficient to support activator stimulated transcription in vitro and TAF_{II}s are required to reconstitute activation (Pugh and Tjian, 1990; Dynalacht et al., 1991; Zhou et al., 1992; Zhou et al., 1993). Second, some TBP mutants which are competent in basal level transcription but defective in activated transcription are defective in binding with $TAF_{II}250$, indicating that TAF_{II}s are important in TBP's response to activators (Tansey et al., 1994). Third, direct interactions between TAFs and

activators have been demonstrated. Using a yeast two-hybrid assay and affinity chromatography approaches, *Drosophila* $TAF_{II}110$ has been identified as the target of the glutamine-rich activator Sp1 (Hoey et al., 1993). Mutational analysis of an Sp1 activation domain established a direct correlation between activation and interaction with *Drosophila* $TAF_{II}110$ (Gill et al., 1994). Subsequently, *Drosophila* $TAF_{II}40$ has been demonstrated as the target of VP16 C-subdomain (453-490 aa) and Epstein-Barr virus nuclear protein 2 (EBNA 2) (Goodrich et al., 1993; Tong et al., 1995a), and $dTAF_{II}30$ as the target of an activation domain of estrogen receptor (Jacq et al., 1994). Recently, human $TAF_{II}55$ was shown to interact with multiple activation domains, including those of activators Sp1, USF, CTF/NF1, YY1, E1A and Tat (Chiang and Roeder, 1995).

TAF_{II}s have been proposed to function as coactivators, which mediate transcriptional activation by bridging or stabilizing the interactions between activators and general transcription factors (Goodrich and Tjian, 1994). In addition to TAF_{II}s, some other proteins have also been proposed to possess this function, including positive cofactors (PCs) PC1-PC4 , E1A coactivator p300, CREB coactivator CBP, yeast mediator proteins SUG1 and GAL11, and yeast adaptor proteins ADA2, ADA3 and GCN5 (Triezenberg, 1995). Functional or physical interactions between activation domains and these coactivators, mediators, or adaptor proteins have been demonstrated in most of the cases. Thus, they are regarded as one class of target proteins for transcriptional activators.

Activators And TFIIB

TFIIB, the bridging factor between promoter bound TFIID and RNAP II, has been initially proposed and actively pursued as the target of activators by Green's lab. By attaching DNA templates to agarose beads, Green and coworkers isolated and analyzed template-associated complexes at various stages of

assembly and found that binding of TFIIB was the rate-limiting step of the preinitiation complex assembly process and that VP16 activation domain functioned by recruiting TFIIB to the promoter (Lin and Green, 1991). They further demonstrated physical interactions between TFIIB and VP16 activation domain by using affinity chromatographic method (Lin et al., 1991). Two TFIIB mutants with double point mutations which severely decreased affinity for VP16 are found defective selectively in activated transcription, but not in basal transcription (Roberts et al., 1993). This demonstrated the specificity and functional significance of interaction between the VP16 activation domain and TFIIB. They also reported that a VP16 point mutant which was transcriptionally inactive also showed strongly decreased affinity to TFIIB (Lin and Green, 1991). However, two other groups could not reproduce this result (Walker et al., 1993; Goodrich et al., 1993).

Using a gel-mobility shift assay, Sundseth and Hansen reported that a cellular activator LSF reduced the lag in the rate of initiation complex formation due to the rate of slow addition of TFIIB (Sundseth and Hansen, 1992). Their results suggest that LSF increases the association of TFIIB with the TFIID-bound template. Green and colleagues recently suggested another mechanism whereby VP16 may enhance transcription through TFIIB (Roberts and Green, 1994). By using affinity chromatography and V8 protease analysis, they showed the amino-terminal domain of TFIIB interacts with its carboxyl-terminal domain. In such a 'closed' conformation, accessibility of TFIIB to TBP, RNAP II and TFIIF was reduced. Binding of VP16 to the carboxyl terminus of TFIIB disrupts the intramolecular interaction and accelerates the access of TBP, RNAP II and TFIIF, driving the preinitiation complex assembly process forward. In vitro interactions have also been shown between TFIIB and steroid receptors, Rel oncoproteins,

CTF/NF1 and EBNA 2 (Baniahmad et al., 1993; Ing et al., 1992; Xu et al., 1993; Kim and Roeder, 1994; Tong et al., 1995a).

Activators And TFIIA

Both in vitro and in vivo functional assays indicate that TFIIA stimulates activator-mediated (such as activators VP16, Sp1, NTF-1, Zta) transcription (Ma et al., 1993; Ozer et al., 1994; Sun et al., 1994; Yokomori et al., 1994). The effect is not simply due to enhancement of basal transcription, but TFIIA directly participates in the activation process. Roles of TFIIA in activation might be two fold. TFIIA could act as the derepressor of TFIID and in conjunction with activators, such as Zta, to overcome a slow step in preinitiation complex formation (Chi and Carey, 1993). Secondly, using gel mobility shift assay, a stable complex of promoter DNA with activator Zta, TFIIA and TFIID formed on a template containing Zta binding site was observed (Lieberman and Berk, 1994). For Zta to increase the stability of the complex, TFIIA is required. Here, TFIIA seems play a more direct role. The activation domain of VP16 behaves in similar fashion as Zta in the same assay. Consistent with TFIIA's direct role in activation, TFIIA has recently been shown to bind the activator Zta in an activation-dependent manner (Ozer et al., 1994).

The general factors which enter the preinitiation complex at early stages (i.e., TBP/TAF_{II}s, TFIIB and TFIIA) could all be targets of some activation domains. Scrutinizing these interactions suggest that two kinds of pathways maybe used by activators. Some pathways are more broadly used. Many activators tested interact with TBP, indicating that the recruitment of TBP/TFIID maybe one of the common pathway. In contrast, some pathway may only be used by a selective sets of activators. For example, direct and specific interaction between GAL4 activation domain and TBP was demonstrated while TFIIB and GAL4 interaction was not detected in a recent study (Melcher and Johnston).

A greater range of targets might contribute to the potency of strong activators such as VP16. TBP, $dTAF_{II}40$, TFIIB and TFIIA have all been demonstrated or implicated as target proteins of VP16. For some activators, these interactions are intermingled and interdependent. For example, $dTAF_{II}40$ and TFIIB each interact with VP16, and $dTAF_{II}40$ is capable of interacting with TFIIB , suggesting a three-way interacting complex (Goodrich et al., 1993). In one study, for Zta activation domain to enhance the stability of the TFIID-TFIIA-promoter complex, both TAFs and TFIIA are found necessary (Lieberman and Berk, 1994). In another study, the effect of GAL4-VP16 on TFIIB recruitment to early initiation complex is disrupted by TBP mutants which is deficient in interacting with VP16 or TFIIB (Kim et al., 1994b). This suggests GAL4-VP16 may function by induction or stabilization of an activation specific TBP-TFIIB-promoter complex. The fourth example comes from the study of ICP4, the herpes simplex virus transcriptional regulatory protein (Smith et al., 1993). ICP4 forms a tripartite complex with TFIIB and TBP/TFIID and the ability of ICP4 to regulate transcription correlates to its ability to form this tripartite complex.

Activators also function at steps after the DAB complex formation. Green and colleagues later suggested that activators function not only through recruiting TFIIB, but also at a second step, after TFIIB (Choy and Green, 1993). The second step was found TAF_{II} dependent.

Activators And TFIIF

TFIIF is an important factor in both initiation phase and elongation phase of transcription, thus an attractive target of activators. TFIIF associated with RNAP II enter the preinitiation complex after TFIIB. Prywes and colleagues reported the role of TFIIF in serum response factor (SRF)-activated transcription (Zhu et al., 1994). Functional studies showed that high amounts of TFIIF were required for SRF-activated transcription and TFIIF could relieve squelching of

SRF in vitro. These results promoted more direct examination of the interaction between SRF and TFIIF by gel mobility shift assay where TFIIF was found bound to DNA in complex with SRF, but not alone. Interestingly, TFIIF had a similar effect on GAL4-VP16, but not on Sp1. Recent identification of the smallest subunit of TFIIF in yeast as $yTAF_{II}30$ points to a common functional requirement for TFIIF and $TAF_{II}s$, possibly interacting with activation domains (Henry et al., 1994).

RNAP II CTD In Activation

Carboxyl terminal domain (CTD) of the largest subunit of RNAP II has been implicated in the response of the transcriptional apparatus to signals from activators at certain promoters (Allison and Ingles, 1989; Scafe et al., 1991; Liao et al., 1991). Yeast strains containing CTD with different length repeats of heptapeptide were equally capable of mediating activation by the acidic activator GAL4 (Allison and Ingles, 1989). Interestingly, when GAL4 activation mutants were assayed in these yeast strains, truncation of the CTD magnified transcriptional defects, while extension of the CTD suppressed the defects. CTD has been postulated to interact with the activation domain of some activators, and in this manner, RNAP II gets recruited to build up the preinitiation complex. The heptapeptide repeats rich in hydroxyl groups have been particularly speculated as the functional redundant motifs to interact with AADs (Sigler, 1988). Direct evidence of CTD-activator interaction has not yet been reported. It is also possible that activators function through coactivators to interact with the CTD.

Activators And TFIIH

TFIIH is the only general factor known which possesses enzymatic activity and it is a multifunctional protein involved in transcription, DNA repair, and possibly cell-cycle control (Drapkin and Reinberg, 1995). Hence, interaction of an

activator with TFIIH could have enormous impact on transcription initiation and perhaps even on the other cellular processes. The TFIIH p62 subunit binds specifically to the AAD of VP16 and p53 (Xiao et al., 1994), and the p62 and p80 subunits both bind specifically to the AAD of EBNA 2 (Tong et al., 1995b). Presumably, both recruitment of TFIIH and its enzymatic activities could be regulated. However, there is no report of stimulation of the enzymatic activities by activators yet.

It has been noted that transcriptional activators work synergistically when multiple regulatory elements are present and the multiple activation subdomains of many activators also act synergistically to increase activator potency (Hori and Carey, 1994). The findings that functional or physical interactions exist between the activation domains and nearly each component of the basal transcriptional machinery suggest that one or a combination of given activation domains may function by targeting one or several steps in the preinitiation complex assembly pathway at a given promoter, regulating transcription of the given gene elaborately or synergistically.

(b) Activators And Holoenzyme Model

According to the holoenzyme model, the major regulation steps in the preinitiation complex assembly are formation of the TFIID-bound complex and recruitment of the holoenzyme. Interactions between TBP/TFIID and activators have been described above. Interactions between activators and the holoenzyme are supported by the following lines of evidence. The holoenzyme (containing RNAP II, SRB proteins, SUG1, GAL11 and general factors TFIIB, TFIIF and TFIIH) is responsive to transcriptional activators as transcription by this holoenzyme is stimulated by GAL4-VP16 (Koleke and Young, 1994). The subcomplex of holoenzyme containing SRB, SUG1 and GAL11 has been identified as a multiprotein mediator of activation (Kim et al., 1994). Young and

colleagues recently demonstrated direct and specific interaction of VP16 AAD and the holoenzyme by immunoprecipitation experiments. Both the holoenzyme and the mediator subcomplex were found bound to an VP16 AAD affinity column (Hengartner, 1995).

The interactions identified between activation domains and individual components of the basal transcription machinery are not contradictory to the holoenzyme model. According to this model, the holoenzyme contains a contiguous surface with multiple contact points (i.e., TFIIB, TFIIF, TFIIH, and mediator subcomplex) for activators andthe activators could contact any binding site along the surface to recruit the complex to the promoter. In fact, a single activator-holoenzyme contact has been shown being capable of triggering gene activation simply by recruitment of the holoenzyme (Barberis et al., 1995). The holoenzyme model can also explain the synergism in gene activation. The ability of multiple activation domains to simultaneously interact different components of the holoenzyme would result in cooperative recruitment of the complex to the core promoter.

(3) Open Complex Formation

After RNAP II and the general transcription factors assemble at the promoter region as the preinitiation complex (also refer to as the closed complex), the duplex DNA around the start site must open (melt) to expose the template strand. This process is referred to as the open complex formation and GAL4-VP16 has been shown to facilitate this process (Wang et al., 1992). Transcriptionally deficient VP16 mutants were found defective in their ability to stimulate the open complex formation (Jiang et al., 1994). These results suggest that the open complex formation step may also be a common target for transcriptional activators.

Specific RNAP II transcription requires ATP β-γ bond hydrolysis (Bunick et al., 1982). ATP hydrolysis is found to be required to open the DNA strands prior to formation of the first phosphodiester bond (Wang et al., 1992). ATP maybe used by DNA helicase to melt the start site or alternatively used by CTD kinase to phosphorylate CTD of RNAP II, inducing a conformational change that causes start site melting. Purified TFIIH has both ATP-dependent helicase activity and CTD kinase activity (Drapkin and Reinberg, 1995). Activators therefore may target TFIIH to facilitate open complex formation.

(4) Promoter Clearance

The open initiation complex is capable of initiating phosphodiester bond synthesis in the presence of all four nucleoside triphosphates. However, RNAP II at this stage can only synthesize very short transcripts several nucleotides in length which can not stably associate with polymerase and are released as abortive transcripts (Jacob et al., 1994). Promoter clearance is the event which results in the transition from the open initiation complex to the elongation complex. This transition must break protein-protein and protein-DNA contacts which establish the initiation complex.

Using defined transcription system, Goodrich and Tjian found that TFIIE, TFIIH and ATP hydrolysis were not required for abortive initiation, but instead required by promoter clearance from a linear template (Goodrich and Tjian, 1994). They further found that TFIIE, TFIIH and the supercoiled template were not required for elongation. The TFIIH-associated DNA helicase appear to be important in the promoter clearance step, rather than in the open complex formation step. These results are somewhat contradictory to the previous observations in which these factors are required for initiation step of transcription. The differences may due to differences in experimental conditions

such as different promoters and different transcription systems. Nonetheless, the activator-TFIIH interaction may stimulate the promoter clearance step. In support of this, PBP, a cAMP response element-binding transcription factor, was found to enhance the rate of promoter clearance rather than open complex formation (Narayan et al., 1994).

(5) Elongation And Termination

After polymerase has escaped from promoter (promoter clearance), it enters the elongation phase during which the transcription complex moves along the DNA and synthesize an RNA transcript. DNA sequences through which the elongating RNAP must pass can lead the enzyme to pause, terminate, or reassume elongation and pass through terminator. Interactions of specific cellular regulatory factors with the RNAP, DNA template and nascent transcript decide fate of the transcription event (Spencer and Groudine, 1990; Kerppola and Kane, 1991; Greenblatt et al., 1993). Eukaryotic genes transcribed by RNAP II are also regulated at the level of elongation. Well documented examples include transcription of several cellular oncogenes c-myc, c-myb and c-fos, human immunodeficiency virus (HIV) and *Drosophila* hsp70 gene (Kerppola and Kane, 1991; Greenblatt et al., 1993; Lis and Wu, 1993).

There are two classes of transcription factors that regulate the elongation phase of RNAP II transcription. One class include the transcription factor TFIIS which promotes read-through of RNAP II through transcription blocks (Rudd et al., 1994). The other class includes TFIIF and SIII which increase the overall rate of RNA chain elongation by RNAP II (Bengal et al., 1991; Garrett et al., 1994).

Two transcriptional activators have earlier been demonstrated to possess antitermination or antipausing activity (Greenblatt et al., 1993; Lis and Wu, 1993). The HIV-1 virally encoded factor Tat not only activates transcriptional initiation

from the promoter in the 5' LTR of HIV-1, but also enhances the processivity of elongating transcription complex. The function of Tat in elongation requires Tat's association with the control sequences (TAR element) in the nascent transcript and its association with some host factors. *Drosophila* unstressed heat shock promoters contain an paused RNAP II and the heat shock factor (HSF) accelerates the rate of escape of the paused polymerase upon heat shock. Recently, effects on processivity of RNAP II transcription by a variety of transcriptional activators, including GAL4-VP16, GAL4-E1a and GAL4-AH, were examined (Yankulov et al., 1994). In the presence of activators, the transcriptional complex was found to have higher processivity and was capable of reading through pausing and termination sites. One possible mechanism by which activators stimulate elongation is that activators recruit elongation factors to the transcription complex. TFIIF is an attractive candidate, as it is important for antitermination by tat in vitro and it works by functionally similar pathway as tat (Kato et al., 1992). Alternatively, activators may target factors which could modify the property of the RNAP II and thus enhance elongation.

(6) Recycling Of General Transcription Factors And RNAP II

Using a defined reconstituted transcription system and a variety of approaches, the fate of each of the general transcription factors during the transition from initiation to elongation were characterized in a recent study (Zawel et al., 1995). Prior to the addition of NTPs, general factors TBP, TFIIB, TFIIF, TFIIE and TFIIH are all in the mature initiation complex. Upon addition of NTP, the complex is disrupted. TBP is the only factor remains bound at the promoter through the transcription cycle. TFIIB is released upon the addition of NTP, TFIIE is released within the first ten nucleotides of the nascent RNA transcript, TFIIH is released after the transcription complex reaches +30. TFIIF is

also released during elongation (after + 10), however, it is the only general factor which can reassociate with RNAP II when the RNAP II is arrested during elongation. After these general transcription factors released, they could reenter the transcription cycle by reassemble the preinitiation complex at the same TFIID- bound promoter. Thus, another role of activators emerges: activators not only initially interact with general transcription factors to establish the first initiation complex but also to target the released general factors to facilitate resetting the cycle after the first polymerase clears the promoter.

The polymerase in the elongation complex is highly phosphorylated at the CTD, which must be dephosphorylated to reassociate the promoter to start another round of transcription. A CTD phosphatase was recently isolated (Chambers and Dhamus, 1994). It is unknown whether transcriptional activators have any effect on the CTD phosphatase.

(7) Dynamic Interactions In Transcription

The process of transcriptional regulation is enormously complex, requiring concerted interactions between and among RNAP II, general transcription factors, elongation factors, activators and coactivators. Regulated transcription is likely not to result from simple static interactions of these various factors but rather may involve dynamic interactions.

Recent studies show that the CTD of RNAP II and the proline-rich transcriptional activation domain (AD) of CTF/NF1 share a common sequence element involved in transcriptional activation. Yet another highly conserved domain of RNAP II shares a functional element with acidic activation domain (AAD) of VP16 (Xiao et al., 1994b; Xiao et al., 1994c). More interestingly, the CTD-like sequence in CTF/NF1 AD interacts specifically with TBP, reminiscent of the specific association between CTD and TBP. The acidic domain in the

RNAP II interacts directly with both TBP and TFIIB, a feature shared with the AAD of VP16. Moreover, the VP16 AAD can compete specifically with the acidic domain in the RNAP II for these interactions. These observations led to the "tether and competition" model of transcription activation (Xiao et al., 1994b; Xiao et al., 1994c). According to this model, at early stage of preinitiation complex assembly, direct interactions of the AD of upstream activators with TBP and TFIIB may help tether general factors to the promoter, accelerating the formation of the transcription complex. The subsequent association of RNAP II with the TFIID-TFIIB-promoter complex may involve direct interactions of the AD-like domains in RNAP II with TFIID and TFIIB. Following assembly, during the transition from initiation to elongation, the AD of upstream activators competes with the AD-like domain in RNAP II to interact with TBP or TFIIB. This competition destablizes or displaces the contacts between the AD-like domain in RNAP II and general factors, facilitating RNAP II to escape from promoter. Thus, these dynamic interaction exchanges facilitate the transcriptional activation process.

Another example of the dynamic nature of the interactions involved in transcription activation is seen in the effect of activators on protein-protein and intra-protein interactions. The interaction between VP16 and TFIIB disrupts the intramolecular interaction between the amino-terminus and carboxyl-terminus of TFIIB and results in exposing the binding sites on TFIIB for TBP, RNAP II and TFIIF, accelerating the subsequent assembly events (Roberts and Green, 1994). Conversely, interaction between activator and general transcription factor also results in conformational change in the activation domain. As revealed by this thesis study, the disordered VP16 activation domain becomes conformationally constrained upon interaction with TBP. The disorder-order transition may be a means to regulate transcription activation.

Dynamic interactions have also been observed in the elongation phase of transcription. The elongating ternary complex composed of RNAP II, DNA template and the nascent RNA chain is not static during elongation. Instead, it is a dynamic apparatus able to assume different structures as it moves along the template (Linn and Luse, 1991; Kerppola and Kane, 1991). The changes in the structural organization of the engaged polymerase is proposed to increase or decrease the ability of the RNAP II to continue transcription and to modulate its interaction with accessory elongation factors. The interaction between TFIIF and RNAP II is also of particularly interest for its dynamic nature (Price et al., 1989; Zawel et al., 1995). TFIIF escorts the RNAP II to the promoter region to build up the preinitiation complex. After the transition from initiation to elongation, TFIIF is released from the RNAP II. However, TFIIF is capable of reassociate with a paused RNAP II transiently and facilitate passage through the pause. Upon resuming elongation, TFIIF is again released from the stalled elongation complex. The dynamic interactions between TFIIF and the RNAP II may contribute to the dual roles of TFIIF in initiation and elongation phase of transcription.

The multiplicity of protein-protein, protein-nucleic acid interactions observed in the transcription process may reflect a complex and dynamic exchange of interactions that result in the regulated transcription cycle. With the development and application of new techniques, more dynamic interactions are expected to be revealed and the dynamic picture of the transcription process will become more clear.

Overview

To understand how transcriptional activators profoundly influence many steps of the transcription cycle, two important and related questions must be

thoroughly studied. First, the structures of the activators; secondly, the dynamic interactions between activators and other components of the transcriptional machinery, particularly the general transcription factors, which eventually lead to the transcriptional activation. This thesis work is aimed at furthering our understanding of the these central issues, using the activation domain of herpes virus activator VP16 as the model system.

Cress and Triezenberg (1991) discovered that the Phe at position 442 of VP16 activation domain is critical for the transcriptional activity of the N-subdomain (413-456 aa). To further characterize the amino acid requirement at position 442, I undertook a saturation mutagenesis approach to thoroughly mutagenize this Phe to nearly all other amino acid substitution in the context of the N-subdomain. Activities of this set of mutants were tested by transient transfection assay and the results support the hypothesis of Cress and Triezenberg (1991) that the aromatic character is critical for this position; mutants bearing aromatic residue Tyr or Trp at this position retains one third of the activity of wild type. Bulky hydrophobic character is also important but less effective as they exhibit 10%-15% activity of the wild type, while all other amino acid substitutions at this position (with the exception of Asn) were less than 10% active. The initial characterization of the amino acid requirement at critical position of VP16 activation domain has inspired other researchers to identify residues important in other activation domains and similar pattern of critical elements appears to be a general requirement for activation domains.

Despite the extensive biochemical and molecular genetic studies of the activation domain, little structural characterization using biophysical approaches have been carried out. In this thesis work, we applied steady-state and time-resolved fluorescence spectroscopy to directly study the structure of VP16 activation domain. In these studies, we used transcriptionally active chimeric

proteins comprising the DNA binding domain of the yeast protein GAL4 (residues 1-147) and the activation domain of VP16 (residues 413-490, or subdomains thereof). Unique intrinsic fluorescent probes were obtained by replacing phenylalanine residues with tryptophan at positions 442 or 473 of VP16. Emission spectra of Trp at either position had maxima near 350 nm, as expected for highly-exposed Trp. The accessibility of these Trp residues to quenching agents was also comparable to that of fully exposed Trp. Decay-associated spectra revealed three lifetimes of 0.9, 3.0 and 5.9 ns. Time-resolved anisotropy decay measurements suggested that both Trp residues were associated with substantial flexibility (segmental motion). In each of these studies, the Trp residues at either position showed nearly identical fluorescence properties in either full-length activation domain or relevant subdomains suggesting that the two subdomains are similarly unstructured. These results will be described in Chapter III.

Previous biochemical demonstration of direct binding between the VP16 activation domain and various components of the basal transcriptional machinery did not yield information about the nature of the interactions in terms of binding affinity and dynamic changes. In Chapter IV I will describe our efforts to examine the interactions between VP16 and two of its potential targets, TBP and TFIIB by fluorescence spectroscopy methods. Two Trp analogs, 5-hydroxy-Trp or 7-aza-Trp were incorporated at amino acid positions 442 or 473 of VP16, providing valuable reagents fluorescence of which can be selectively excited in complexes with other Trp-containing proteins. TBP (but not TFIIB) caused concentration-dependent changes in the steady-state anisotropy of VP16, from which equilibrium binding constants were calculated. In anisotropy decay experiments using 5-hydroxy-Trp at either position, TBP induced a more ordered structure in the VP16 domain. In contrast, TFIIB induced only a slight change

and only for VP16 labeled at 473. The 7-aza-Trp residue at either position showed a spectral shift in the presence of TBP (but not TFIIB), indicating a change to a more hydrophobic environment. Quenching analyses also demonstrated that both residues became less solvent accessible in the presence of TBP. In contrast, TFIIB reduced the solvent accessibility only for the fluorophore at position 473. Our results support models of TBP as a target protein for transcriptional activators and suggest that ordered structure in the VP16 activation domain is induced upon interaction with target proteins.

These fluorescence spectroscopy approaches provided new insights into the structural and functional relationship of the VP16 activation domain, offering an attractive prospect for future study. Additional experiments that could be proposed using these techniques will be described in the final section. I will also describe another experimental design in which isotope-edited FTIR (Fourier transformed infrared) spectra will be used as the means to identify the induced secondary structure in the VP16 AAD.

REFERENCES

Allison, L. A., Wong, J. K., Fitzpatrick, D., Moyle, M., & Ingles, J. C. (1988) *Mol. Cell. Biol. 8,* 321-329.

Allison, L. A., & Ingles, J. C. (1989) *Proc. Natl. Acad. Sci. USA 86,* 2794-2798.

Arndt, K. M., Ricupero-Hovasse, S. & Winston, F. (1995) *EMBO. J. 14,* 1490-1497.

Axelrod, J. D., Reagan, M. S., & Majors, J. (1993) *Genes Dev. 7,* 857-869.

Barberis, A., Müller, C. W., Harrison, S., & Ptashne, M. (1993) *Proc. Natl. Acad. Sci. USA 90,* 5628-5632.

Barberis, A., Pearlberg, J., Simkovich, N., Farrel, S., Reinagel, P., Bamdad, C., Sigal, G., & Ptashne, P. (1995) *Cell 81,* 359-368.

Bartolomei, M. S., Halden, N. F., Cullen, C. R., & Corden, J. L. (1988) *Mol. Cell. Biol. 8, 330-339.*

Baniahmad, A., Ha, I., Reinberg, D., Tsai, S., Tsai, M. J., & O'Malley, B. W. (1993) *Proc. Natl. Acad. Sci. USA 90,* 8832-8836.

Bengal., E., Flores, O., Krauskopf, A., Reinberg, D., Aloni, Y. (1991) *Mol. Cell. Biol. 11,* 1195-1206.

Berroteran, R. W., Ware, D. E., & Hampsey, M. (1994) *Mol. Cell. Biol. 14,* 226-237.

Berger, S. L., Cress, W. D., Cress, A., Triezenberg, S. J., & Guarente, L. (1990) *Cell 61,* 1199-1208.

Blair, W. S., Bogerd, H., & Cullen, B, R. (1994a) *J. Virol. 68,* 3803-3808.

Blair, W. S., Bogerd, H. P., Madore, S. J., & Cullen, B, R. (1994b) *Mol. Cell. Biol. 14,* 7226-7234.

Bunick, D., Zandomeni, R., Ackerman, S., & Weinmann, R. (1982) *Cell 29*, 877-886.

Buratowski, S., Hahn, S., Guarente, L., & Sharp, A. (1989) *Cell 56*, 549-561.

Buratowski, S., & Zhou, H. (1993) *Proc. Natl. Acad. Sci. USA 90*, 5633-5637.

Cadena, D., & Dahmus, M. J. (1987) *J. Biol. Chem. 262*, 12468-12474.

Caron, C., Rousset, R., Béraud, C., Moncollin, V., Egly, J-M., & Jalinot, P. (1993) *EMBO. J. 12*, 4269-4278.

Chang, C. H., Kostrub, C. F., & Burton, Z. F. (1993) *J. Biol. Chem. 268*, 20482-20489.

Chang, C. H. (1995) Ph. D. thesis. Michigan State University.

Chasman, D. I., Flaherty, K. M., Sharp, P. A., & Kornberg, R. D. (1993) *Proc. Natl. Acad. Sci. USA 90*, 3174-3178.

Chatterjee, S., & Struhl, K. (1995) *Nature 374*, 820-822.

Chen, X-B., Farmer, G., Zhu, H., Prywes, R., & Prives, C. (1993) *Genes Dev. 7*, 1837-1849.

Chiang, C. M., & Roeder, R. G. (1995) *Science 267*, 531-536.

Chi, T., & Carey, M. (1993) *Mol. Cell. Biol. 13*, 7045-7055.

Choy, B., & Green, M. R. (1994) *Nature 366*, 531-536.

Conaway, R. C., & Conaway, J. W. (1993) *Ann. Rev. Biochem. 62*, 161-90.

Corden, J. L. (1990) *Trends in Biochem. Sci. 15*, 383-387.

Cormack, B. P., Strubin, M., Ponticelli, A. S., & Struhl, K. (1991) *Cell 65*, 341-348.

Cress, W. D., & Triezenberg, S. J. (1991) *Science 251*, 87-90.

Croston, G. E., Kerrigan, L. A., Lira, L. M., Marshak, D. R., & Kadonaga, J. T. (1991) *Science 251*, 643-649.

Dahlman-Wright, K., Baumann, H., McEwan, I. J., Almlof, T., Wright, A. P. H., Gustafsson, J., & Hard, T. (1995) *Proc. Natl. Acad. Sci. USA 92*, 1699-1703.

Darst, S. A., Edwards, A. M., Kubalek, E. W., & Kornberg, R. D. (1991) *Cell 66*, 121-128.

DeJong, J., & Roeder, R. G. (1993) *Genes Dev. 7*, 2220-2234.

Donaldson, L., & Capone, J. P. (1992) *J. Biol. Chem. 267*, 1411-1414.

Drapkin, R., Reardon, J. T., Ansari, A., Huang, J. C., Zawel, L., Ahn, K., Sancar, A., & Reinberg, D. (1994) *Nature 368*, 769-772.

Drapkin, R., & Reinberg, D. (1994) *Trends in Biochem. Sci. 19*, 504-508.

Drysdale, C. M., Dueñas, E., Jackson, B. M., reusser, U., Braus, G. H., & Hinnebusch, A. G. (1995) *Mol. Cell. Biol. 15*, 1220-1233.

Emili, A., Greenblatt, J., & Ingles, J. C. (1994) *Mol. Cell. Biol. 14*, 1582-1593.

Emili, A., & Ingles, J. C. (1995) *J. Biol. Chem. 270*, 13674-13680.

Feaver, W. J., Gileadi, O., Li, Y., & Kornberg, R. D. (1991) *Cell 67*, 1223-1230.

Feaver, W. J., Svejstrup, J. Q., Henry, N. L., & Kornberg, R. D. (1994) *Cell 79*, 1103-1109.

Fischer, L., Gerard, M., Chalit, C., Lutz, Y., Humbert, S., Kanno, M., Chambon, P., & Egly, J. M. (1992) *Science 257*, 1392-1395.

Finkelstein, A., Kostrub, C. F., Li, J., Chavez, D. P., Wang, B-Q., Fang, S-M., Greenblatt, J., & Burton, Z. F. (1992) *Nature 355*, 464-467.

Flores, O., Lu, H., Killeen, M., Greenblatt, J., Burton, Z. F., & Reinberg, D. (1991) *Proc. Natl. Acad. Sci. USA 88*, 9999-10003.

Garrett, K. P., Tan, S-Y., Bradsher, J. N., Lane, W. S., Conaway, J. W., & Conaway, R. C. (1994) *Proc. Natl. Acad. Sci. USA 91*, 5237-5241.

Gasch, A., Hoffman, A., Horikoshi, M., Roder, R. G., & Chua, N. H. (1990) *Nature 346*, 390-394.

Gill, G., & Tjian, R. (1991) *Cell 65*, 333-340.

Gill, G., & Tjian, R. (1992) *Curr. Opin. Genetics Dev.,2*, 232-242.

Gill, G., Pascal, E., Tseng, Z. H., & Tjian, R. (1994) *Proc. Natl. Acad. Sci. USA 91*, 192-196.

Goodrich, J., Hoey, T., Thut, C. J., Admon, A., & Tjian, R. (1993) *Cell 75*, 519-530.

Goodrich, J., & Tjian, R. (1994) *Cell 77*, 145-156.

Goodrich, J., & Tjian, R. (1994) *Curr. Opin. Cell Biol. 6*, 403-409.

Greenblatt, J., Nodwell, J. R., & Mason, S. W. (1993) *Nature 364*, 401-406.

Ha, I., Lane, W. S., & Reinberg, D. (1991) *Nature 352*, 689-695.

Ha, I., Roberts, S., Maldonada, E., Sun, X-Q., Kim, L-U., Green, M., & Reinberg, D. (1993) *Genes Dev. 7*, 1021-1-32.

Hardwick, J. M., Tse, L., Applegren, N., Nicholas, J., & Veliuona, M. A. (1992) *J. Virol. 66*, 5500-5508.

Hahn, S., Buratowski, P. A., Sharp, P. A., & Guarente, L. (1989) *Cell 58*, 1173-1181.

Hahn, S., & Blanco, J. A. (1992) *Cell 71*, 1055-1064.

Hahn, S. (1993) *Nature 363*, 672-673.

Hagemeier, C., Walker, S., Caswell, R., & Kouzarides, T. (1992) *J. Virol. 66*, 4452-4466.

Hagemeier, C., Bannister, A. J., Cook, A., & Kouzarides, T. (1993) *Proc. Natl. Acad. Sci. USA 90*, 1580-1584.

Hengartner, C. J., Thompson, C. M., Zhang, J-H., Chao, D. M., Liao, S-M., Koleske, A. J., Okamura, S., & Young, R. A. (1995) *Genes Dev. 9*, 897-910.

Henry, N. L., Campbell, A. M., Feaver, W. J., Poon, D., Weil, P. A., & Kornberg, R. D. (1994) *Genes Dev. 8*, 2868-2878.

Hoey, T., Dynlacht, B. D., Peterson, M. G., Pugh, B. F., & Tjian, R. (1990) *Cell 60*, 1179-1186.

Hoey, T., Weinzier, R. O. J., Gill, G., Chen, J-L., Dynlacht, B. D., & Tjian, R. (1993) *Cell 72*, 247-270.

Hope, I. A., & Struhl, K. (1986) *Cell 46*, 885-894.

Hoopes, B. C., LeBlanc, J. F., & Hawley, D. K. (1992) *J. Biol. Chem. 267*, 11539-11547.

Hori, R. & Carey, M. (1994) *Curr. Opin. Genetics Dev. 4*, 236-244.

Horikoshi, M., Wang, C. K., Fuji, H., Cromlish, J. A., Weil, P. A., & Roeder, R. G. (1990) *Nature 341*, 299-301.

Humbert, S., Van Vuuren, H., Lutz, Y., Hoeijmakers, J. H., Egly, J-M., & Mancollin, V. (1994) *EMBO. J. 13*, 2393-2398.

Ing, N. H., Beekman, J. M., Tsai, S. Y., & O'Malley, B. W. (1992) *J. Biol. Chem. 267,* 17617-17623.

Ingles, C. J., Cress, W. D., Triezenberg, S. J., & Greenblatt, J. (1991) *Nature 351,* 588-590.

Jacob, G. A., Kitzmiller, J. A., & Luse, D. (1994) *J. Biol. Chem. 269,* 3655-3663.

Jacq, X., Brou, C., Lutz, Y., Davidson, I., Chambon, P., & Tora, L. (1994) *Cell 79,* 107-117.

Jiang, Y., Triezenberg, S. J., & Gralla, J. D. (1994) *J. Biol. Chem. 269,* 1-4.

Johnson, P. F., & McKnight, S. L. (1989) *Ann. Rev. Biochem. 58,* 799-839.

Kao, C. C., Lieberman, P. M., Schmidt, M. C., Zhou, Q., Pei, R., & Berk, A. J. (1990) *Science 248,* 1646-1650.

Kashanchi, F., Piras, G., Radonovich, M. F., Duvall, J. F., Fattaey, A., Chiang, C-M., Roeder, R. G., & Brady, J. N. (1994) *Nature 367,* 295-299.

Katan, M., Haigh, A., Verrijzer, C. P. van der Vliet, P. C., & O'Hare, P. (1990) *Nucleic Acid Res. 18,* 6871-6880.

Kato, H., Sumimoto, H., Pognonec, P., Chen, C. H., Rosen, C. A., & Roeder, R. G. (1992) *Genes Dev. 6,* 655-666.

Kassavetis, G. A., Joazeiro, C. A. P., Pisano, M., Geiduschek, E. P., Colbert, T., Kelleher, R. J., Flanagan, P. M., & Kornberg, R. D. (1990) *Cell 61,* 1209-1215.

Kerppola, T. K., & Kane, C. M. (1991) *FASEB J. 5,* 2833-2842.

Kim, J. L., Nikolov, D, B., & Burley, S. K. (1993a) *Nature 365,* 520-527.

Kim, T. K., & Roeder, R. G. (1994) *Proc. Natl. Acad. Sci. USA 91,* 4170-4174.

Kim, T. K., Hashimoto, S., Kelleher, R. J. III., Flanagan, P. M., Kornberg, R. D., Horikoshi, M., & Roeder, R. G. (1994b) *Nature 369*, 252-255.

Kim, Y., Geiger, J. H., Hahn, S., & Sigler, P. B. (1993b) *Nature 365*, 512-520.

Kim, Y-J., Björklund, S., Li, Y., Sayre, M. H., & Kornberg, R. D. (1994a) *Cell 77*, 599-608.

Kingston, R. E., & Green, M. R. (1994) *Curr. Biol. 4*, 325-332.

Klein, C., & Struhl, K. (1994) *Science 266*, 280-282.

Kraus, V. B., Inostroza, J. A., Yeung, K., Reinberg, D., & Nevins, J. R. (1994) *Proc. Natl. Acad. Sci. USA 91*, 6279-6282.

Kristie, T. M., & Roizman, B. (1984) *Proc. Natl. Acad. Sci. USA 81*, 4065-4069.

Kristie, T. M., & Sharp, P. A. (1993) *J. Biol. Chem. 268*, 6525-6534.

Koleske, A. J., Buratowski, S., Nonet, M., & Young, R. A. (1992) *Cell 69*, 883-894.

Koleske, A. J., & Young, R. A. (1994) *Nature 368*, 466-469.

Koleske, A. J., & Young, R. A. (1995) *Trends in Biochem. Sci. 20*, 113-116.

Laybourn, P. L., & Dahmus, M. E. (1990) *J. Biol. Chem. 264*, 6693-6698.

Lee, W. S., Kao, C. C., Bryant, G. O., Liu, X., & Berk, A. J. (1991) *Cell 67*, 365-376.

Leuther, K. K., Salmeron, J. M., & Johnston, S. A. (1993) *Cell 72*, 575-585.

Lewin, B. (1994) *Cell 79*, 397-406.

Li, Y., Flanagan, P. M., Tschochner, H., & Kornberg, R. D. (1994) *Science 263*, 805-807.

Liao, S-M., Taylor, I. C., Kingston, R. E., & Young, R. A. (1991) *Genes Dev. 5*, 2431-2440.

Lieberman, P. M., & Berk, A. J. (1991) *Genes Dev. 5*, 2441-2454.

Lieberman, P. M., Schmidt, M. C., Kao, C. C., & Berk, A. J. (1991) *Mol. Cell. Biol. 11*, 63-74.

Lieberman, P. M., & Berk, A. J. (1994) *Genes Dev. 8*, 995-1006.

Lin, Y-S., & Green, M. R. (1991) *Cell 64*, 971-981.

Lin, Y-S., Ha, I., Maldonado, E., Reinberg, D., & Green, M. R. (1991) *Nature 353*, 569-571.

Lin, J., Chen, J., Elenbaas, B., & Levine, A. J. (1994) *Genes Dev. 8*, 1235-1246.

Linn, S. C., & Luse, D. S. (1991) *Mol. Cell. Biol. 11*, 1508-1522.

Lis, J., & Wu, C. (1993) *Cell 74*, 1-4.

Lobo, S. M., Tanaka, M., Sullivan, M. L., & Hernandez, N. (1992) *Cell 71*, 1029-1040

Lu, H., Flores, O., Weimann, R., & Reinberg, D. (1991) *Proc. Natl. Acad. Sci. USA 88*, 10004-10008.

Lu, H., Zawel, L., Fisher, L., Egly, J. M., & Reinberg, D. (1992) *Nature 358*, 641-645.

Ma, D-M., Watanabe, H., Mermelstein, F., Admon, A., Oguri, K., Sun, X-Q., Wade, T., Imai,T., Shiroya, T., Reinberg, D., & Handa, H. (1993) *Genes Dev. 7*, 2246-2257.

Ma, J., & Ptashne, M. (1987) *Cell 48*, 847-853.

Maldonado, E., & Reinberg, D. (1995) *Curr. Opin. Cell Biol. 7*, 352-361.

Marsden, H. S., Campbell, M. E. M., Haarr, L., Frame, M. C., Parris, D. S., Murphy, M., Hope, R. G., Muller, M. T., & Preston, C. M. (1987) *J. Virol. 61*, 2428-2437.

Maxson, M. E., Goodrich, J. A., & Tjian, R. (1994) *Genes Dev. 8*, 515-524.

Metz, R., Bannister, A. J., Sutherland, J. A., Hagemeier, C., O'Rourke, E. C., Cook, A., Bravo, R., & Kouzarides, T. (1994) *Mol. Cell. Biol. 14*, 6021-6029.

Melcher, K., & Johnston, S. A. (1995) *Mol. Cell. Biol. 15*, 2839-2848.

Mitchell, P. J., & Tjian, R. (1989) *Science 245*, 371-378.

Mu, D., Park, C-H., Matsunaga, T., Hsu, D., Reardon, J. T., & Sancar, A. (1995) *J. Biol. Chem. 270*, 2415-2418.

Narayan, S., Widen, S. G., Beard, W. A., & Wilson, S. H. (1994) *J. Biol. Chem. 269*, 12755-12763.

Nikolov, D. B., Hu, S., Lin, J., Gasch, A., Hoffman, A., Horikoshi, M., Chua, N., Roeder, R. G., & Burley, S. K. (1992) *Nature 360*, 40-46.

O'Hare, P., & Williams, G. (1992) *Biochemistry 31*, 4150-4156.

Ohkuma, Y., Sumimoto, H., Hoffman, A., Ahimasaki, S., Horikoshi, M., & Roeder, R. G. (1991) *Nature 354*, 399-404.

Ohkuma, Y., & Roeder, R. G. (1994) *Nature 368*, 160-163..

Ozer, J., Moore, P. A., Bolden, A. H., Lee, A., Rosen, C. A., & Lieberman, P. M. (1994) *Genes Dev. 8*, 2324-2335.

Pabo, C. O., & Sauer, R. T. (1992) *Ann. Rev. Biochem. 61,* 1053-1095.

Paranjape, S. M., KAmakaka, R. T., & Kadonaga, J. T. (1994) *Ann. Rev. Biochem. 63,* 265-297.

Parvin, D. P., & Sharp, P. A. (1993) *Cell 73,* 533-540.

Pascal, E., & Tjian, R. (1991) *Genes Dev. 5,* 5005-5012.

Pellett, P., McKnight, J. L. C., Jenkins, F., & Roizman, B. (1985) *Proc. Natl. Acad. Sci. USA 82,* 5870.

Peterson, C. L., & Tamkun, J. W. (1995) *Trends in Biochem. Sci. 20,* 143-146.

Peterson, M. G., Tanse, N., Pugh, B. F., & Tjian, R. (1990) *Science 248,* 1625-1630.

Peterson, M. G., Inostroza, J., Maxon, M. E., Flores, O., Admon, A., Reinberg, D., & Tjian, R. (1991) *Nature 354,* 369-373.

Peterson, M. G., & Tjian, R. (1992) *Nature 358,* 620-621.

Pino, I., Ware, D. E., & Hampsey, M. (1992) *Cell 68,* 977-988.

Price, D. H., Sluder, A. E., & Greenleaf, A. L. (1989) *Mol. Cell. Biol. 9,* 1465-1475.

Poon, D., Schroeder, S., Wang, C. K., Yamamoto, T., Horikoshi, M., Roeder, R. G., & Weil, P. (1991) *Mol. Cell. Biol. 11,* 4809-4821.

Ranish, J. A., Lane, W. S., & Hahn, S. (1992) *Science 255,* 1127-1129.

Reese, J. C., Apone, L., Walker, S. S., Griffin, L. A., & Green, M. R. (1994) *Nature 371,* 523-527.

Regier, J. L., Shen, F., & Triezenberg, S. J. (1993) *Proc. Natl. Acad. Sci. USA 90,* 883-887.

Roberts, S. G. E., Ha, I., Maldonado, E., Reinberg, D., & Green, M. R. (1993) *Nature 363*, 741-744.

Roberts, S. G. E., & Green, M. R. (1994) *Nature 371*, 717-720.

Roy, R., Adamczewski, J. P., Seroz, T., Vermeulen, W., Tassan, J-P., Schaeffer, L., Nigg, E. A., Hoeijmakers, J. H. J., & Egly, J-M. (1994) *Cell 79*, 1093-110.

Rudd, M. D., Izban, M. G., & Luse, D. S. (1994) *Proc. Natl. Acad. Sci. USA 91*, 8057-8061.

Sadowski, I., Ma, J., Triezenberg, S., & Ptashne, M. (1988) *Nature 355*, 563-564.

Sadowski, C. L., Henry, R. W., Lobo, S. M., & Hernandez, N. (1993) *Genes Dev. 7*, 1535-1548.

Sawadogo, M., & Sentenac, A. (1990) *Ann. Rev. Biochem. 59*, 711-754.

Scafe, C., Chao, D., Lopes, J., Hirsh, J. P., Henry, S., & Young, R. (1990) *Nature 347*, 491-494.

Schaeffer, L., Roy, R., Humbert, S., Moncollin, V., Vermeulen, W., Hoeijmakers, J. H., Chambon, P., & Egly, J-M. (1993) *Science 260*, 58-63.

Schmidt, M. C., Zhou, Q., & Berk, A, J. (1989) *Mol. Cell. Biol. 9*, 3299-3307.

Schmitz, M. L., Silva, M. A. D. S., Altman, H., Czisch, M., Holak, T. A., & Baeuerle, P. A. (1994) *J. Biol. Chem. 269*, 25613-25620.

Seipel, K., Georgiev, O., & Schaffner, W. (1994) *Biol. Chem. Hoppe-Seyler 375*, 463-470.

Serizawa, H., Conaway, J. W., & Conaway, R. C. (1993) *Nature 363*, 371-374.

Serizawa, H., Mäkelä, T. P., Conway, J. W., Conaway, R. C., Weinberg, R. A., & Young, R. A. (1995) *Science 374*, 280-287.

Shen, F., Triezenberg, S. J., Hensley, P., Porter, D., & Knutson, J. (1995a) Manuscript in preparation.

Shen, F., Triezenberg, S. J., Hensley, P., Porter, D., & Knutson, J. (1995b) Manuscript in preparation.

Sigler, P. (1988) *Nature 347*, 491-494.

Smith, C. A., Bates, P., Rivera-Gonzalez, R., Gu, B-H., & DeLuca, N. A. (1993) *J. Virol. 67*, 4676-4687.

Sopta, M., Burton, Z. F., & Greenblatt, J. (1989) *Nature 341*, 410-414.

Spector, D., Purves, F., & Roizman, B. (1990) *Proc. Natl. Acad. Sci. USA 87*, 5268-5272.

Spencer, C. A., & Groudine, M. (1990) *Oncogenes 5*, 777-785.

Stern, S., Tanaka, M., & Herr, W. (1989) *Nature 341*, 624-630.

Sun, X-Q., Ma, D-M., Sheldon, M., Yeung, K., & Reinberg, D. (1994) *Genes Dev. 8*, 2336-2348.

Sundesch, R., & Hansen, U. (1992) *J. Biol. Chem. 267*, 7845-7855.

Sutherland, J. A., Cook, A., Banister, A. J., & Kouzarides, T. (1992) *Genes Dev. 6*, 1810-1819.

Taggart, A. K. P., Fisher, T. S., & Pugh, B. F. (1992) *Cell 71*, 1015-1028.

Tamura, T., Sumita, K., Fujino., K., Aoyama, A., & Horikoshi, M. (1991) *Nucleic Acids Res. 19*, 3861-3865.

Tanaka, M., & Herr, W. (1994) *Mol. Cell. Biol. 14*, 6056-6067.

Tansey, W. P., Ruppert, S., Tjian. R., & Herr, W. (1994) *Genes Dev. 8*, 2756-2769.

Thompson, C. M., Koleske, A. J., Chao, D. M., & Young, R. A. (1993) *Cell 73*, 1361-1375.

Thompson, C. M., & Young, R. A. (1995) *Proc. Natl. Acad. Sci. USA 92*, 4587-4590.

Thompson, N. E., Steinberg, T. H., Aronson, D. A., & Burgess, R. R. (1989) *J. Biol. Chem. 264*, 11511.

Tjian, R., & Maniatis, T. (1994) *Cell 77*, 5-8.

Tong, X., Wang, F., Thut, C. J., & Kieff, E. (1995a) *J. Virol 69*, 585-588.

Tong, X., Drapkin, R., Reinberg, D., & Kieff, E. (1995b) *Proc. Natl. Acad. Sci. USA 92*, 3259-3263.

Truant, R., Xiao, H., & Greenblatt, J. (1993) *J. Biol. Chem. 268*, 2284-2287.

Triezenberg, S. J., Kingsbury, R. C., & McKnight, S. L. (1988a) *Genes Dev. 2*, 718-729.

Triezenberg, S. J., LaMarco, K. L., & McKnight, S. L. (1988b) *Genes Dev. 2*, 730-742.

Triezenberg, S. J. (1995) *Curr. Opin. Genetics Dev. 5*, 190-196.

Tyree, C. M., Geoge, C. P., Lira-Devito, L. M., Wampler, S. L., Dahmus, M. E., Zawel, L., & Kadonaga, J. T. (1993) *Genes Dev. 7*, 1254-1265.

Usheva, A., Maldonado, E., Goldring, A., Lu, H., Houbavi, C., Reinberg, D., & Aloni, Y. (1992) *Cell 69*, 871-881.

Usheva, A., & Shenk, T. (1994) *Cell 76*, 1115-11221.

Van Hoy, M., Leuther, K. K., Kodadek, T., & Johnston, S. A. (1993) *Cell 72*, 587-594.

Wagner, E. K. (1990) In *Herpesvirus Transcription and Its Regulation*, CRC Press, Boca Raton, FL., pp. 1-16.

Wagner, A., & Green, M. R. (1994) *Curr. Opin. Cell Biol. 6*, 410-414.

Walker, S., Greaves, R., & O'Hare, P. (1993) *Mol. Cell. Biol. 13*, 5233-5244.

Wampler, S. L., & Kadonaga, J. T. (1992) *Genes Dev. 6*, 1542-1552.

Wang, W-D., Carey, M., & Gralla, J. D. (1992) *Science 255*, 450-453.

Weis, L., & Reinberg, D. (1992) *FASEB J. 6*, 3300-3309.

White, R. J., & Jackson, S. P. (1992) *Cell 71*, 1041-1054.

Wilson, A. C., LaMarco, K., Peterson, M. G., & Herr, W. (1993) *Cell 74*, 115-125.

Workman, J. L., Taylor, I. C. A., & Kingston, R. E. (1991) *Cell 64*, 533-544.

Xiao, H., Pearson, A., Coulombe, B., Truant, R., Zhang, S., Regier, J. L., Triezenberg, S. J., Reinberg, D., Flores, O., Ingles, C. J., & Greenblatt, J. (1994a) *Mol. Cell. Biol. 14*, 7013-7024.

Xiao, H., Friesen J. D., & Lis, J. T. (1994b) *Mol. Cell. Biol. 14*, 7507-7516.

Xiao, H., Lis, J. T., Xiao, H., Greenblatt, J., & Friesen J. D. (1994c) *Nucleic Acids Res. 22*, 1966-1973.

Xiao, P., & Capone, J. P. (1990) *Mol. Cell. Biol. 10*, 4974-4977.

Xu, X., Prorock, C., Ishikawa, H., Maldonado, E., Ito, Y., & Gelinas, C. (1993) *Mol. Cell. Biol. 13*, 6733-6741.

Yankulov, K., Blau, J., Purton, T., Roberts, S., & Bentley, D. L. (1994) *Cell 77*, 749-759.

Yokomori, K., Admon, A., Goodrich, G., Chen, J-L., & Tjian, R. (1993) *Genes Dev. 7*, 2235-2245.

Yokomori, K., Zeider, M. P., Chen, J-L., Verrijzer, C. P., Mlodzik, M., & Tjian, R. (1994) *Genes Dev. 8*, 2313-2323.

Young, R. A. (1991) *Ann. Rev. Biochem. 60, 689-715.*

Zawel, L., & Reinberg, D. (1993) In *Progress in Nucleic Acids Research and Molecular Biology*, Cohn, W. E., & Moldave, K., Eds., Academic Press, San Diego, pp. 67-108.

Zawel, L. R., & Reinberg, D. (1995) *Ann. Rev. Biochem. 64*, 533-561.

Zawel, L. R., Kumar, K. P., & Reinberg, D. (1995) *Genes Dev. 9*, 1479-1490.

Zehring, W. A., Lee, J. M., Weeks, J. R., Jokerst, R. S., & Greenleaf, A. L. (1988) *Proc. Natl. Acad. Sci. USA 85*, 3698-3702.

Zhou, Q., Lieberman, P. M., Boyer, T. G., & Berk, A. J. (1992) *Genes Dev. 6*, 1964-1974.

Zhou, Q., Boyer, T. G., & Berk, A. J. (1993) *Genes Dev. 7*, 180-187.

Zhu, H., Joliot, V., & Prywes, R. (1994) *J. Biol. Chem. 269*, 3489-3497.

Zwilling, S., Annweiler, A., & Wirth, T. (1994) *Nucleic Acids Res. 22*, 1655-1622.

CHAPTER I

INTRODUCTION

SECTION 2 FLUORESCENCE SPECTROSCOPY OF PROTEINS

Fluorescence spectroscopy has proven to be a powerful tool for studying the structure, dynamics, and interactions of proteins in solution (Badea and Brand, 1979; Lakowicz, 1983; Eftink, 1991). It can reveal a variety of molecular details of proteins, such as exposure of amino acid side chains, local pH, local potential, local viscosity and restraint of the fluorescence probe, different protein conformations, conformational flexibility, distance between sites on protein and interactions between protein and other macromolecules. This approach is highly sensitive and responsive to various molecular processes, thus it is distinctively useful in studies with protein.

Basic Principles Of Fluorescence (Lakowicz, 1983; Eftink, 1991)

Fluorescence is emitted light generated when a molecule relaxes from one electronic state to another state of lower energy. The absorption and emission of photons by a molecule is illustrated in Figure 1. This modified Jablonski diagram shows two electronic energy levels, the lower or ground state (G) and one higher or first excited state (S_1) and some of the vibration levels of each. The absorption of light into G results in an almost instaneous (~10^{-15} s) promotion to the excited state. This is followed by rapid internal conversion or vibrational relaxation (~10^{-12} s) to the lowest vibrational level of S_1. The excited molecule then returns

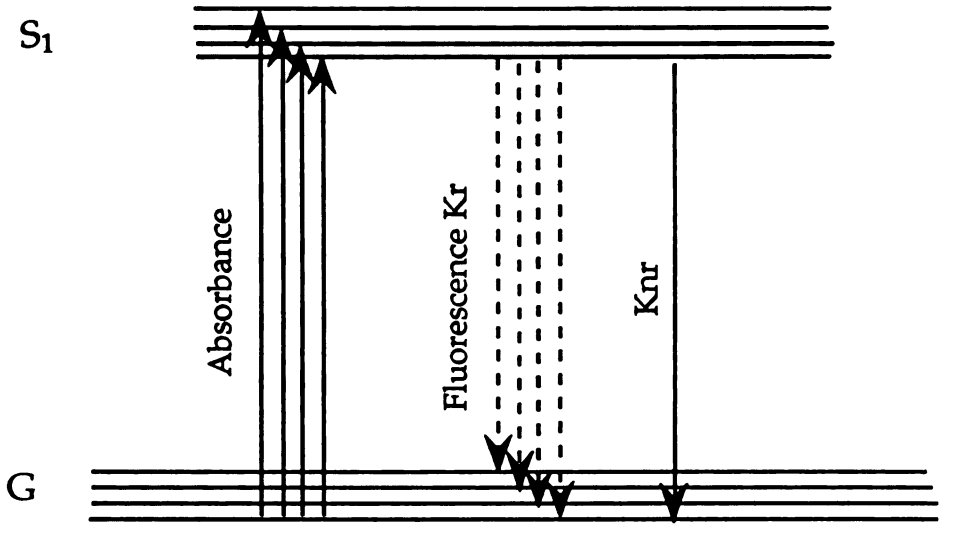

Figure 1. Modified Jablonski diagram. G and S_1 indicate the ground and first excited states, respectively.

to G either by radiative decay with rate constant k_r to produce fluorescence or by nonradiative transitions with the sum of rate constants Σk_{nr}. These nonradiative decay processes include radiationless relaxation, inter-system crossing, photochemical reactions, solute quenching and resonance energy transfer. The measured fluorescence properties of a molecule depend on the competition between the radiative decay process and the nonradiative decay processes. These fluorescence spectral properties are very responsive to changes in the environment of a fluorophore. This is the basis that fluorescence can reveal information on protein structure, dynamics, protein-ligand, protein-protein interaction. The important spectral parameters include excitation and emission spectra contour, emission maxima position, fluorescence lifetime, polarization properties and the responses of these parameters to various solution conditions.

The lifetime of the excited state is the average time the molecule remains in the excited state prior to return to the ground state. It is defined as:

$$\tau = \frac{1}{k_r + \Sigma k_{nr}} \qquad (1)$$

The quantum yield of a fluorophore is the ratio of the number of emitted to absorbed photons. It is defined as:

$$Q = \frac{K_r}{k_r + \Sigma k_{nr}} \qquad (2)$$

Instrumentation For Fluorescence Spectroscopy

Figure 2 is a schematic representation of a fluorimeter. The steady-state fluorimeter operates with a constant beam of light striking the sample and continuous emission collection. A high-pressure xenon arc lamp is used in these studies. The excitation light passes through a monochromator for wavelength selection. A beam splitter shunts some of the excitation light to a reference cell for ratio correction. Emission light is recorded at right angle to the incident beam. The fluorescence passes through a monochromator at which the emission wavelength is selected. A photomultiplier tube is used as the detector.

An emission spectrum is the wavelength distribution of the emission, measured with a single constant excitation wavelength. To collect an emission spectrum, a wavelength for excitation is selected and fixed with the excitation monochromator. Conversely, one can record an excitation spectrum by fixing the emission wavelength with the emission monochromator , and varying the excitation wavelength.

Adjustable polarizers can be placed both in the path of excitation light and the path of emission light. For fluorescence anisotropy measurements (illustrated in Figure 3), the sample is excited with vertically polarized light. The electric vector of the excitation is oriented parallel to the z axis. The intensities of emission (I_{vv} and I_{vh}) are measured through a polarizer. I_{vv} and I_{vh} are observed intensity when the observing polarizer is oriented parallel or perpendicular to the vertically polarized excitation, respectively.

Experiments described in this thesis employed a time-correlated single photon counting (TCSPC) fluorimeter to measure the time-resolved fluorescence (Lakowicz, 1983). In this method, the sample is excited with a brief pulse of light and the time between the pulse and the arrival of the first fluorescent photon to a

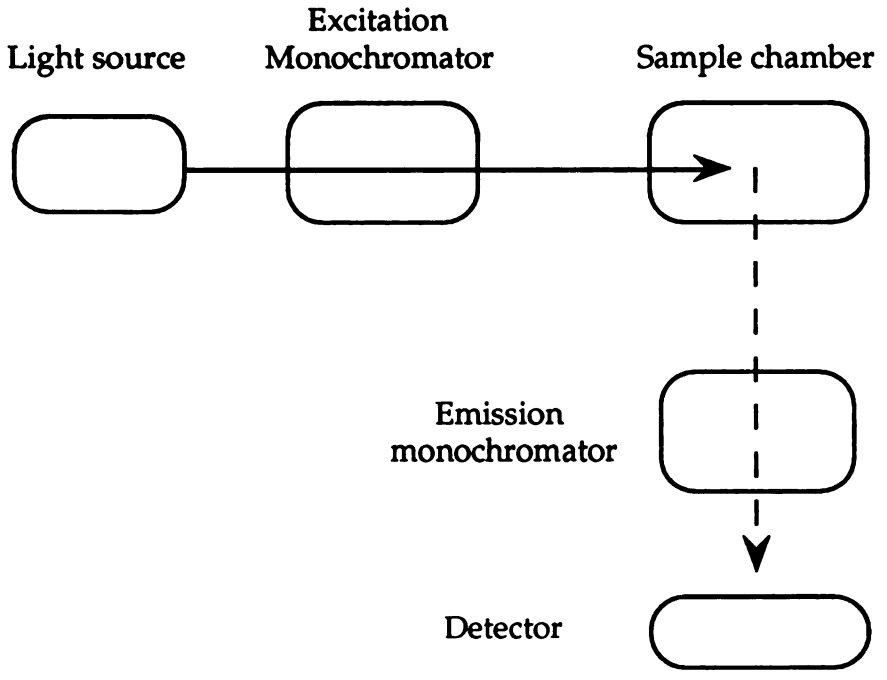

Figure 2. Schematic diagram of a spectrofluorimeter.

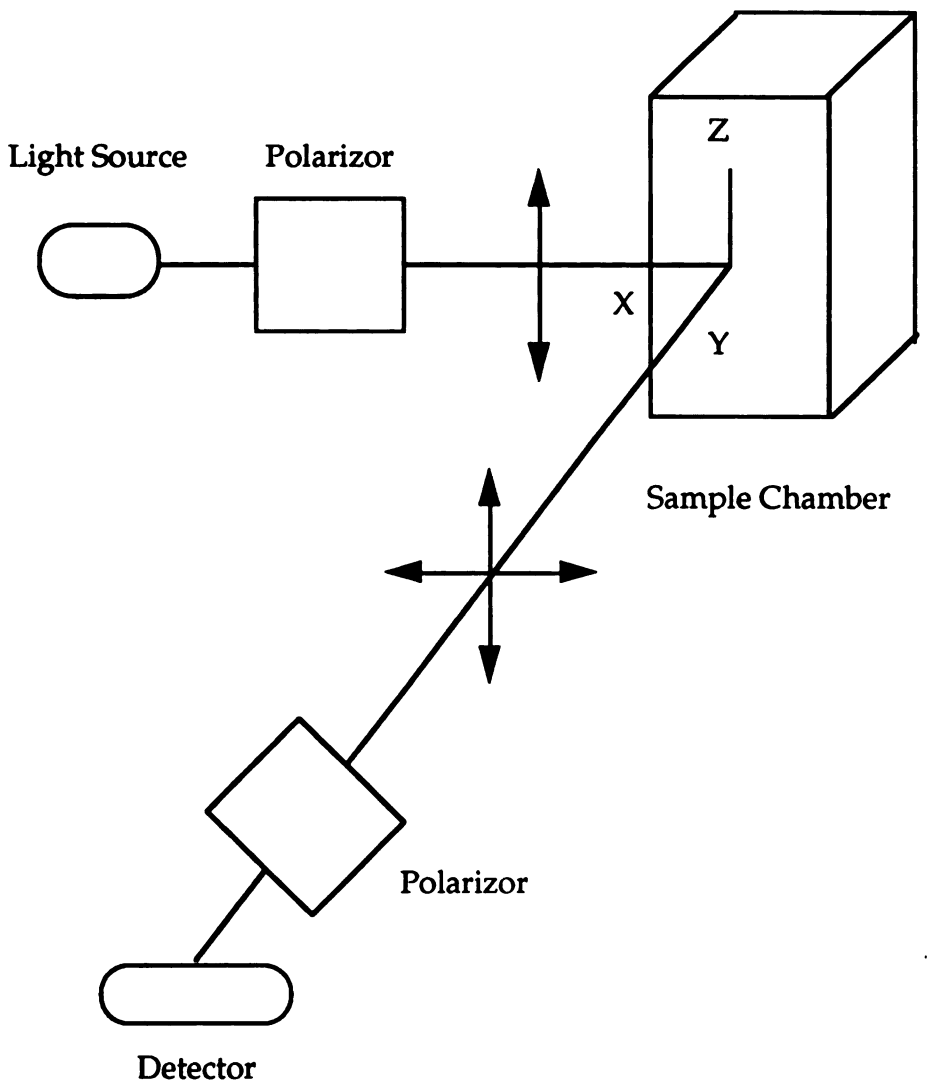

Figure 3. Schematic diagram of experimental arrangements for anisotropy measurement.

detector is recorded. Arrival times for a large number of photons are recorded and the distribution of the arrival times represent the decay curve. Individual fluorescence decay curves, instrument response curves corresponding to the various emission wavelengths monitored are analyzed simultaneously by the global analysis to obtain the decay parameters α_i and τ_i which will be described in detail in a following section (Knutson et al., 1983).

Intrinsic And Extrinsic Probes

Two types of fluorescence probes are used to study macromolecules, the intrinsic probes and the extrinsic probes. Intrinsic probes are contained in the macromolecules themselves while extrinsic probes are added fluorescent molecules which form covalent or noncovalent adducts with the macromolecules.

In proteins, phenylalanine, tyrosine and tryptophan are capable of contributing to its fluorescence. The intrinsic fluorescence of proteins is dominated by tryptophan fluorescence, because phenylalanine has a very low quantum yield and tyrosine fluorescence in proteins is frequently very weak. Tyrosine fluorescence can be quenched by the presence of a nearby carboxyl group or amino group, by energy transfer to the tryptophan, and by ionization of itself. Since tryptophan has higher extinction coefficient and its fluorescence properties are very sensitive to its environment, this residue is the most valuable intrinsic probe in proteins. Tryptophan can be selectively excited at wavelength above 295 nm.

Using site-directed mutagenesis techniques it is feasible to change the number and type of intrinsic probes found in a protein. One can replace the

or Tyr, or introduce single Trp residue into sites of interest, again typically replacing Try or Phe. These replacements involving Trp usually have no severe effect on the functions of the proteins. Thus, tryptophan fluorescence has wide applications in studies of proteins. In this study, we replaced a Trp residue in DNA binding domain of the chimeric protein and introduced Trp codons into the VP16 activation domain. These replacements did not cause major consequences on the protein activity.

In addition to these intrinsic probes, extrinsic fluorophores can be introduced into protein either by chemical coupling or by simple binding. The most commonly used extrinsic probes for proteins include 1-anilino-8-naphathalene sulfate (ANS), 1-dimethylaminonaphthalene-5-sulfonate (DNS), 2-p-toluidylnaphthalene-6-sulfonate (TNS), dansyl chloride, rhodamine and fluorescine. The extrinsic probes have the advantages that they can be used to study systems with no intrinsic fluorescence. In addition, one can choose appropriate probes to study a specific site in protein other than the aromatic amino acids, extending the range of what can be studied. Moreover, probes can be chosen to possess unique fluorescence properties which do not overlap with other molecules in the system. However, one must ensure that the addition of extrinsic probes do not affect the protein activity and the spectroscopy properties of the bound probes can be distinguished from those of the unbound probes.

Emission Spectra

The emission maximum of tryptophan will vary depending on the general solvent polarity and on specific interactions between the solvent and the indole ring. Therefore the emission maxima of proteins are dependent on the location of the tryptophan residues in the proteins. The fluorescence λ_{max} of free

tryptophan in aqueous solution is at 348 nm (Teale and Weber, 1957). Tryptophans in proteins exhibit a large range of emission maxima (Lakowicz, 1983). The fluorescence λ_{max} of the protein azurin (308 nm) is the most blue-shifted known for protein tryptophan, indicating a very nonpolar environment. X-ray crystallographic results showed that the single Trp in azurin is completely buried inside the protein, surrounded by alkyl side chains and having no hydrogen bonds. Ribonuclease T_1 also has a single buried Trp, and its emission spectrum is blue-shifted with the maximum at 324 nm. In contrast, proteins such as glucagon and adrenocorticotropin have fully solvent exposed Trp with emission maxima around 350 nm. Thus, emission spectra of proteins provide information about the exposure extent of the tryptophan residues. Emission spectral shifts can also indicate structural changes in proteins such as that caused by association with substrate, other proteins and membrane. For instance, the emission maximum of lysozyme shifts from 340 nm to 331 nm upon binding substrate (Lakowicz, 1983). This blue shift of emission maxima suggests shielding of the tryptophan from water.

Solute Quenching (Eftink and Ghiron, 1981)

Certain compounds when added to solution can quench fluorescence. There are two types of quenching, dynamic (collisional) quenching and static quenching. Dynamic quenching results from collisional encounters between the fluorophore and the quencher. The dynamic quenchers act by competing with the radiative process and decrease the lifetime of the fluorescence. Static quenching results from the formation of a nonfluorescent complex between the fluorophore and the quencher. The static quenchers act in a way that do not compete with the radiative process and no change in the fluorescence lifetime

occurs. Both dynamic and static quenching requires molecular contact between quencher and fluorophore. Solute quenching has been widely used to assess degrees of exposure of fluorophores in proteins. The commonly used quenchers include neutral quenchers (such as oxygen and acrylamide), anionic quenchers (such as iodide) and cationic quenchers (such as cesium ion). In addition to steric factors, charged quenchers are also affected by the electrostatic interaction between the quencher and the charges on the protein neighboring the tryptophan residues.

The pure dynamic quenching is described by the Stern-Volmer equation:

$$F_0/F = 1 + K_{sv}[Q] = 1 + k_q < \tau > [Q] \qquad (3)$$

where F_0 and F are the fluorescence intensity in the absence and presence of quencher, [Q] is the quencher concentration, K_{sv} is the Stern-Volmer dynamic quenching constant, k_q is the bimolecular collisional quenching constant, $< \tau >$ is the mean lifetime of the fluorophore before quenching. The Stern-Volmer plot (F_0/F vs. [Q]) is linear for pure dynamic quenching.

In the instance that fluorescence is quenched by both dynamic and static process, the Stern-Volmer plot is upward curved. A modified Stern-Volmer equation can describe this instance:

$$F_0/F = (1+K_{sv}[Q]) \exp(V[Q]) \qquad (4)$$

V is the static quenching constant, which can be interpreted as an association constant for a dark complex between the quencher and the fluorophore, or as a active volume element surrounding the fluorophore. In the latter interpretation,

instantaneous quenching occurs when the quencher happens to be within this volume at the time of excitation.

Equation 4 applies for systems having homogeneous emission (i.e., single fluorophore in one environment). If there is ground-state heterogeneity (i.e., the different tryptophanyl residues of the protein or the different environments of a single tryptophan) in the system, then more than one K_{sv} and V are needed. The appropriate form of the Stern-Volmer equation for the heterogenously emitting systems is:

$$F_0/F = \left(\Sigma \frac{f_i}{(1+K_{sv,i}[Q])\exp(V_i[Q])} \right)^{-1} \qquad (5)$$

where $K_{sv,i}$ and V_i are the dynamic and static quenching constants for fluorescent component i, and f_i is the fractional contribution of component i to the total fluorescence. For two emitting species, one of which is inaccessible to quencher, assuming no static quenching, the modified Stern-Volmer equation is:

$$F_0/F = \frac{1+K_a[Q]}{1+K_a(1-f_a)[Q]} \qquad (6)$$

where f_a is the fractional contribution of the fluorophores which are accessible to the quencher and K_a is the Stern-Volmer constant for the accessible fraction. The Stern-Volmer plot in such circumstance is downward curved.

Tryptophan residues in protein have a wide range of accessibility to quenchers, depending on how deeply the residue is located in the protein (Eftink, 1991). The buried tryptophans have the lowest values of quenching rate k_q. For example, the k_q values for acrylamide quenching of the buried Trps in apoazurin and ribonuclease T_1 are 0.05 $M^{-1}ns^{-1}$ and 0.17 $M^{-1}ns^{-1}$, respectively. Conversely,

exposed tryptophans in flexible polypeptides show largest k_q values, 3.2 and 3.5 $M^{-1}ns^{-1}$ for glucagon and adrenocorticotropin, by acrylamide quenching.

Solute quenching is very useful for monitoring protein conformation change (Eftink and Ghiron, 1976). Dissociation of tetrameric aldolase to monomer in low pH condition caused a extensive structural change throughout the protein, as suggested by the drastic increase of K_{sv} from 0.2 M^{-1} to 6.8 M^{-1}. This approach can also detect subtle conformational change. For example, binding of one competitive inhibitor to trypsin modestly decreased tryptophanyl exposure as suggested by decrease of K_{sv} from 2.8 M^{-1} to 2.0 M^{-1}.

Time-Resolved Intensity Decay (Beechem and Brand, 1985)

Steady-state fluorescence spectroscopy provides time-averaged information on diverse phenomena. Time-resolved fluorescence spectroscopy monitors events that occur during the lifetime of the excited state. It can reveal more detailed information about excited-state processes than can steady-state fluorescence measurements.

The fluorescence intensity of a population of excited fluorophore molecules is expected to decay in an exponential manner with time. With an infinitely short pulse of light, intensity decays as following:

$$I(\lambda,t) = I_0(\lambda) \exp(-t/\tau) \qquad (7)$$

where $I(\lambda,t)$ is the fluorescence intensity at time t and wavelength λ following excitation, $I_0(\lambda)$ is the intensity at t = 0 and wavelength λ, and τ is the fluorescence lifetime. If i species of unique fluorophores, or one fluorophore in i

unique environments, are present, then the decay is said to be heterogeneous or multi-exponential:

$$I(\lambda,t) = I_0(\lambda)\sum \alpha_i(\lambda) \exp(-t/\tau_i) \quad (8)$$

where τ_i is the emission wavelength independent decay time of the ith decay component and α_i is the preexponential term representing the fractional contribution to the time-resolved decay of the ith component.

A relationship exists between the steady-state spectrum and a time-resolved spectra (Knutson et al., 1982). This relationship can be used to extract i emission spectra associated with i individual decay time components, forming decay-associated spectra (DAS):

$$I_i(\lambda) = I_{ss}(\lambda)\,[\alpha_i(\lambda)\tau_i \,/\, \Sigma\alpha_i(\lambda)\tau_i] \quad (9)$$

where $I_i(\lambda)$ is the intensity spectrum (DAS) of the ith component, $I_{ss}(\lambda)$ is the intensity of the steady-state spectrum. The fractional intensity, $f_i(\lambda)$, of the ith component at wavelength λ is given by :

$$f_i(\lambda) = \alpha_i(\lambda)\tau_i \,/\, \Sigma\alpha_i(\lambda)\tau_i \quad (10)$$

The mean lifetime $\langle\tau\rangle$ is defined by:

$$\langle\tau\rangle = \Sigma\, \alpha_i\tau_i^2 \,/\, \Sigma\, \alpha_i\tau_i \quad (11)$$

The fluorescence of free tryptophan shows biexponential decay kinetics. The existence of different rotamers of tryptophan have been suggested for the

deviation from monoexponential decay behavior (Szabo and Rayner, 1980). The average lifetimes of tryptophan in proteins range from 1 to 7 nsec, depending on the protein and its tertiary structure. Most of the single tryptophan-containing proteins also show multiexponential decay (Beechem and Brand, 1985). In addition to the complex decay of a single tryptophan, single tryptophan residues in proteins may be subjected to multiple environments corresponding to the multiple conformational states of the protein. In this case, tryptophan in each conformation experiences a different environment and has a different decay time and spectrum. The individual lifetime τ_i reflects the different environment experienced in the conformation, and the amplitude α_i associated with the different lifetime components can be approximately proportional to the relative fractional populations of the various conformations.

DAS can be used roughly to "fingerprint' the protein structure. DAS can monitor whether changes such as truncation, point mutation, or ligand binding in a protein change the environment of the tryptophan. For example, the single-Trp-containing protein azurin in its copper-binding form shows a biexponential decay: a long-lived component of 4-5 ns and a short-lived component of 0.1-0.5 ns. However, the apoazurin only shows monoexponential decay kinetics. The addition of copper creates a microheterogenous environment for the tryptophan. The two lifetimes have been suggested may originate from two conformers of the copper binding sites which interact differently with Trp residue (Szabo et al., 1983). Another example is seen in the structural perturbation effect on the conformation of the parathyroid hormone (Willis and Szabo, 1992). This hormone has a single Trp at position 23. DAS were measured for the intact hormone and the deletion mutant which retains amino acids 1-34. DAS parameters of both protein are closely similar, suggesting that truncation has no significant effect on the structure or environment in the region of Trp-23.

Steady-State Anisotropy And Time-Resolved Anisotropy Decay (Lakowicz, 1983; Bucci and Steiner, 1988)

When a solution of fluorophore is excited with plane polarized light, only those fluorophores whose transition moment is parallel to the plane of polarization will be excited. If emission occurs before significant molecular motion, the fluorescence will also be polarized. Conversely, rotational diffusions before emission will lead to loss of the ordered orientation of the excited molecules (i.e., the loss of the anisotropic distribution of states) and the emission will be only partially polarized. By monitoring the emission that occurs parallel, I_{vv}, and perpendicular, I_{vh}, to the vertically polarized excitation light, one can measure the anisotropy, r, of the emission:

$$r = (I_{vv} - I_{vh}) / (I_{vv} + 2I_{vh}) \qquad (12)$$

Rotational diffusion of fluorophores is a dominant cause of fluorescence depolarization. For an isotropically rotating sphere with a rigidly fixed fluorophore, the steady-state anisotropy is related to the fluorescence lifetime, τ, and the rotational correlation time, ϕ, by the Perrin equation:

$$r = \frac{r_0(app)}{1+(\tau / \phi)} \qquad (13)$$

where $r_0(app)$ is the apparent limiting anisotropy in the absence of motion or energy transfer. The value of ϕ is governed by the viscosity (η) and temperature (T) of the solution and by the effective hydrodynamic molar volume of the rotating unit (V):

$$\phi = \frac{\eta V}{RT} \tag{14}$$

where R is the gas constant. The parameter V is related to the molecular weight (M) and the hydration of the molecule (h) by:

$$V = M\,(v + h) \tag{15}$$

where v is the partial specific volume of the molecule.

Measurements of fluorescence anisotropy have been widely used to quantify association reactions between biological molecules, such as protein-protein association (Lakowitz, 1983). As an example, I will describe the interaction studied in this work: association between 5-OH-Trp incorporated GAL4-VP16 (V) and TBP (T). The fluorophore (5-OH-Trp) can exist in either the free form (V) or in the bound form (V-T complex). The fluorescence anisotropy measured, r, when both forms are present is given by:

$$r = f_F r_F + f_B r_B = (1-f_B) r_F + f_B r_B \tag{16}$$

where r_B and r_F are the anisotropy of the free and bound fluorophores, and f_B and f_F refer to the fraction of the total fluorophore which is present in the bound and free forms. Considering the intensity change of the fluorophore upon binding:

$$r = \frac{r_B f_B I_B + r_F (1 - f_B) I_F}{f_B I_B + (1 - f_B) I_F} \tag{17}$$

where I_B and I_F are the fluorescence intensities of the fluorophore in bound or free forms. Assume GAL4-VP16 (V) and TBP (T) form a 1: 1 binary complex:

$$V + T \Leftrightarrow [V\text{-}T] \tag{18}$$

The dissociation constant for this interaction, K_D, is given by:

$$K_D = \frac{[V][T]}{[V\text{-}T]} \tag{19}$$

and the fraction of the fluorophore in the bound form is given by:

$$f_B = \frac{([V]_0 + [T] + K_D) - \sqrt{([V]_0) + [T] + K_D)^2 - 4[V]_0[T]}}{2[V]_0} \tag{20}$$

where $[V]_0 = [V] + [V\text{-}T]$ is the total concentration of the 5-OH-Trp incorporated GAL4-VP16 used in the study and [T] is the concentration of the added TBP. K_D can be determined by fitting experimental data to equations 17 and 20.

The time dependence of the anisotropy r(t) for a fluorophore rigidly attached to a spherical macromolecule is a single exponential:

$$r(t) = r_0(app) \exp(-t/\phi) \tag{21}$$

If a fluorophore is rigidly attached to an asymmetric structure, the anisotropy decay is more complex. More importantly, for many biopolymer systems, some form of internal motion is present, so that another rotational motion is superimposed upon that of the entire macromolecule. Consequently, protein anisotropy decay kinetics are usually double (or triple) exponential:

$$r(t) = r_0(app)\Sigma\, \beta_j \exp(-t/\phi_j) \tag{22}$$

where ϕ_j is the rotational correlation time of the jth component and β_j is its preexponential term. There are three types of possible internal rotations: (1) rotation of the tryptophan about the bond linking it to the protein; (2) rotational wobble of a segment of the protein associated with the tryptophan; (3) rotation of a molecular domain as a unit about a flexible hinge point. If one assumes the internal motion in terms of the probe wobbling within a cone, with the protein rotating isotropically, then the anisotropy decay is given by the following expression:

$$r(t) = \beta_1 \exp[-t(\phi_m^{-1} + \phi_i^{-1})] + \beta_2 \exp(-t\phi_m^{-1}) \tag{23}$$

when $\phi_m \gg \phi_i$, $\phi_m^{-1} + \phi_i^{-1} \approx \phi_i^{-1}$

$$r(t) = \beta_1 \exp(-t\phi_i^{-1}) + \beta_2 \exp(-t\phi_m^{-1}) \tag{24}$$

where ϕ_m and ϕ_i are the rotational correlation time corresponding to the global rotational motion of the protein and the effective correlation time of the internal motion. β_1 and β_2 are the contribution of the internal motion and the global motion, respectively. This equation has been widely used to describe the protein anisotropy decay when more than one rotational decay mode is present. The cone semiangle, Θ, of the cone within which the fluorophore wobbles is given by:

$$\frac{\beta_2}{r_0} = \left[\frac{1}{2}(\cos\Theta)(1+\cos\Theta)\right]^2 \tag{25}$$

The magnitude of this cone semiangle provides an index of the extensiveness of the wobbling motion.

The motions of tryptophan in proteins vary greatly. The single Trp in ribonuclease T_1 (James et al., 1985; Chen et al., 1987) and in nuclease B (Munro, et al., 1979) are examples of tryptophans with little independent rotational freedom. These two tryptophans only rotate with the protein as a whole, as indicated by monoexponential anisotropy decay fit. The recovered correlation time in both cases are comparable to that predicted for global rotation of the proteins. Conversely, the single Trp in the flexible polypeptides adrenocortiocotropin (Ross et al., 1981), glucagon (Tran et al., 1982), and apolipoprotein (Joans et al., 1982) demonstrate independent rotation. In these proteins, anisotropy decays were well represented as two or three exponentials. The subnanosecond short rotational correlation time was attributed to the localized motion of the Trp.

Time-resolved anisotropy decay can detect protein conformational changes caused by different solution conditions (pH, ionic strength, temperature, etc.) or by association reactions. The single Trp in human serum albumin at 8°C only showed a single rotational correlation time representing rotation of the entire protein (Munro et al., 1979). However, this Trp showed two rotational correlation times at 43°C. The appearance of the subnanosecond short time representing localized Trp motion indicates that at 43°C this protein exists in a conformation where the local mobility of the single Trp is significantly increased. Another example is the monomer $\Leftrightarrow$ tetramer equilibrium of melittin (Lakowicz et al., 1987). Melittin, the major component of bee venom, is monomeric in 0.01 M Tris. The monomeric protein has little three-dimensional structure and behaves as a flexible coil. Its anisotropy decay was best fit to two correlation times. Almost 60% of the anisotropy decay was associate with the rapid rotation

mode, with a correlation time of 160 ps. The remainder decay was associated with a correlation time of 1.7 ns. In the presence of 2 M NaCl, the flexible melittin monomer folds into α-helix and a tetramer is formed (Terwilliger and Eisenberg, 1982). Under this condition, the anisotropy decay was also biexponential. However, two-thirds of the decay was now dominated by the slow rotation mode. The long correlation time is 3.5 ns, larger than that of the monomer. These results are consistent with the larger size and globular-like structure of tetramer.

The molecular motion elucidated by time-resolved anisotropy decay may directly connect to biological function of proteins. Anisotropy decay played an important role in revealing the correlation between molecular dynamics and flexibility in immunoglobulins. More importantly, functional relevance of the internal flexibility of immunoglobulin has been suggested (Oi et al., 1984). The ability of different classes of antibodies to fix complement are directly proportional to their segmental flexibility. The extent of segmental flexibility and the capacity to fix complement were greatest for IgG2b, intermediate for IgG2a, and least for IgG1 and IgE. The data strongly suggest that biological function of immunoglobulins are partially controlled by the segmental mobility of the Fab arms.

Tryptophan Analogs As Intrinsic Probes

Incorporation of unusual Trp analogs into proteins was initially used to study the effect of specific amino acids on enzyme activity (Pardee et al., 1956; Schlesinger, 1968). Large effects on the absorption and fluorescence properties of these analog-incorporated enzymes were observed (Schlesinger, 1968). The use of incorporated Trp analogs to study protein structure, dynamics and function

with modern fluorescence techniques was later suggested (Hudson et al., 1986). After the first report of site-specific incorporation of Trp analog 5-hydroxy-tryptophan (5HW) in place of Trp in an E. coli expression system (Hogue et al., 1992), several groups have incorporated Trp analogs 5HW and 7-aza-tryptophan (7AW) into different proteins (Ross et al., 1992; Lau et al., 1993; Heyduk et al., 1993; Hogue, 1994; Sato et al., 1994).

There are many advantages of using the Trp analogs (5HW and 7AW, shown in Figure 4) as intrinsic fluorescence probes. First, both analogs have red shifted absorbancies, compared to Trp (Hogue and Szabo, 1993). One can selectively excite either analog (at excitation wavelength ≥ 310 nm) in the presence of Trp-containing proteins or DNA. This enables the utility of fluorescence spectroscopy to study protein-protein or protein-DNA interaction. In one study, fluorescence analysis of the interaction between 5HW-incorporated oncomodulin and anti-oncomodulin antibody provided information about complex formation and epitope identification that could not be obtained with the natural amino acid (Hogue et al., 1992). In the study of binding between 5HW-incorporated bacteriophage λ *c*I repressor and DNA, important oligomeric states of the protein were revealed (Sato et al., 1994). Second, these analogs can be readily and specifically incorporated into proteins. By using Trp auxotrophic E. coli strain and with the separation of protein synthesis from cell growth, these two analogs have been successfully incorporated into several proteins. Using a linear combination of spectra analysis, the incorporation efficiency of 5HW into λ *c*I repressor is estimated to be 95% (Ross et al., 1992). Third, these analogs are generally nondisruptive in their effects on protein structure and function. For example, functional properties and structural properties of 5HW incorporated λ *c*I repressor are indistinguishable from those of the native repressor (Ross et al., 1992).

Tryptophan

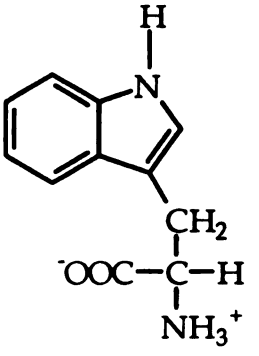

5-hydroxytryptophan

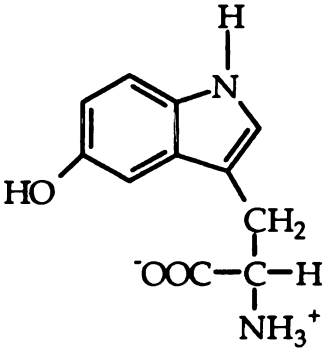

7-azatryptophan

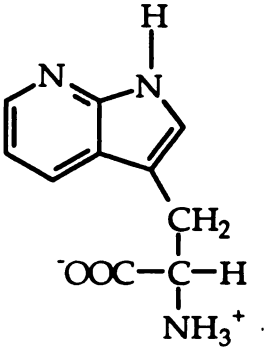

Figure 4. Structure of tryptophan and two tryptophan analogs 5HW and 7AW.

In addition to the above advantages, these analogs have special photophysical features compared to Trp and thus provide unique utility for protein fluorescence study. 7AW is an extremely sensitive probe of environment. Fluorescence properties of the parent fluorophore, 7azaindole (7AI), are dramatically different in different solvent (Chapman and Maroncelli). 7AI undergoes tautomerizations induced by solvent hydroxyl groups as found in water and alcohols (shown in Figure 5). In aprotic solvents such as acetonitrile, emission maximum of 7AI is at 362 nm and quantum yield is 0.38. In water, emission maximum is at 402 nm and quantum yield is very low (0.032). In alcohols, 7AI showed two populations of fluorescence, neither of which is efficient. These two fluorescence populations were attributed to normal 7AI and tautomer 7AI. When 7AW is incorporated into protein, the characteristics of the emission spectra are directly connected with the polarity of the environment of the probe. Emission of 7AW in alkaline phosphatase is intense and has the emission maximum at 370 nm, suggesting a hydrophobic environment (Schlesinger, 1968). Upon denaturation, the 7AW fluorescence dramatically decreased and red-shifted. 7AW in tryptophanyl-tRNA synthetase also showed intense, blue-shifted (λ_{max} = 350 nm) fluorescence (Hogue, 1994), indicating buried nature of this residue. In contrast, 7AW incorporated into GAL4-VP16 in this study has emission maxima at 396 nm, suggesting that these residues are solvent exposed. Thus, 7AW is a very sensitive environment indicator and can be used to monitor protein-folding, conformational change, protein-ligand and protein-protein interaction.

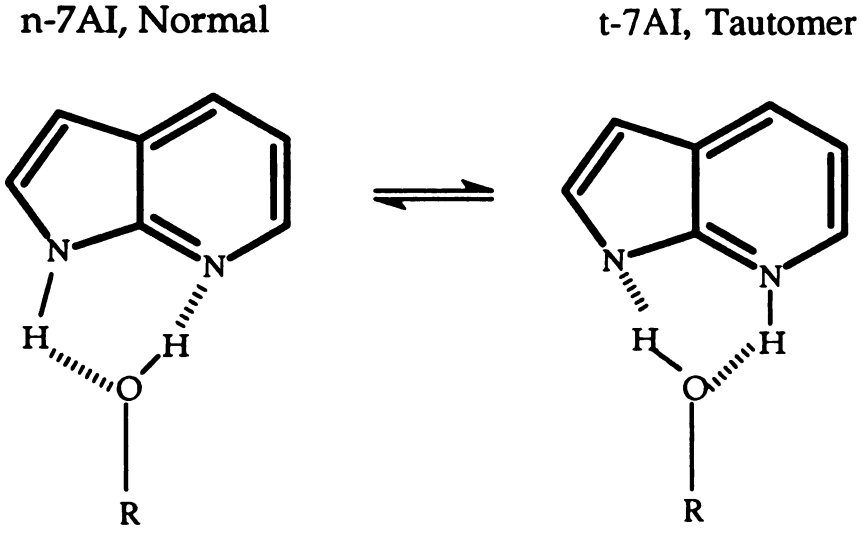

Figure 5. Tautomerization reactions of 7AI in protic solvents such as water or alcohols.

Fluorescence Approaches To Transcriptional Regulation

Transcriptional regulators participate in a large number of protein-DNA and protein-protein interactions. Various fluorescence approaches have been adopted to study the stoichiometries and binding affinities of these interactions, to analyze dynamics of these multimacromolecular assembly and to monitor structural changes in the transcriptional regulation process.

Fluorescence emission spectra is very sensitive to conformational changes in protein. For example, conformational changes in transcription factor Jun/Fos dimer, induced by DNA binding, were detected by monitoring the emission intensity change of extrinsically labeled Jun (Patel et al., 1990). Tryptophan fluorescence emission has also been used to probe the structural differences between wild-type and mutant homeodomains (Shang et al., 1994).

Several groups have applied fluorescence anisotropy to study the binding between transcriptional regulators and DNA. In these studies, researchers labeled DNA fragments containing binding sites for transcription factors with extrinsic fluorescence probes and then monitored changes in fluorescence anisotropy of the labeled DNA when bound to protein. For example, LeTilly and Royer (1993) studied binding of *trp* repressor (TR) of E. coli to a fluorescently labeled oligonucleotide containing the *trp* operator sequence. Binding profiles under different concentrations of corepressor, operator DNA and protein suggested that TR could interact with DNA in different modes, having different protein/DNA stoichiometries. Other examples of such studies include binding between the E. coli *lac* promoter and cAMP receptor protein (CRP), binding between TBP and TATA box, and interactions between glucocorticoid receptor DNA binding domain and a variety of DNA targets (Heyduk and Lee, 1990; Perez-Howard et al., 1995; Hill and Royer, 1995).

The solution-based methodology described above is sensitive, rapid and reliable. Protein-nucleic acid interaction can be characterized under different solution conditions such as pH, temperature, effector ligand and other proteins. Several investigators have extracted information other than protein-DNA interaction from this kind of analyses. Using this fluorescence anisotropy technique, Heyduk et al. (1993) showed that E. coli catabolite gene activator protein (CAP) interacted with RNA polymerase in solution in the absence of promoter DNA. However, a CAP mutant defective in transcription activation was found not capable of interacting with RNA polymerase. In another similar study, the equilibrium binding constant between transcription factor CREB and nuclear protein CBP was determined (Kwok et al., 1994).

In addition to using the extrinsically labeled DNA in the anisotropy studies, intrinsic tryptophan fluorescence anisotropy can be used to study oligomerization states of transcription factors in solution. Interactions between *trp* repressor dimers as a function of solution conditions have been investigated (Martin and Royer, 1994). The oligomerization of TBP in solution has also been reported (Perez-Howard et al., 1995).

Another fluorescence technique, resonance energy transfer measurement, can be used to map distances between sites in macromolecular assemblies and to monitor the thermodynamics and kinetics of protein-protein and protein-DNA interaction in solution. Resonance energy transfer describes the event that under certain circumstances energy absorbed by one molecule (donor) can be transferred to another fluorophore (acceptor) at some distance away. The efficiency of transfer is a function of the separation of the fluorophores and therefore can be used to measure molecular distance. The efficiency of transfer can be experimentally determined by measuring the emission of the donor or acceptor. Using this technique, a 3Å reduction between the fluorophores placed

on Jun and Fos upon DNA binding was detected (Patel et al., 1994). In addition, binding affinity of the Jun-Fos interaction was determined, and the kinetics of dimerization and DNA binding as well as the rate of subunit exchange were examined.

Time-resolved and stopped-flow fluorescence studies may be very informative in studying the spatially and temporally regulated interactions in transcription processes. For instance, DNA, protein, or nucleotide could be labeled with different types of probes, and then various time-resolved and kinetic fluorescence techniques could be used to monitor different events in transcription (such as DNA-protein interaction, DNA bending transition, transcription bubble formation and mRNA synthesis) in real-time scale (Beechem, 1994).

The great potential offered by Trp analogs as intrinsic probes has also be explored to study transcription regulation. 5HW-incorporated λ *c*I repressor protein has been very useful in studies of λ *c*I repressor-operator interactions including the demonstration of important oligomeric states of the λ *c*I repressor (Ross et al., 1992; Sato et al., 1994). In another study, 5HW was incorporated into cAMP receptor protein and the α and β subunits of E. coli RNA polymerase with the aim to investigate activator-polymerase interaction (Heyduk et al., 1993).

Most of the studies employing fluorescence techniques in transcription regulation focus on DNA binding aspects of transcription factors. Applying various fluorescence approaches to characterize structural features of activation domain (or repression domain) of transcription activators (or repressors), to study the dynamics of multicomponent transcription machinery will be very informative. Knowledge gained from these studies will be essential for a full appreciation of the mechanisms of transcriptional regulation.

REFERENCES

Beechem, J. M., & Brand, L. (1985) *Ann. Rev. Biochem. 54*, 43-71.

Beechem, J. M. (1994) *Biophys. J. 66(2)*, A233.

Bucci, E., & Steiner, R. F. (1988) *Biophys. Chem. 30*, 199-224.

Chapman, C. F., & Maroncelli, M. (1992) *J. Phys. Chem. 96*, 8430.

Chen, L. X-Q., Longworth, J. W., & Fleming, G. R. (1987) *Biophys. J. 51*, 865-873.

Eftink, M. R., & Ghiron, C. A. (1976) *Biochemistry 15*, 672-680.

Eftink, M. R., & Ghiron, C. A. (1981) *Anal. Biochem. 114*, 199-227.

Eftink, M. R. (1991) In *Protein Structure Determination*, Suelter, C. H. Eds., John Wiley & Sons, Inc., pp. 127-206.

Heyduk, T., & Lee, J. C. (1990) *Proc. Natl. Acad. Sci. USA 87*, 1744-1748.

Heyduk, E., & Heyduk, T. (1993) *Cellular and Molecular Biology Research 39*, 401-407.

Heyduk, T., Lee, J. C., Ebright, Y-H. W., Blatter, E. E., Zhou, Y., & Ebright, R. H. (1993) *Nature 364*, 548-549.

Hill, J. J., & Royer, C. A. (1995) *Biophys. J. 68(2)*, A223.

Hogue, C. W. V., Rasquinha, I., Szabo, A. G., & MacManus, J. P. (1992) *FEBS Lett. 310*, 269-272.

Hogue, C. W. V., & Szabo, A. G. (1993) *Biophys. Chem. 48*, 159-169.

Hogue, C. W. V. (1994) Ph. D. thesis. University of Ottawa, Canada.

Hudson, B. S., Harris, D. L., Ludescher, R. D., Ruggiero, A., Cooney-Freed, A., & Cavalier, S. (1986) Fluorescence Probe Studies of proteins and membranes. In *Application of Fluorescence in the Biochemical Sciences*, D. L. Taylor et al., Eds., A. R. Liss Inc., New York, pp. 159-202.

James, D. R., Demmer, D. R., Steer, R. P., & Verrall, R. E. (1985) *Biochemistry 24*, 5517-5526.

Jonas, A., Privat, J., Wahl, P., Osborne, J. C. Jr. (1982) *Biochemistry 21*, 6205-6211.

Kinosta, K., Kawato, S. & Ikegami. (1977) *Biophys. J. 20*, 289-305.

Knutson, J. R., Walbridge, D. G., & Brand, L. (1982) *Biochemistry 21*, 4671-4679.

Knutson, J. R., Beechem, J. M., & Brand, L. (1983) *Chem. Phys. Lett. 102*, 501-507.

Kwok, R. P. S., Lundblad, J. R., Chrivia, J. C., Richards, J. P., Bächinger, H. P., Brennan, R. G., Roberts, S. G. E., Green, M. R., & Goodman, R. H. (1994) *Nature* 370, 223-226.

Lakowicz, J. R. (1983) In *Principles of Fluorescence Spectroscopy*, Plenum Press, pp 145-150.

Lakowicz, J. R., Cherek, H., Gryczynski., Joshi, N., & Johnson, M. L. (1987) *Biophys. J. 51*, 755.

Laue, T. M., Snear, D. F., & Ross, J. B. A. (1993) *Biochemistry 32*, 2469-2472.

LeTilly, V., & Royer, C. A. (1993) *Biochemistry 32*, 7753-7758.

Martin, K. S., & Royer, C. A. (1994) *Biophys. J. 66(2)*, A. 358.

Munro, L., Pecht, I., & Stryer, L. (1979) *Proc. Natl. Acad. Sci. USA 76*, 56-60.

Oi, V. T., Vuong, T. M., Hardy, R., Reidler, J., Dangl, J., Herzenberg, L. A., & Stryer, L. (1984) *Nature 307*, 136-140.

Pardee, A. B., Shore, V. G., & Prestidge, L. S. (1956) *Biochim. Biophys. Acta 21*, 406-407.

Patel, L. R., Abate, C., & Curran, T. (1990) *Nature 347*, 572-575.

Patel, L. R., Curran, T., & Kerppola, T. K. (1994) *Proc. Natl. Acad. Sci. USA 91*, 7360-7364.

Perez-Howard, G. M., Poon, D., Weil, P. A., & Beechem, J. M. (1995) *Biophys. J. 68(2)*, A295.

Ross, J. B., Rousslang, K. W., & Brand, L. (1981) *Biochemistry 20*, 4361-4369.

Ross, J. B. A., Senear, D. F., Waxman, E., Kombo, B. B., Rusinova, E., Huang, Y. T., Laws, W. R., & Hasselbacher, C. (1992) *Proc. Natl. Acad. Sci. USA 89*, 12023-12027.

Sato, A., Bitten, E., Lambert, D., & Rousslang, K. (1994) *SPIE Procedings 2137*, 343-352.

Schlesinger, S. (1968) *J. Biol. Chem. 243*, 3877-3883.

Shang, Z-G., Isaac, V. E., Li, H-C., Patel, L., Catron, K. M., Curran, T., Montelione, G. T., & Abate, C. (1994) *Proc. Natl. Acad. Sci. USA 91*, 8373-8377.

Szabo, A. G., Stepanik., T. M., Wayner, D. M., & Young, N. M. (1983) *Biophys. J. 411*, 233-244.

Szabo, A. G., & Rayer, D. M. (1980) *J. Am. Chem. Soc. 102*, 554-563.

Teale, F. W. J., & Weber, G. (1957) *Biochem. J. 65*, 476-482.

Terwilliger, T., & Eisengerg, D. (1982) *J. Biol. Chem. 257*, 6016-6022.

Tran, C. D., Beddard, G. S., & Osborne, A. D. (1982) *Biochim. Biophys. Acta 709*, 256-264.

Willis, K. J., & Szabo, A. G. (1992) *Biochemistry 31*, 8924-8931.

INT

spe
the
"dc
dis
del
doı
sev
in t
ricl
cor
hav
acti

effe
stu
acti
mo
wa

CHAPTER II

SATURATION MUTATIONAL STUDY OF THE CRITICAL PHE-442 IN THE VP16 TRANSCRIPTIONAL ACTIVATION DOMAIN

INTRODUCTION

Transcriptional activators are the class of proteins which bind to gene specific regulatory sequences and increase the rate of transcription. Following the cloning of many transcriptional activator proteins, deletion analysis and "domain-swap" experiments have shown that activators usually have several distinct functional domains. One domain, usually a DNA binding domain, delivers the activator to the gene specific regulatory sequence while the other domain mediates transcriptional activation. In contrast to the well defined several classes of DNA binding domains, there are no clear sequence homologies in the activation domains of activator proteins (Mitchell and Tjian, 1989). The richness of certain types of amino acids in the activation domains has led to the conventional amino acid composition-based classification of activators. They have been broadly classified into acidic, glutamine-rich and proline-rich activators.

Acidic activation domains (AAD), being among the most prevalent and effective activators, have been the major focus of transcriptional activation studies. Two models were previously proposed for the structure of acidic activation domains. One model, dubbed the "acid blob" or "negative noodle" model by Sigler, proposed that AADs acted as random coils; net negative charge was the sole determinant of activity and a specific secondary structure was not a

critical requirement for its function (Sigler, 1988). This model was mainly based on the following lines of evidence. First, progressive deletion of the AAD of the yeast activator GCN4 resulted in progressive loss of transcriptional activity and a general correlation between transcriptional activity and net negative charge was observed (Hope et al., 1988). There was no sudden complete loss in activity as might be expected if the activation function resided in a globular protein. In the second set of experiments, the acidic activation region I of the yeast activator GAL4 was subjected to chemical mutagenesis (Gill and Ptashne, 1987). Interestingly, mutants with increased activity were all invariably found to have gained negative charge while some mutants with decreased activity were associated with decreased acidity. Thirdly, E. coli genomic DNA fragments were fused to the GAL4 DNA binding domain and the resulted chimeric proteins which could activate transcription were all found to have a net negative charge. Among these so called 'activating sequences', the least active members had less negative charge (Ma and Ptashne, 1987).

In the second model regarding the structure of AAD, an acidic activation domain was modeled as an amphipathic α–helix (AAH), with the acidic residues forming one face of the helix and the hydrophobic residues forming the other. Standard computer algorithms predicted that many AADs, including that of VP16 and GCN4, have the potential to form AAHs (Zhu et al. 1990; Hope et al., 1988). Experimental evidence supporting this model came from the differential activities of two synthetic peptides which contain the same amino acids but in a different order such that only one of the two peptides could potentially form an amphipathic α–helix (Giniger and Ptashne, 1987). When each of these peptides was linked to the DNA-binding domain of GAL4, only the AAH-forming peptide could activate transcription.

As a model system for transcription activation, our lab studies the herpesvirus activator VP16. Deletion analysis defined the carboxyl terminal 78 aa as the activation domain of VP16 (Triezenberg et al., 1988). This domain is the prototype AAD. It is rich in acidic amino acids; 21 acidic residues are found in the 78 aa activation domain (Figure 1). This AAD comprises two subdomains, namely, the N-subdomain (413-456 aa) and the C-subdomain (453-490 aa) (Seipel et al., 1992; Regier et al., 1993). Each subdomain has roughly half the activation strength of the full-length activation domain. As one of the most potent activation domains yet identified, a great deal about the eukaryotic transcriptional activation should be learned from detailed studies of the VP16 AAD (Sadowski et al., 1988).

To test the two proposed models regarding the structure of AADs (i.e. the "acid blob" model and the amphipathic α–helix model), Cress and Triezenberg (1991) performed elaborate mutational analysis of the VP16 AAD N-subdomain. This study showed that the key aspects of both models were inadequate for VP16. To test the "acid blob" model, the acidic amino acids in the VP16 AAD, in various combinations, were replaced by their neutral counterparts (i.e., glutamine for glutamic acid, or asparagine for asparatic acid). In general, replacement of an increasing number of acidic residues led to a progressive decrease in transcriptional activation. However, the correlation between activity and acidity is only general but not strict. In some cases, VP16 derivatives with different combination of changes but identical net charge had dramatically different activities, suggesting that negative charge alone was not sufficient for activation and some structural elements were important for its function.

To test the amphipathic α–helix model, two sets of VP16 AAD mutants aimed at two aspects of the model were constructed. In the set of mutants designed to test the predicted amphipathy, groups of four negative residues

L S T A P P T **D** V S L G **D** **E**
CTG TCG ACG GCC CCC CCG ACC GAT GTC AGC CTG GGG GAC GAG
410 420

L H L **D** G **E** **D** V A M A H A **D**
CTC CAC TTA GAC GGC GAG GAC GTG GCG ATG GCG CAT GCC GAC
430

A L **D** **D** F **D** L **D** M L G **D** G **D**
GCG CTA GAC GAT TTC GAT CTG GAC ATG TTG GGG GAC GGG GAT
440 442 450

S P G P G F T P H **D** S A P Y
TCC CCG GGT CCG GGA TTT ACC CCC CAC GAC TCC GCC CCC TAC
460
Δ456

G A L **D** M A **D** F **E** F **E** Q M F
GGC GCT CTG GAT ATG GCC GAC TTC GAG TTT GAG CAG ATG TTT
470

T **D** A L G I **D** **E** Y G G END
ACC GAT GCC CTT GGA ATT GAC GAG TAC GGT GGG TAG
480 490

Figure 1. Nucleotide and deduced amino acid sequences of the VP16 transcriptional activation domain (codons 410-490 aa). The truncated VP16 activation domain (410-456 aa) is indicated. Acidic amino acids are in bold letters and the phenylalanine at position 442 is underlined.

were changed to their neutral counterparts in a circularly permuted manner around the predicted helix in VP16 AAD. If the AAH model were correct, then altering negative residues in the center of the charged face of the helix should be more detrimental to transcription activity, whereas, removal of negative residues at the periphery of the charged face would have a weaker effect. However, no correlation was observed between amphipathy and activity. The second set of mutants were designed to test whether this activation domain could form an α–helix. The α–helix incompatible amino acid proline were inserted in several locations along the predicted helix. Substitution of proline at position 425 had no effect on its activity; moreover, simultaneous substitution of two prolines in the region with the strongest predicted helix-forming tendency (at positions 432 and 436) also had no effect on activity. Together, these results argued against the amphipathic α–helix model.

In addition to rebuttal of the two earlier models, the study of Cress and Triezenberg (1991) discovered critical elements for VP16 AAD and raised new hypotheses. In the course of testing the helix-forming tendency of the VP16 AAD, Pro substitution of Phe at 442 abolished its activity. However, this diminished activity was not due to a disrupted helix, as substitution of Phe-442 with helix compatible residues Ala or Ser also abolished its activity. Interestingly, substitution with another aromatic residue Tyr restored activity to about one-third of wild type activity, suggesting that aromaticity at this position was important for the activity of VP16 AAD. Illuminated by the importance of bulky hydrophobic amino acid in the VP16 AAD, Cress and Triezenberg subsequently aligned the sequences of many activation domains, using the six bulky hydrophobic residues of the VP16 AAD as a guide. An interesting pattern of bulky hydrophobic residues flanking carbonyl-containing amino acids, similar

to the sequence surrounding the Phe-442 of VP16, was observed among the sequences of several activation domains from different classes.

In previous work, Cress and Triezenberg (1991) discovered the importance of the phenylalanine at position 442 of VP16 AAD and their results suggested the importance of aromaticity at that position. Below, I will describe the saturation mutagenesis analysis of the Phe-442 which I undertook to thoroughly examine the amino acid requirement at this critical position.

EXPERIMENTAL PROCEDURES

Oligonucleotide-Directed Mutagenesis

A SalI/BamHI fragment corresponding to the truncated VP16 activation domain (codons 411-456, with point mutation Ser (TCC) instead of Phe (TTC) at position 442) was cloned into M13mp19 (Norrander et al., 1983). Single-stranded uracil-containing template DNA was further prepared and purified(Kunkel, 1985). This mutagenesis template was provided by Doug Cress.

The degenerate oligonucleotide 5'--GTCCAGATC (c/a) (t/a/c) (t/g/c) ATCGTCTAA--3' was synthesized by the Macromolecular Structure Facility at Michigan State University. Oligonucleotide-directed mutagenesis was performed as described (Zoller and Smith, 1982; Kunkel, 1985; Cress and Triezenberg, 1991). Synthesis of the second strand was performed in vitro using the mutagenic oligonucleotide as a primer. The mutagenic primer was first phosphorylated by T4 polynucleotide kinase and then annealed to the template in the annealing buffer (20 mM Tris-HCl, pH 7.4, 2 mM $MgCl_2$ and 50 mM NaCl) by heating to 65°C followed by graduating cooling to 4°C . 10X extension buffer (175 mM Tris-HCl, pH 7.4, 37.5 mM $MgCl_2$, 215 mM DTT, 7.5 mM ATP, 4 mM each deoxynucleotide triphosphate) along with T4 DNA polymerase and T4

DNA ligase (final concentration 0.1 units/ml) were added to the annealed reaction to synthesize the complementary strand. The synthesis reaction was then carried out on ice, at 25°C and 37°C for 5, 5, and 90 minutes, respectively. The mutagenesis reaction was then used to transform competent dut^+ ung^+ MV1193 cells [Δ (lac-pro AB), rpsL, thi, endA, spcB15, hsdR4, Δ(srl-recA)306::Tn10(tet^r) F'(traD36, $proAB^+$, $lacI^qZ\Delta M15$)]. Transformation of the duplex DNA into dut^+ ung^+ E. coli results in selection against the uracil-containing template strand. Transformant plaques were screened for mutations by dideoxy sequencing (Sanger et al., 1977).

Construction Of Mutant VP16 Expression Plasmids

The plasmids used to express VP16 and VP16 derivatives in mammalian cells are pMSVP16β58 and pMSVP16β41. pMSVP16β58 expresses full length VP16 (codons 1-490), whereas pMSVP16β41 expresses truncated VP16 (codons 1-456), termed VP16Δ456. In these plasmids, the VP16 gene is fused downstream of the Long Terminal Repeat (LTR) of Moloney murine sarcoma virus (MSV). The MSV LTR provides the transcriptional enhancer, promoter and mRNA cap site (Triezenberg et al., 1988).

Construction of mutant VP16 expression plasmids was accomplished as follows. pMSVP16β58 was linearized with BamHI, then partially digested with SalI to yield the 6.1 kb vector fragment which contains VP16 codons 1-410. Double strand M13mp19 phage DNA containing the desired mutant VP16 activation domains were prepared. The 135 bp insert fragments encoding the truncated mutant VP16 activation domains (codons 411-456) were excised by digestion with BamHI and SalI. After cloning the mutant activation domains into the expression vector, double-stranded DNA sequencing was performed to confirm the mutation.

Transient Transfection Assay

One day prior to transfection, $8x10^5$ mouse L cells (tk^-, $aprt^-$) were plated per 60-mm culture dish in Dulbeco's modified Eagle medium (Gibco), supplemented with 10% fetal calf serum (Hyclone Laboratories). 50 ng of activator expression plasmid (pMSVP16β41 or derivatives thereof), along with 2 μg of reporter plasmid pSJT703 and 2 μg of internal control plasmid pMSV-tk (thymidine kinase) were cotransfected into the cells by DEAE-dextran / DMSO shock method (Lopata et al., 1984). pSJT703 contains the IE regulatory sequences of HSV-I ICP4 gene fused to the HSV-1 tk gene. pMSV-tk contains the MSV LTR fused to the HSV-1 tk gene. The location of the transcription start site in the reporter and the internal control tk genes are different. Forty eight hours after transfection, total RNA was harvested by the proteinase K / DNase I method (Eisenberg et al., 1985).

Primer Extension Assay (Cress and Triezenberg, 1991)

The primer used was a synthetic oligonucleotide complementary to the sequence between +53 and +77 of HSV-1 tk gene, relative to the tk gene mRNA cap site. The ^{32}P-labeled primer was incubated with total RNA in the hybridizationn buffer (10 mM Tris-HCl, pH 8.3, 150 mM KCl, 1 mM EDTA) at 65 °C for 1.5 hour. After the reaction cooled to 25 °C, 1.5X extension buffer (30 mM Tris-HCl, pH 8.3, 15 mM $MgCl_2$, 9 mM DTT, 225 μg/ml actinomycin D, 0.45 mM each deoxynucleotide triphosphate) and AMV reverse transcriptase (final concentration 1 units/ml) were added to the reaction and the primer was extended at 37 °C for 1 hour. Extension products from transcripts of pSJT703 and pMSV-tk were 81 and 55 bp, respectively. These products were separated by

electrophoresis on a 9% polyacrylamide-7M urea gel, and detected by autoradiography.

The developed film and the dried gel were aligned and the portions of the gel corresponding to bands on the film were cut out. Radioactivity of each gel slice was detected by a 5 minute scan on the tritium setting of a Packard 300 liquid scintillation counter.

Mutant Protein Stability Determination

Mouse L cells were transfected with 10 μg of wild-type or mutant pMSVP16β41. Forty eight hours after transfection, cells were lysed with lysis buffer (10 mM Tris-Hcl, pH 8.0, 5 mM EDTA and 1% SDS). The lysate was sonicated and total protein was precipitated with cold acetone. The protein pellets were then resuspended in SDS-PAGE sample buffer and electrophoresed on a 4% stacking-10% resolving SDS-PAGE minigel (Hoefer Scientific). Protein was transferred to nitrocellulose membrane using a Western Transphor TE22 apparatus (Hoefer Scientific) and probed with C8-series anti-VP16 antisera (Triezenberg et al., 1988). An avidin:biotin:peroxidase conjugate detection system was used to visualize the primary antibody (Vector Laboratories).

RESULTS

Cress and Triezenberg (1991) suggested that Phe-442 was critical to the function of the VP16 AAD. Several substitutions of this amino acid (FY, FW, FP, FA, FL, FS 442 VP16 mutants) have been previously tested by Doug Cress and Jeff Regier in our laboratory. However, certain classes of substitutions have not yet been made. A saturation mutagenesis of this position was designed and performed to characterize the amino acid requirement at position 442 more

thoroughly. This work was done in the context of VP16Δ456 (1-456 aa) which has the VP16 AAD N-subdomain.

A single degenerate oligonucleotide was synthesized to produce most of the possible substitutions. This allowed the replacement of Phe-442 by eleven amino acids, including Ile, Met, Val, His, Asp, Asn, Glu, Gln, Lys, Arg and Gly. A VP16 mutant which has the codon for Ser (TCC) instead of Phe (TTC) at position 442 of VP16 was chosen as mutagenic template so that the degenerate oligonucleotide would not contain the template bases. This choice of template avoided the selection for particular combinations of changes, therefore increasing the probability of obtaining each of the desired mutations. Out of 80 plaques screened, there were 56 mutants, including all desired mutations.

The abilities of the VP16 AAD mutants to activate HSV-1 IE gene transcription was tested by transient expression assay. Mouse L cells were transfected with the plasmid expressing the VP16 mutant along with the reporter plasmid expressing HSV-1 tk gene under control of a VP16-responsive promoter. A plasmid which constitutively expressing the HSV-1 tk gene was cotransfected as an internal control. Total RNA was harvested and the amount of HSV-1 tk transcripts were measured by primer extension assay. The result of a primer extension assay is shown in Figure 2. The 81 bp VP16-specific transcript and the 55 bp internal control transcript bands were then quantitated by scintillation spectroscopy. The relative activity of each VP16 mutant was represented by the ratio of the reporter signal (radioactive counts of the 81 bp band) to the internal control signal (radioactive counts of the 55 bp band), normalized to the activity of the wild-type VP16Δ456. The relative activities of the eleven VP16 mutants generated from this saturation mutagenesis analysis along with those of six previously generated Phe-442 mutants are shown in Table 1. Four independent transient transfection experiments were performed for every mutant and primer

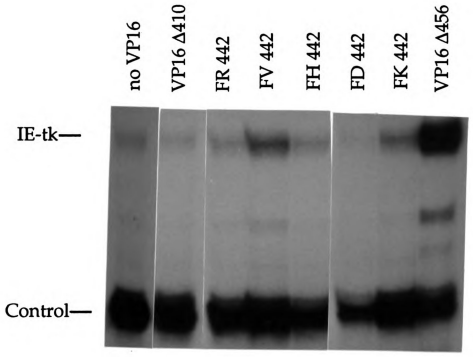

Figure 2. Autoradiogram of primer extension assay measuring the transcriptional activities of the truncated VP16 derivatives altered at Phe-442. The positions of extension products corresponding to transcripts from the reporter plasmid and the internal control plasmid are indicated. VP16Δ410 (1-410 aa) is the VP16 mutant which lacks the carboxyl-terminal 80 aa activation domain.

Table 1. Relative activities of truncated VP16 (Δ456) mutants altered at position 442. Relative activities are obtained as the ratio of the reporter signal to the internal control signal, normalized to the activity of the wild-type VP16Δ456. Means and standard deviations are calculated from at least four independent experiments. Asterisks indicate the mutants constructed and assayed by Doug Cress and Jeff Regier. The other eleven mutants are generated and tested in this study.

Amino acid substitutions at position 442	Relative activities (% of wild-type VP16Δ456)
Asp	≤ 10
Glu	≤ 10
Asn	11 ± 2
Gln	≤ 10
His	≤ 10
Arg	≤ 10
Lys	≤ 10
Gly	≤ 10
Ser*	≤ 10
Pro*	≤ 10
Val	11 ± 2
Ile	14 ± 2
Met	12 ± 1
Leu*	14 ± 2
Ala*	14 ± 3
Tyr*	30 ± 10
Trp*	36 ± 6

extension assays were repeated for each transfection. None of the eleven mutants generated from this study showed an activity greater than fifteen percent of that of the wild type protein. All these VP16 mutants were expressed at a size and level indistinguishable from the wild-type VP16Δ456 protein demonstrated by western blot analysis (Figure 3), indicating that the effects of the Phe-442 substitutions were not due to any stability change of the mutant proteins, but rather due to the structural change caused by the mutation.

The results of this Phe-442 saturation mutagenesis are consistent with previous mutational analysis of the VP16 AAD (Cress and Triezenberg, 1991; Regier, 1993). Further, the extensiveness of this mutational analysis extends our understanding of the amino acid requirement at the critical position of the AAD. Several aspects revealed from the study are summarized as follows:

(1) VP16 mutants with substitutions of the other two aromatic residues Trp or Tyr at position 442 decreased activity to 35% of wild-type VP16Δ456. The eleven nonaromatic amino acid substitution mutants tested here showed much less activity than FW442 and FY442. In fact, out of the seventeen Phe-442 mutants generated, no other substitution mutants had an activity greater than 15% relative to wild-type VP16Δ456 (Table 1).

(2) Substitution with bulky hydrophobic residues Ile, Met and Val at position 442 reduced activity to approximately fifteen percent of wild type. The activity seemed slightly higher than that of polar or charged amino acids substitution mutants. Two previously tested hydrophobic amino acids substitution mutants (FL442 and FA442) also showed somewhat higher activity.

(3) Activity of VP16 mutants with substitutions of polar or charged residues (i.e., Asp, Glu, Gln, His, Arg, Lys, Ser) and Gly or Pro were no more than 10% active (i.e., equivalent to controls lacking VP16 protein), with the exception of the Asp substitution (11%).

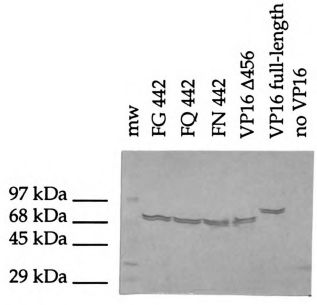

Figure 3. Western blot analysis of the stability of the truncated VP16 derivatives altered at Phe-442. Lanes corresponding to each VP16 derivative are indicated as are the positions and sizes (in kilodaltons, kDa) of molecular weight markers.

(4) Interestingly, the two acidic amino acid substitution mutants (FE442 and FD442), although having increased acidity, was less than ten percent active relative to the wild-type VP16Δ456. The increased net negative charge had no positive effect on transcriptional activities. This argues against the "acid blob" model in which the net negative charge of activation domain was the only determinant of activity. Similarly, activity of VP16 mutants with substitution of helix compatible residues Ile, Met and Val was not capable of retaining activity of the VP16 AAD. The inability to retain activity with these helix compatible substitutions argues against the AAH model in which the amphipathic helix was the determinant of activity.

Together, the saturation mutagenesis results reported here strengthen the discovery that the aromatic character of amino acid at position 442 is particularly important and that other hydrophobic residues at this position is less effective but retain some function (Cress and Triezenberg, 1991). These results also supported previous suggestions that neither the "acid blob" model nor the AAH model regarding the secondary structure of acidic activation domains is appropriate for VP16.

DISCUSSION

The critical role of a previously identified residue Phe-442 of the VP16 activation domain has been thoroughly tested by oligonucleotide-directed saturation mutagenesis and transient transfection assays. The experimental results strengthen the conclusions of Cress and Triezenberg (1991): (1) Neither the "acid blob' model nor the AAH model is suitable to describe the secondary structure of VP16 activation domain; and (2) The aromatic, bulky hydrophobic character at position 442 is critical to VP16 activity. Promoted by our initial

discovery from mutational analysis of the VP16 AAD (Cress and Triezenberg, 1991; Regier et al., 1993), many researchers started to explore the amino acid requirements in various activation domains. Results from these studies generally confirm the conclusions drawn from the studies of the VP16 AAD and together suggest a common theme of activation domains, which is that the most abundant amino acids of the activation domains may not be the most important for their function and hydrophobic and aromatic amino acids are equally or even more important (Triezenberg, 1995). Below, I will discuss the experimental results that reflect on the importance of the most abundant amino acids and the hydrophobic amino acids to the activity of activation domains.

The Most Abundant Amino Acids

For acidic activation domains, the net negative charge generally correlates with the strength of the activation domain. This was initially shown by deletion analysis of the yeast activator GCN4 (Hope et al., 1988), and subsequently demonstrated by the "neutralization" mutagenesis analysis of the VP16 AAD in which the acidic residues were substituted by their neutral counterparts (Cress and Triezenberg, 1991) as well as by recent studies of the AADs of GAL4, RelA and gluococorticoid receptor (Leuther et al., 1993; Blair et al., 1994; Almlöf et al., 1995). Despite the general correlation, mutational analysis of VP16 AAD first suggested that the acidic amino acids are not sufficient for the function of AADs (Cress and Triezenberg, 1991). Indeed, this conclusion has been supported by mutational studies of various AADs, including those of GCN4, GAL4, RelA and gluococorticoid receptor (Hope et al., 1988; Leuther et al., 1993; Blair et al., 1994; Almlöf et al., 1995). In all the cases, the correlation between AAD activity and the number of acidic amino acids is not strict, suggesting that certain structural element is required for their activities. The saturation mutational analysis

reported here further supports this conclusion. First, many of the Phe-442 mutations of VP16 do not change the net charge, and yet they dramatically reduced transcriptional activity of VP16. Moreover, increasing the net negative charge of VP16 by substituting Phe-442 with Asp or Glu decreased rather than increased its transcriptional activity. Mutational analysis of the GAL4 AAD yielded the most extreme results in which mutants with no net charge, or even a net positive charge, were found as nearly active as wild-type activator (Leuther et al., 1993). In this case, the interspersal of acidic residues are proposed to increase the accessibility of hydrophobic residues which interact with other transcription factors, rather than to their direct involvement in protein-protein interaction with other transcription factors..

Mutational studies of other classes of activators also revealed that the most abundant amino acids in the activation domains may not be the most required for their functions. The glutamine rich activator Sp1 has been proposed to interact with $TAF_{II}110$ to activate transcription. However, substitution of multiple glutamine residues with alanine residues in the Sp1 activation domain had no effect on its interaction with $TAF_{II}110$ nor on its transcriptional activity (Gill et al., 1994). Another example is seen in the glutamine rich activator Oct-2 (Tanaka and Herr, 1994). In this case, although glutamine residues were found important for high level of activation, they were not absolutely essential for low levels of activity.

Hydrophobic Amino Acids

Earlier mutagenesis analysis of the VP16 AAD suggested that aromatic charter of Phe-442 is critical for the activity of VP16 (Cress and Triezenberg, 1991). This saturation mutational study of Phe-442 of VP16 reported here conclusively demonstrated that aromaticity, to a less extent, hydrophobicity at

position 442 is important for transcriptional activation. Aromatic amino acid substitutions retained approximately 30 percent of wild-type VP16Δ456 activity. Bulky hydrophobic amino acid substitutions decreased activity to approximately 15 percent of wild-type VP16Δ456 while all other substitutions reduced activity to no more than 10 percent. In addition to the critical Phe-442, Cress and Triezenberg (1991) observed a pattern of bulky hydrophobic residues flanking carbonyl-containing amino acids, similar to the sequence surrounding the Phe-442 of VP16, among all three different classes of activators. Mutational analysis of Leu-439 and Leu-444 of the VP16 AAD indicated that, although to a less extent, these hydrophobic residues flanking Phe-442 contribute to the activity of the VP16 truncated activation domain (Regier et al., 1993). These results confirm the role for hydrophobic residues in the trans-activation of VP16 and suggest a role in possibly other classes of transactivators.

After the demonstrated importance of hydrophobic residues in VP16 AAD, the roles of hydrophobic residues in various activation domains started to be addressed (reviewed in Triezenberg, 1995). Later studies confirmed the importance of hydrophobic residues for the function of VP16, as the minimal transcription activation domain identified in VP16 AAD consists a specific array of acidic and hydrophobic residues (Seipel et al., 1994). Moreover, a pattern of bulky hydrophobic residues were found to be equally, or more critical than the most abundant residues in many other acidic activation domains (Triezenberg, 1995). The list includes the varicella-zoster viruse protein ORF10, the Epstein-Barr virus protein Rta, the foamyvirus Bel-1 protein, the yeast activators GAL4 and GCN4, and the mammalian proteins p53 and RelA (Moriuchi et al., 1995; Hardwick et al., 1992; Blair et al., 1994a; Leuther et al., 1993; Drysdale et al., 1995; Lin et al., 1994; Blair et al., 1994b; Schmitz et al., 1994). As a detailed example, the phenylalanine at position 28 and a motif centered at this residue in the varicella-

zoster virus protein ORF10, a VP16 homolog, resembles Phe-442 and the sequence surrounding Phe-442 of VP16 (Moriuchi et al., 1995). As shown previously for VP16, substitution of ORF10 Phe-28 by various amino acids demonstrated the importance of aromatic or bulky hydrophobic residues at this position. Hydrophobic residues flanking Phe-28 were also found to contribute to the transcriptional activity of ORF10.

The importance of the pattern of bulky hydrophobic residues is not limited in the acidic activation domains. Hydrophobic residues have also been found necessary for the activities of two glutamine-rich activators, Sp1 and Oct-2 (Gill et al., 1994; Tanaka and Herr, 1994). Both activators showed higher dependence on hydrophobic residues than on glutamine residues.

The requirements of aromatic or bulky hydrophobic amino acids in the activation domains have been widely observed, however, the reasons for the requirements are not well understood. Two potential roles of these amino acids are either that they are important for maintaining the structure of the activation domains or they are directly involved in interactions with their target proteins. This question can be addressed by probing the structure of these activation domains and exploring their interactions with putative target proteins. In the case of VP16, our fluorescence studies suggest that the amino acid at position 442 of VP16 AAD is solvent exposed and that the conformation around this Phe-442 becomes constrained upon interaction with basal transcription factors (Shen et al., 1995a; 1995b). Therefore, it is most likely that Phe-442 is directly involved in protein-protein interactions and thus is critical for transcriptional activation.

Transcriptional activators have been shown to interact with several components of the transcriptional apparatus, such as TBP, TAF_{II}, TFIIB and TFIIH (Zawel and Reinberg, 1995). Considering the wide range of target proteins, having bulky hydrophobic amino acids, in particularly, aromatic amino

acids in the protein-protein interaction face of activation domains maybe very beneficial. Aromatic residues can participate in many kinds of interactions such as hydrophobic interactions, cation-pi interactions between the aromatic rings and charged groups and, in some cases, hydrogen-bonding. Thus, having aromatic residues in the interaction face of activation domain, permits it to interact with structurally diverse target proteins. In addition, aromatic residues have the largest surface area which enable them to elicit substantial changes in binding site topography. Having these residues in the interaction face of the activation domains could permit them to alter the stereochemical features of the binding sites to interact with various target proteins. Unusually frequent utilization of aromatic residues at the protein-protein interaction face has been shown in the antibody combining sites, where aromatic residues enable the antibodies to bind different antigens (Mian et al., 1991).

Our mutational analysis of the VP16 activation domain has yielded important information about the critical structural elements in the acidic activation domains. However, the molecular biology approaches can not define protein structure directly. Another important question, related to the structural features identified in the VP16 activation domain, is how this acidic activation domain fulfills its function. Although the activation mechanisms have been studied intensively by various biochemical techniques, they are still poorly understood.

Biophysical approaches are very powerful for probing protein structures and exploring protein-protein interactions. Thus, their application in the study of transcription would be very informative. Unfortunately, few such studies have been carried out. In the following chapters, I will introduce various fluorescence spectroscopy methods to study these two important questions in the

field of eukaryotic transcription activation. Important insights on the structure of the activation domain and the activation mechanism have been gained from these studies. Our fluorescence analyses of the VP16 AAD structure and the interactions between the VP16 AAD and its putative target proteins will be described in the following two chapters.

REFERENCES

Almlöf, T., Wright, A. P. H., & Gustafsson, J-Å. (1995) *J. Biol. Chem. 270,* 17535-17540.

Blair, W. S., Bogerd, H., & Cullen, B, R. (1994a) *J. Virol. 68,* 3803-3808.

Blair, W. S., Bogerd, H. P., Madore, S. J., & Cullen, B, R. (1994b) *Mol. Cell. Biol. 14,* 7226-7234.

Cress, W. D., & Triezenberg, S. J. (1991) *Science 251,* 87-90.

Eisenberg, S. P., Coen, D. M., & McKnight, S. L. (1985) *Mol. Cell. Biol. 5,* 1940-1947.

Drysdale, C. M., Dueñas, E., Jackson, B. M., Reusser, U., Braus, G. H., & Hinnebusch, A. G. (1995) *Mol. Cell. Biol. 15,* 1220-1233.

Gill, G., & Ptashne, M. (1987) *Cell 51,* 121-126.

Gill, G., Pascal, E., Tseng, Z. H., & Tjian, R. (1994) *Proc. Natl. Acad. Sci. USA 91,* 192-196.

Gininger, E., & Ptashne, M. (1987) *Nature 330,* 670-672.

Hardwick, J. M., Tse, L., Applegren, N., Nicholas, J., & Veliuona, M. A. (1992) *J. Virol. 66,* 5500-5508.

Hope, I. A., Mahadeven, S., & Struhl, K. (1988) *Nature 333,* 635-640.

Kunkel, T. A. (1985) *Proc. Natl. Acad. Sci. USA 82,* 488-492.

Leuther, K. K., Salmeron, J. M., & Johnston, S. A. (1993) *Cell 72,* 575-585.

Lin, J., Chen, J., Elenbaas, B., & Levine, A. J. (1994) *Genes Dev. 8,* 1235-1246.

Lopata, M. A., Cleveland, D. W., & Sollner-Webb, B. (1984) *Nucleic Acids Res. 12*, 5707- 5717.

Ma, J., & Ptashne, M. (1987) *Cell 51*, 113-119.

Mian, S., Bradwell, A. R., & Olson,A. J. (1991) *J. Mol. Biol. 217*, 133-151.

Mitchell, P. J., & Tjian, R. (1989) *Science 245*, 371-378.

Moriuchi, H., Moriuchi, M., Pichyangkura, R., Triezenberg, S. J., Straus, S. E., & Cohen, J. I. (1995) *Proc. Natl. Acad. Sci. USA 92*, in press.

Norrander, J., Kempe, T., & Messing, J. (1983) *Gene 26*, 101-106.

Regier, J. L. (1993) Ph. D. thesis. Michigan State University.

Regier, J. L., Shen, F., & Triezenberg, S. J. (1993) *Proc. Natl. Acad. Sci. USA 90*, 883-887.

Sadowski, I., Ma, J., Triezenberg, S., & Ptashne, M. (1988) *Nature 355*, 563-564.

Sanger, F., Nicklen, S., & Coulson, A. R. (1977) *Proc. Natl. Acad. Sci. USA 74*, 5463-5467.

Schmitz, M. L., Silva, M. A. D. S., Altman, H., Czisch, M., Holak, T. A., & Baeuerle, P. A. (1994) *J. Biol. Chem. 269*, 25613-25620.

Seipel, K., Georgiev, O., & Schaffner, W. (1994) *Biol. Chem. Hoppe-Seyler 375*, 463-470.

Shen, F., Triezenberg, S. J., Hensley, P., Porter, D., & Knutson, J. (1995a) Manuscript in preparation.

Shen, F., Triezenberg, S. J., Hensley, P., Porter, D., & Knutson, J. (1995b) Manuscript in preparation.

Sigler, P. (1988) *Nature 333*, 210-212.

Tanaka, M., & Herr, W. (1994) *Mol. Cell. Biol. 14*, 6056-6067.

Triezenberg, S. J., Kingsbury, R. C., & McKnight, S. L. (1988) *Genes Dev. 2*, 718-729.

Triezenberg, S. J. (1995) *Curr. Opin. Genetics Dev. 5*, 190-196.

Walker, S., Greaves, R., & O'Hare, P. (1993) *Mol. Cell. Biol. 13*, 5233-5244.

Zawel, L. R., & Reinberg, D. (1995) *Ann. Rev. Biochem. 64*, 533-561.

Zhu, Q., Smith, T. F., Lathrop, R. H., & Figge, J. (1990) *Proteins 8*, 156-163.

Zoller, M. J., & Smith, M. (1982) *Nucleic Acids Res. 10*, 6487-6500.

CHAPTER III

CRITICAL AMINO ACIDS IN THE TRANSCRIPTIONAL ACTIVATION DOMAIN OF THE HERPESVIRUS PROTEIN VP16 ARE SOLVENT EXPOSED IN HIGHLY MOBILE PROTEIN SEGMENTS: AN INTRINSIC FLUORESCENCE STUDY

INTRODUCTION

Transcription initiation by RNA polymerase II in eukaryotic cells requires the assembly of a basal transcription complex containing the polymerase and several general transcription factors (Zawel and Reinberg, 1995). The actual level of transcription, however, is regulated by gene specific proteins termed transcriptional activators or repressors. These proteins usually contain two functional domains. One domain directs the gene-specific binding (Nelson, 1995) and the other domain performs the transcription activation or repression function (Hahn, 1993; Tjian and Maniatis, 1994; Triezenberg, 1995).

VP16 is a virion protein of herpes simplex virus that specifically activates viral immediate early gene expression (Hayward, 1993; O'Hare, 1993). The amino-terminal region of this protein interacts with host DNA binding proteins to associate with the immediate early gene promoter sequences (Walker et al., 1994; Wilson et al., 1993). The activation function resides within the carboxyl -terminal 78 amino acids (Triezenberg et al., 1988; Cousens et al., 1989; Sadowski et al., 1988). As one of the most potent activators known, the VP16 activation domain has been studied widely in many systems and by various experimental designs. In light of these studies, several models have been proposed for the

mechanisms of activation. Activators might function by relieving the repression effect of chromatin structure (Paranjape et al., 1994). Alternatively, they may interact with components of the basal transcription complex, directly or indirectly, to either speed up or stabilize the formation of the preinitiation complex (Ingles et al., 1991; Choy and Green, 1994; Xiao et al., 1994a; Goodrich et al., 1993; Berger et al., 1992). Some activators may affect initiation, promoter clearance or transcriptional elongation (Narayan et al., 1994; Yankulov et al., 1994).

Despite their central importance in gene regulation, the structures of the transcriptional activation domains remain a mystery. No activation domain structure has yet been solved by X-ray crystallographic analyses or NMR. Most clues to the structures of activation domains come from mutational analyses. Many activation domains are rich in acidic amino acids; in the case of VP16, 21 acidic residues are found in the 78 amino acid domain. Initially, an "acidic blob" random coil model was suggested for these acidic activation domains (AAD) (Sigler, 1989). According to this model, AADs would function primarily through electrostatic interactions. Subsequent mutational analyses provided evidence against this model (Cress and Triezenberg, 1991; Ma and Ptashne, 1987; Leuther et al., 1993), in that no strict correlation between negative charge and activity was observed. An alternative, the so called amphipathic α helix model (Ptashne, 1988), was also refuted by mutational analyses of the VP16 AAD (Cress and Triezenberg, 1991; Regier et al., 1993). No relation was observed between predicted amphipathy and activity, and proline substitutions introduced into the putative helix had no effect on activity. Instead, particular aromatic and bulky hydrophobic residues were found important for function. These and other studies also suggested that VP16 AAD had two subdomains, namely, the N-terminal subdomain (413-456) and the C-terminal subdomain (453-490) (Regier et

al., 1993; Goodrich et al., 1993; Walker et al., 1993). Phe-442 was deemed the most critical residue in the N-subdomain and its aromaticity was the most important feature. Although the pattern of amino acids surrounding Phe-473 resembled that surrounding Phe-442, Phe-473 was not as sensitive to mutations. Thus, these two subdomains apparently depend on different patterns of residues and might function through different mechanisms.

Few biophysical studies of transcriptional domains have been reported. Both 1D and 2D NMR of the isolated VP16 AAD demonstrated that this domain lacked stable secondary and tertiary structure (O'Hare and Williams, 1992). Similarly, circular dichroism (CD) experiments indicated that this isolated domain was devoid of any stable α-helical or β-strand structure (Donaldson and Capone, 1992), although more α-helical structure was induced under hydrophobic conditions or at low pH. Parallel studies by CD spectroscopy revealed that the AADs of yeast activators GAL4 and GCN4 were conformationally mobile at neutral pH and underwent a transition to β-sheet in acidic solution (Van Hoy et al., 1993). Taken together, the limited biophysical studies have not detected secondary structure of AADs under physiological conditions.

Fluorescence spectroscopy can provide a rich variety of information about protein conformation, including the local environment of specific residues, populations of protein conformers and dynamics (Eftink, 1991). Here, we describe a fluorescence analysis employing chimeric proteins comprising the DNA-binding domain of yeast protein GAL4 fused to the AAD of VP16. Trp residues were substituted for Phe (at either position 442 or 473) to provide unique intrinsic probes within each subdomain. The results of fluorescence quenching, time-resolved intensity decay and time-resolved anisotropy decay studies show that the VP16 AAD is largely unstructured.

EXPERIMENTAL PROCEDURES

Mutagenesis And Cloning

A SphI/SalI fragment corresponding to the GAL4 gene sequences encoding amino acids 10 to 147 was cloned into M13mp18. A Trp codon at position 36 in GAL4 was changed to a Val codon using oligonucleotide directed mutagenesis (Kunkel, 1985). The SphI/XhoI fragment encoding the desired mutant GAL4 DNA binding domain (WV36) was cloned into pLA31ΔSma which was the E. coli expression vector for GAL4-VP16C (453-490). Using directional cloning, the WV36 mutation at GAL4 was introduced into pFS12182 and pAC-del456, which express GAL4-VP16 (413-490) and GAL4-VP16N (413-456) respectively. The plasmids pFS12182, pAC-del456 and pLA31ΔSma are all derived from pJL2 (Chasman et al., 1988; F. Shen, A. Cress, L. Alexander and S. J. Triezenberg, unpublished data). Previously mutated VP16 activation domains (FW442 or FW473) were further subcloned into these E. coli expression plasmids from mammalian VP16 expression vectors derived from pMSVP16 (Cress and Triezenberg, 1991; Regier et al., 1993).

Expression And Purification Of Proteins

Various GAL4WV36-VP16 proteins were expressed in E. coli XA90 cells under control of the hybrid tac promoter. A previously reported purification protocol (Chasman et al., 1989) was significantly modified to improve the purity. Cells containing the expression plasmid were grown at 37°C in LB medium containing 50 mg/l ampicillin. At a cell density of A_{600} = 0.7, IPTG was added to 1 mM to induce the synthesis of fusion proteins. Zinc acetate was added to 100 μM at this point to provide divalent cations for the GAL4 zinc binding domain.

Three hours after induction, cells were harvested and resuspended in (40 ml/liter culture) ice cold buffer A (20 mM HEPES, pH 7.5, 20 mM 2-mercaptoethanol, 10 μM zinc acetate, 2 μg/ml leupeptin, 2 μg/ml pepstatin, 20 μg/ml benzamidine and 0.2 mM phenylmethylsulfonyl fluoride) plus 200 mM NaCl. The cells were then lysed by sonication, and cell debris was pelleted by centrifugation. Polyethylenimine was added to the cleared lysate to 0.30% (wt/vol). The precipitated proteins were resuspended in buffer A plus 750 mM NaCl and precipitated by addition of solid ammonium sulfate to 35% for GAL4-VP16 and GAL4-VP16C and to 40% for GAL4-VP16N. Ammonium sulfate pellets were resuspended in buffer A and dialyzed against standard column buffer (SCB; 20 mM HEPES, pH 7.5, 10 mM zinc acetate, 1 mM dithiothreitol) plus 100 mM NaCl. The crude proteins were then loaded onto a pre-equilibrated Whatman P-11 column at 4° C. The column was first washed with SCB plus 100 mM NaCl, and then eluted with a linear gradient of 100 mM to 1000 mM NaCl in SCB. The relatively pure fractions (as judged by SDS-PAGE) were combined and dialyzed against SCB plus 200 mM NaCl (for GAL4-VP16) or 150 mM NaCl (for GAL4-VP16N and GAL4-VP16C), and then loaded onto a pre-equilibrated DE-52 column at room temperature. This column was washed with SCB plus 200 mM NaCl (for GAL4-VP16) or 150 mM NaCl (for GAL4-VP16N and GAL4-VP16C) first, and then eluted with a linear gradient (to 400 mM NaCl in SCB). Fractions containing purified proteins (as judged by SDS-PAGE) were pooled and stored as aliquots at -70°C. GAL4 (1-147) was purified by a modified procedure of a method previously described (Pan and Coleman, 1989).

In Vitro Transcription Assay

In vitro transcription reactions were performed as described (Berger et al., 1990). The DNA template, pCZ3GAL, contains the yeast CYC1 gene promoter

which includes two TATA box sequences and multiple initiation sites. It also contains three tandem binding sites for GAL4. In vitro synthesized RNAs were analyzed by primer extension using avian myeloblastoma virus reverse transcriptase (Life Sciences, St. Petersburg, FL). Primer extension products were separated on 9% polyacrylamide-7 M urea gel.

Fluorescence Measurements

All proteins were dialyzed against PBS buffer (pH 7.4, 8.1 mM Na_2HPO_4, 1.4 mM KH_2PO4, 137 mM NaCl and 2.7 mM KCl) with three changes. Concentrations of samples were determined using the following extinction coefficients derived from amino acid composition (Gill and von Hippel, 1989): ε_{280nm} = 9890 $cm^{-1}M^{-1}$ for GAL4WV36-VP16FW442, GAL4WV36-VP16FW473 and GAL4WV36-VP16C FW473 and ε_{280nm} = 7370 $cm^{-1}M^{-1}$ for GAL4WV36-VP16N FW442. Absorbance measurements were obtained using Perkin-Elmer Lambda 4B UV/VIS spectrophotometer. Concentrations of all proteins used in this study were in the range of 10-20 μM. The optical densities of all samples were less than 0.1 at the excitation wavelengths to avoid inner filter effects.

The steady-state fluorescence spectra were obtained on a SLM 8000 spectrofluorometer operated in a ratio mode. "Magic angle" configuration was used to avoid rotational artifacts (Badea and Brand, 1979). The bandwidths for excitation and emission slits were 4 nm. The excitation wavelength was 297 nm.

Quenching experiments were performed at an excitation wavelength of 297 nm. Aliquots of stock quenching solutions (4 M KI, 4 M CsCl and 8 M acrylamide) were added to 1.4 ml protein samples. The values of fluorescence emission intensity at 350 nm were corrected for dilution prior to data analysis. Quenching data were analyzed by the Stern-Volmer equation for dynamic quenching:

$$F_0/F = 1+K_{sv}[Q] \quad (1)$$

or by the single species dynamic-static quenching equation:

$$F_0/F = (1+K_{sv}[Q]) \exp(V[Q]) \quad (2)$$

where F_0 and F are the fluorescence intensity in the absence and presence of quencher, [Q] is the quencher concentration, K_{sv} is the Stern-Volmer dynamic quenching constant and V is the static quenching constant (or "active volume"). K_{sv} and V values were determined using least-squares regression (IGOR, Wavemetrix, Lake Oswego, OR). The bimolecular collisional quenching constant k_q was calculated from:

$$k_q = K_{sv} / \langle \tau \rangle \quad (3)$$

where $\langle \tau \rangle$ is the mean (intensity weighted) fluorescence lifetime obtained from time-resolved measurements.

Time-resolved fluorescence was measured on a single photon counting fluorometer (Green et al., 1990). A synchronously pumped, mode-locked, cavity-dumped dye laser (Spectra-Physics 3520) was used as the light source, providing pulses of width <10 ps at 297 nm with a repetition rate of 4 MHz and an average power of 200 μW. The vertically polarized UV pulses were obtained by frequency doubling of horizontally polarized dye laser pulses. The exciting light time profile was obtained with a light-scattering suspension (Ludox, Dupont de Nemours Co.). The intensity decay profiles were collected through an emission sheet polarizer oriented 55° from the vertical symmetry axis (Badea and Brand,

1979). Emission was selected by computer-controlled JYH10 monochromator with the bandwidth set at 8 nm and a 3-mm glass slide added to further reject stray excitation. Decay curves were recorded at 5-nm intervals across the emission band (310-460 nm) by using standard TCSPC modules and an Ortec ADCAM multichannel analyzer under computer control. The decay-associated spectra (Knutson et al., 1982) were obtained from global analysis (Knutson et al., 1983). The fluorescence intensity decay, $I(\lambda,t)$, was fit to a sum of exponentials:

$$I(\lambda,t) = \sum \alpha_i(\lambda) \exp(-t/\tau_i) \qquad (4)$$

where τ_i is the emission wavelength independent decay time of the ith decay component and α_i is its preexponential term at emission wavelength λ. The fractional fluorescence, $f_i(\lambda)$, of the ith component at wavelength λ is given by (Ross et al., 1981a):

$$f_i(\lambda) = \alpha_i(\lambda)\tau_i \; / \; \sum \alpha_i(\lambda)\tau_i \qquad (5)$$

The mean lifetime $\langle\tau\rangle$ is defined by:

$$\langle\tau\rangle = \sum \alpha_i\tau_i^2 \; / \; \sum \alpha_i\tau_i \qquad (6)$$

Anisotropy decay curves were obtained by alternatively recording emission oriented parallel and perpendicular to the plane of excitation at emission wavelength of 350 nm. Time per channel was 90 ps and 512 channels were recorded. Data were analyzed by the "sum and difference" method (Dale et al., 1977). The anisotropy decay curve, r(t), was obtained from the difference curve and total intensity curve by:

$$r(t) = (I_{vv} - I_{vh}) / (I_{vv} + 2I_{vh}) \quad (7)$$

where I_{vv} and I_{vh} are emission intensities measured parallel and perpendicular to the excitation plane, respectively. r(t) was modeled by a sum of exponentials:

$$r(t) = \Sigma \beta_j \exp(-t/\phi_j) \quad (8)$$

where ϕ_j is the rotational correlation time of the jth component and β_j is its preexponential term. A fixed 50 ps component was introduced to compensate for both scattering and color shift artifacts. If one assumes segmental motion can be reconciled with the "wobbling in cone" model (Kinosita et al., 1977; Lipari and Szabo, 1980), the cone semiangle, Θ, is given by:

$$\frac{\beta_2}{r_0} = \left[\frac{1}{2}(\cos\Theta)(1+\cos\Theta)\right]^2 \quad (9)$$

where β_2 is the preexponential term for the global rotation of the macromolecule and r_0 is the limiting ("time zero") anisotropy. Time-resolved fluorescence data were analyzed by Denise Porter and Jay Knutson at National Institutes of Health.

RESULTS

Production Of GAL4-VP16 Fusion Proteins With Unique Trp Substitutions

The chimeric transactivator GAL4-VP16, which contains the DNA-binding domain (residues 1-147) of GAL4 and the activation domain of VP16 (residues 413-490 or derivatives thereof), was utilized in our study. The GAL4 domain

initially had a tryptophan at position 36. To exclusively study the fluorescence properties of the VP16 activation domain, Trp-36 was replaced with Val using oligonucleotide-directed mutagenesis. This substitution was chosen because Val is present at homologous positions in proteins related to GAL4 (Kraulis et al., 1992). Gel mobility shift assays demonstrated that GAL4WV36-VP16 produced in E. coli bound to DNA containing the GAL4 recognition sequence as well as did GAL4-VP16 (data not shown), implying that this Trp to Val substitution did not significantly change the structure of GAL4 DNA binding domain.

The wild-type VP16 AAD has no indigenous tryptophan residues. To obtain unique intrinsic fluorescence probes at key positions within the VP16 AAD, Phe to Trp mutations were introduced at either position 442 or 473. These mutations had modest or no effects on transcriptional activation when tested in transient transfection assays (Regier et al., 1993). For this study, these mutations were transferred to the expression vector for the GAL4-VP16 fusion protein as both full-length AAD and as relevant subdomains (413-456 or 453-490). These fusion proteins (represented in Figure 1) were purified to more than 95% homogeneity judged by SDS-PAGE. These proteins were transcriptionally active when tested by in vitro transcription assays (Figure 2). Addition of GAL4WV36-VP16, GAL4WV36-VP16FW442 and GAL4WV36-VP16FW473 to the in vitro transcription reactions strongly stimulated transcription from the multiple start sites of yeast CYC1 promoter (lanes 3-5), while addition of no activator or addition of the GAL4 DNA binding domain alone resulted in basal level transcription only (lanes 1 and 2). Thus, the structural features revealed by Trp-442 or Trp-473 should reflect those of the wild-type VP16 AAD.

Figure 1. Schematic representations of the various transactivators used in this study. All proteins contain the GAL4 DNA binding domain (1-147) with the valine substitution at position 36, designated as GAL4WV36. All proteins also contain a 2 or 3 amino acid linker between GAL4 domain and VP16 domain. GAL4WV36-VP16 (413-490), GAL4WV36-VP16FW442 or GAL4WV36-VP16FW473 contains the in-frame fused wild-type full-length VP16 activation domain (413-490) or with the tryptophan substitution at position 442 or 473, respectively. GAL4WV36-VP16N FW442 contains the in-frame fused VP16 activation N subdomain (411-456) with the tryptophan substitution at position 442. GAL4WV36-VP16C FW473 contains the in-frame fused VP16 activation C subdomain (453-490) with the tryptophan substitution at position 473.

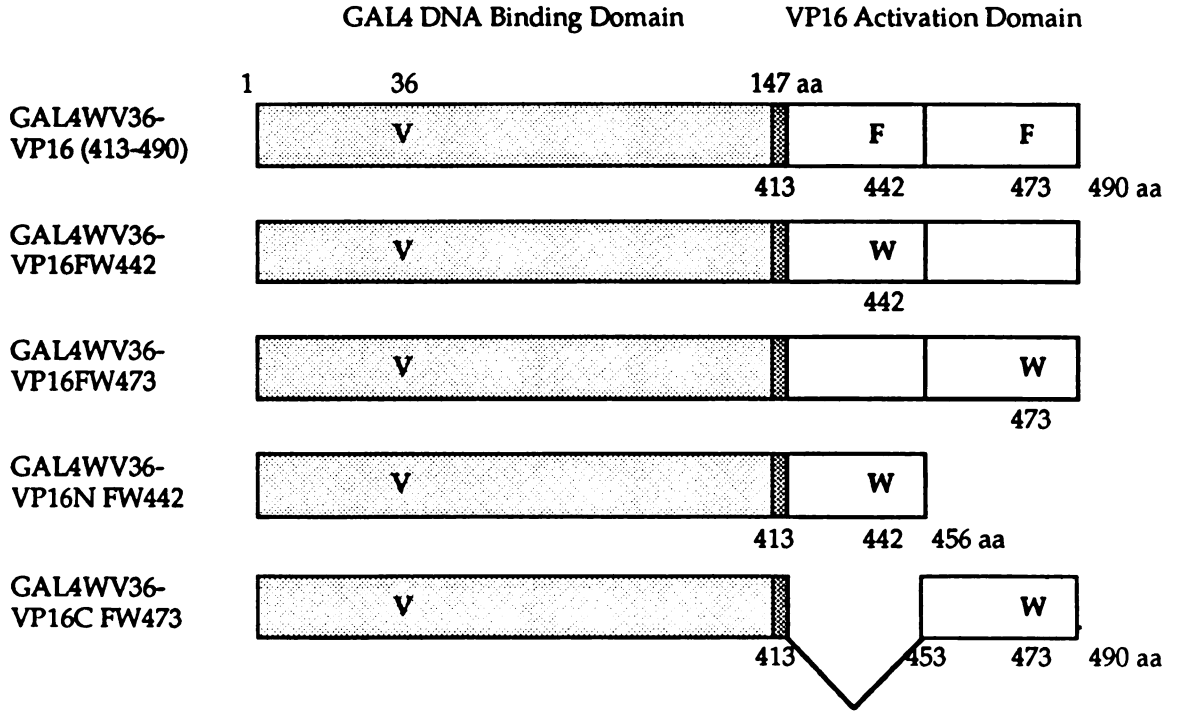
GAL4 DNA Binding Domain
VP16 Activation Domain
1
36
147 aa
GAL4WV36-
VP16 (413-490)
V
F
F
413
442
473
490 aa
GAL4WV36-
VP16FW442
V
W
442
GAL4WV36-
VP16FW473
V
W
473
GAL4WV36-
VP16N FW442
V
W
413
442
456 aa
GAL4WV36-
VP16C FW473
V
W
413
453
473
490 aa

Figure 1

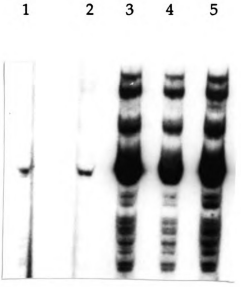

Figure 2. Autoradiogram of primer extension assay reflecting the transcriptional activities of the transactivators used in this study. No transactivator (lane 1); 2 pmol of GAL4 (1-147) (lane 2); 2 pmol of GAL4WV36-VP16 (413-490) (lane 3); 2 pmol of GAL4WV36-VP16FW442 (lane 4) and 2 pmol of GAL4WV36-VP16FW473 (lane 5) was added to the in vitro transcription reactions. Protein concentrations were determined by the Bradford assay.

Steady-State Fluorescence

The steady-state emission spectra of various GAL4WV36-VP16 proteins are presented in Figure 3. The excitation wavelength at 297 nm was chosen to avoid excitation of tyrosine fluorescence. The maximum of Trp-442 emission in either the full-length activation domain or in the N subdomain was centered at 350 nm. The Trp-473 in full-length activation domain context displayed an emission maximum at 349 nm, while a C subdomain yielded 348 nm. All of these emission wavelength maxima resemble those of fully-exposed Trp residues, suggesting that both Trp-442 and Trp-473 are accessible to solvent.

To further assess the solvent access to the surroundings of Trp-442 and Trp-473, quenching studies were undertaken using anionic (iodide), cationic (cesium), and neutral polar (acrylamide) quenching agents. The results of these studies are given in Figure 4 and the results of the analysis in terms of equations 1-3 are given in Table 1. The Stern-Volmer plot of acrylamide for GAL4WV36-VP16FW442 was linear (Figure 4A), giving a Stern-Volmer quenching constant (K_{sv}) of 15.7 M^{-1}. The Stern-Volmer plot of acrylamide for GAL4WV36-VP16FW473 showed upward curvature (Figure 4A); a single-species dynamic-static model fit the data significantly better than did a pure dynamic model. This analysis gave a K_{sv} of 6.6 M^{-1} and a static quenching constant (V) of 2.3 M^{-1}. V measures the strength of the ground state complex between the quencher and Trp. The quenching rate constants for GAL4WV36-VP16FW442 and GAL4WV36-VP16FW473 were 4.2 $M^{-1}ns^{-1}$ and 2.0 $M^{-1}ns^{-1}$, respectively, within the range (2-4 $M^{-1}ns^{-1}$) typically seen for exposed Trp residues in proteins with little secondary structure (Eftink and Ghiron, 1981). These results suggest that both Trp residues are highly exposed.

Using iodide as a quenching agent (Figure 4B), the Stern-Volmer constants K_{sv} for GAL4WV36-VP16FW442 and GAL4WV36-VP16FW473 were 3.1 M^{-1} and

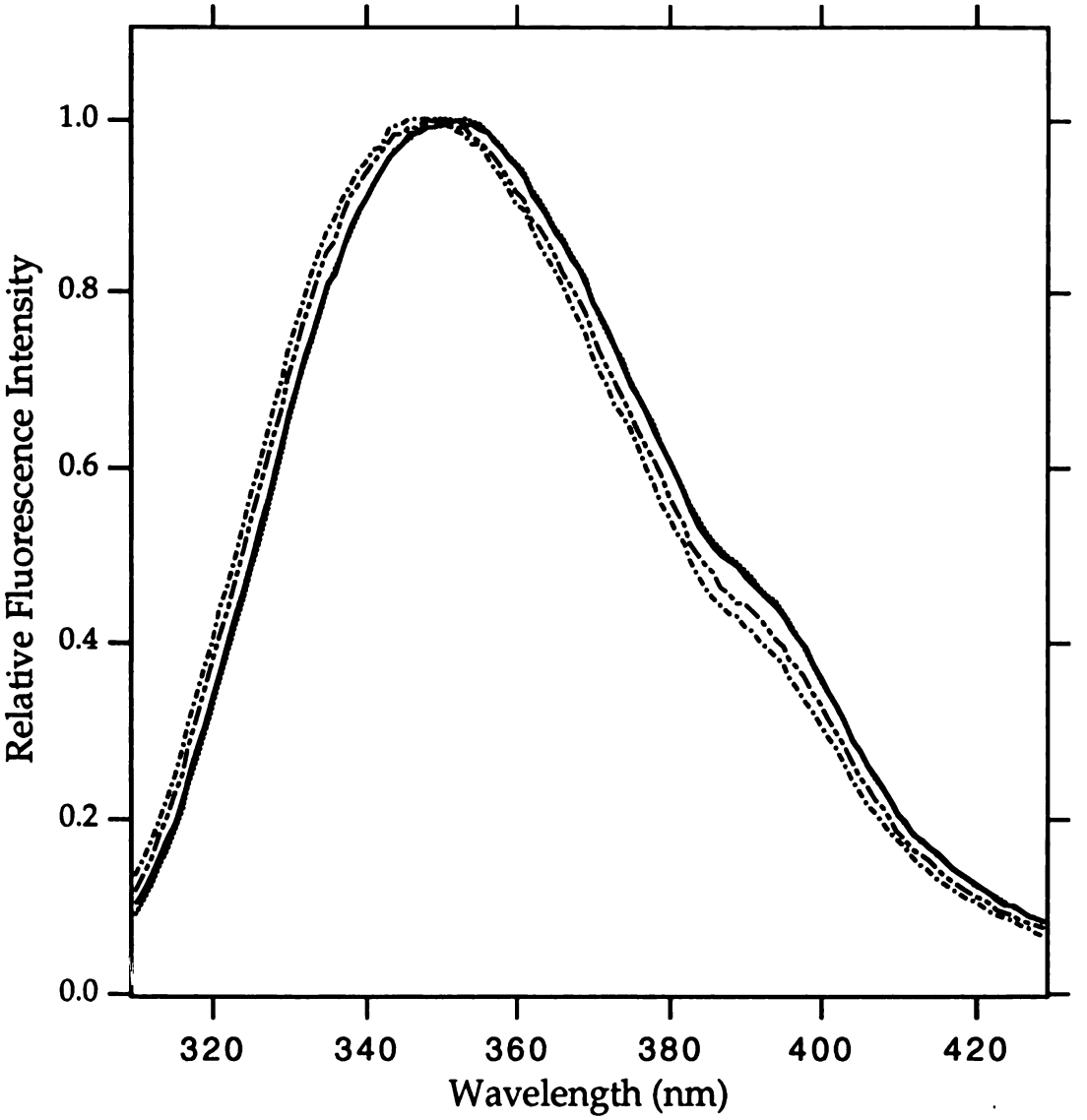

Figure 3. Normalized emission spectra of various transactivators used in this study. Solid line represents GAL4WV36-VP16FW442, long dash-dotted line represents GAL4WV36-VP16FW473, dotted line represents GAL4WV36-VP16N FW442 and short dash-dashed line represents GAL4WV36-VP16C FW473.

Figure 4. Stern-Volmer plots for the quenching of the fluorescence of various transactivator proteins used in this study. Panel A, Panel B and Panel C represents quenching by acrylamide, KI and CsCl, respectively. Closed circles are for the GAL4WV36-VP16FW442; open circles are for the GAL4WV36-VP16N FW442; closed triangles are for the GAL4WV36-VP16FW473; open triangles are for the GAL4WV36-VP16C FW473. constants are very close to those observed for the full-length activators. Thus, truncation of the activator has no effect on the extent of exposure of Trp-442 and Trp-473.

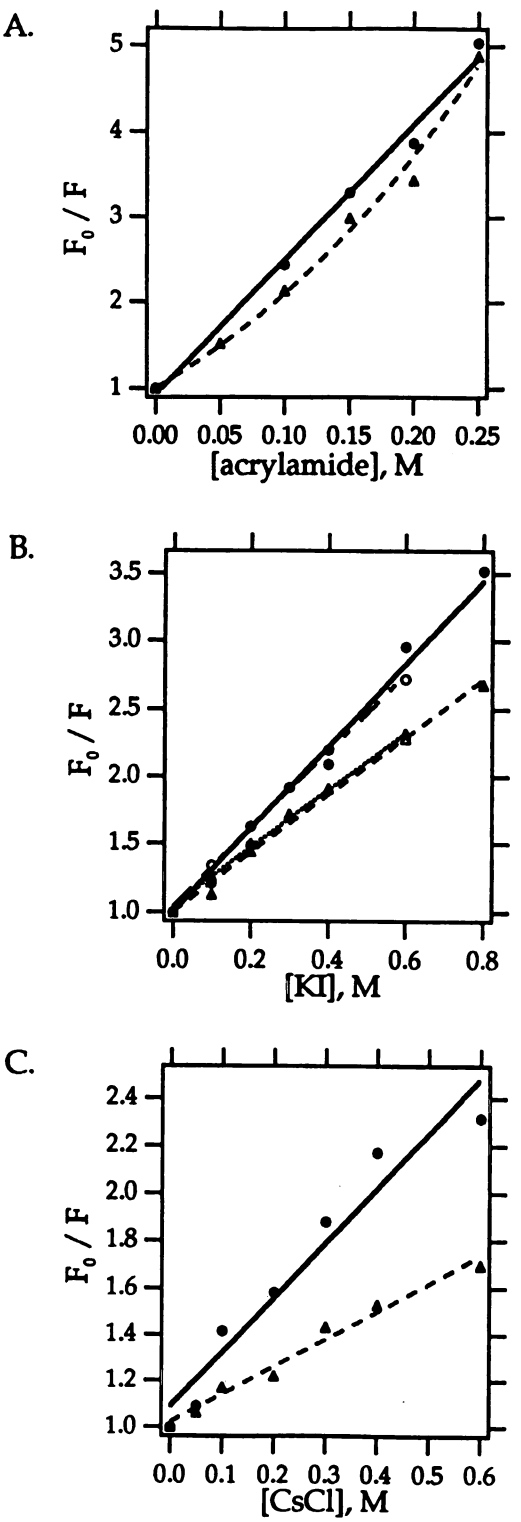
A.
F_0 / F
5
4
3
2
1
0.00 0.05 0.10 0.15 0.20 0.25
[acrylamide], M
B.
F_0 / F
3.5
3.0
2.5
2.0
1.5
1.0
0.0 0.2 0.4 0.6 0.8
[KI], M
C.
F_0 / F
2.4
2.2
2.0
1.8
1.6
1.4
1.2
1.0
0.0 0.1 0.2 0.3 0.4 0.5 0.6
[CsCl], M

Figure 4

Table 1. Analysis of acrylamide quenching data for various GAL4WV36-VP16 proteins.

proteins	quenchers	K_{sv} (M^{-1})	k_q ($M^{-1}ns^{-1}$)	V (M^{-1})	χ^2
GAL4WV36-VP16FW442	acrylamide	15.7	4.2		0.08
	KI	3.1	0.8		0.06
	CsCl	2.3	0.6		0.09
GAL4WV36-VP16FW473	acrylamide	6.6	2.0	2.3	0.09
	KI	2.2	0.7		0.01
	CsCl	1.2	0.4		0.009
GAL4WV36-VP16N FW442	KI	2.9	0.7		0.004
GAL4WV36-VP16C FW473	KI	2.1	0.5		0.005

2.2 M^{-1}, respectively. Similar results are usually obtained for acrylamide and iodide quenching when shielding by the protein matrix is only steric (Eftink, 1991). The apparent lower K_{sv} of KI quenching for both tryptophans in VP16 activation domain indicate that their microenvironments are negatively charged. The fact that there are 4 or 5 acidic amino acids in the vicinity of the tryptophans and the unusually large number of acidic residues in the VP16 activation domain makes these lower K_{sv} values understandable. The Stern-Volmer constants K_{sv} of KI for the two VP16 subdomains (GAL4WV36-VP16N FW442 and GAL4WV36-VP16C FW473) were 2.9 M^{-1} and 2.1 M^{-1}, respectively. These constants are very close to those observed for the full length activators. Thus, truncation of the activator has no effect on theextwnt of exposure of Trp-442 and Trp-473.

Analysis of cesium quenching (Figure 4C) for the full-length proteins with Trp-442 or Trp-473 using the dynamic quenching model gave K_{sv} of 2.3 M^{-1} and 1.2 M^{-1}, respectively. The quenching efficiency of cesium for an indole ring is much lower than that of iodide (Eftink and Ghiron, 1981). The similar values of K_{sv} of both quenchers for both proteins again indicate that the microenvironments surrounding both tryptophans are negatively charged. Additional studies of the ionic strength dependence and pH dependence of the quenching reactions would be needed to further characterize the local electric potentials in the vicinity of these tryptophans (Ando and Asai, 1980).

Time-Resolved Fluorescence Intensity Decay

The fluorescence decays for all the proteins studied were recorded as a function of wavelength across the emission spectrum. By using global analysis, nanosecond time-resolved decay associated spectra (DAS) were obtained. Figure 5 shows the resolved DAS for various samples. A summary of these recovered

Figure 5. Resolution of the total fluorescence spectrum into the decay-associated spectra (DAS). Total, $\tau 1$, $\tau 2$ and $\tau 3$ stand for the total spectrum, the spectrum associated with the short-lifetime component, the spectrum associated with the middle-lifetime component and the spectrum associated with the long-lifetime component, respectively. In panel A, the spectra of GAL4WV36-VP16FW442 are denoted by the solid lines and the spectra of GAL4WV36-VP16FW473 are denoted by the dotted lines. In panel B, the spectra of GAL4WV36-VP16FW442 are denoted by the solid lines and the spectra of GAL4WV36-VP16N FW442 are denoted by the dotted lines.

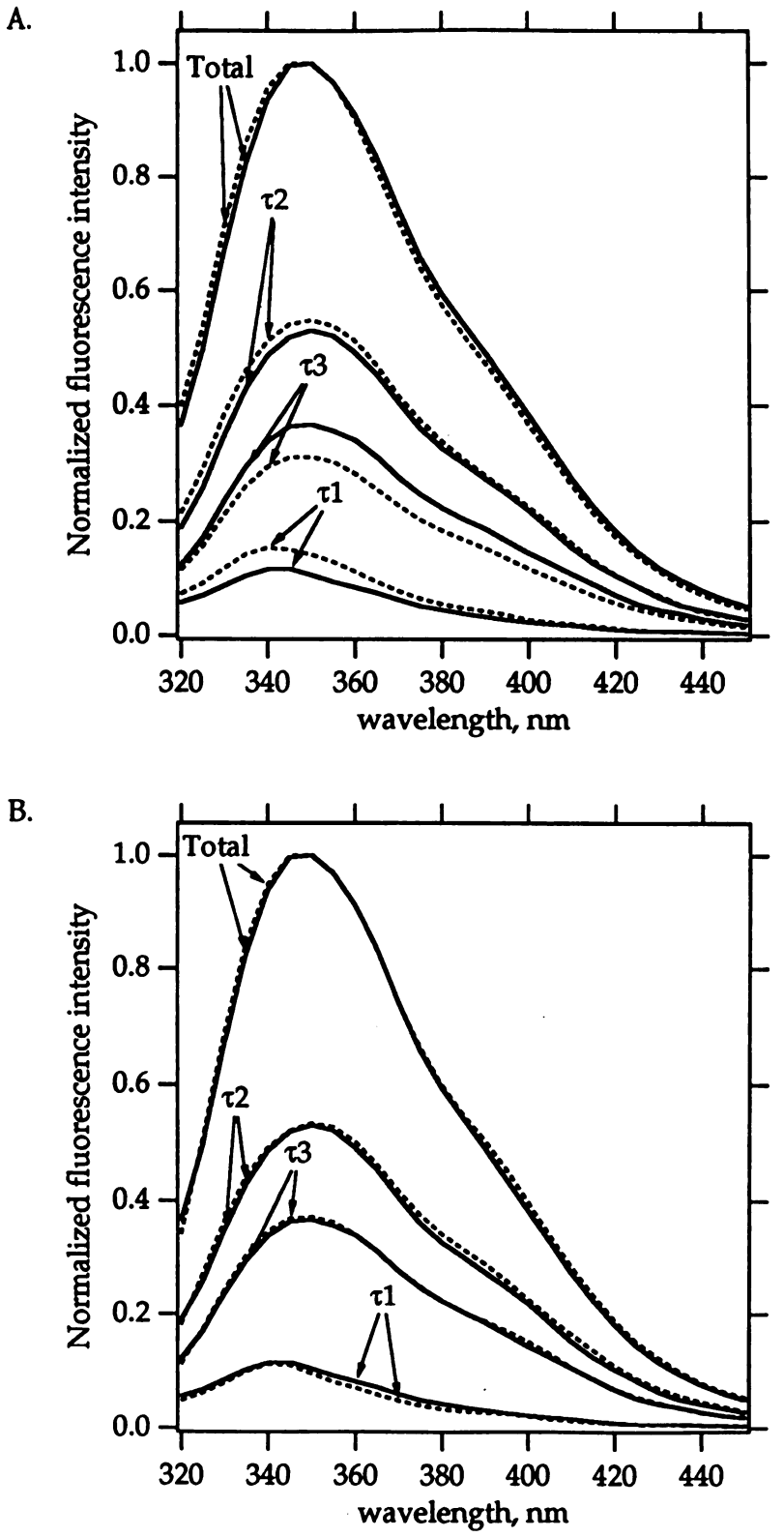
A.
Total
τ2
τ3
τ1
Normalized fluorescence intensity
1.0
0.8
0.6
0.4
0.2
0.0
320
340
360
380
400
420
440
wavelength, nm
B.
Total
τ2
τ3
τ1
Normalized fluorescence intensity
1.0
0.8
0.6
0.4
0.2
0.0
320
340
360
380
400
420
440
wavelength, nm

Figure 5

DAS parameters is shown in Table 2. In all cases, three decay times and a fourth short-lived fixed component (compensating for any scattered excitation or color shift) gave the best fit. The three decay times (0.9, 3.0 and 5.9 ns) are very similar for all proteins. Furthermore, in all four proteins, the relative intensity of the intermediate lifetime contributed about half of the total emission intensity, whereas the long lifetime contributed one-third and the short lifetime contributed one-sixth. The DAS for short lifetimes in all proteins were blue-shifted, with emission maxima near 340 nm. The middle and long lifetimes in both full-length VP16 activation domains had emission maxima at 350 nm, the same as the steady-state emission maxima. In the truncated VP16 N-subdomain, the emission maximum of middle lifetime of Trp- 442 was slightly red shifted (to 355 nm) while the long lifetime maximum was at 350 nm. For the C-subdomain, the emission maximum of long lifetime of Trp- 473 was slightly blue shifted (to 345 nm) while the middle lifetime maximum was at 350 nm. Despite these fairly small differences, the environments surrounding both Trp-442 and Trp-473 seem to be very similar.

Time Resolved Fluorescence Anisotropy Decay

Time-resolved fluorescence anisotropy decay was analyzed for all these proteins. Figure 6 shows the anisotropy decay curves for various samples. The resulting decay parameters are summarized in Table 3. The steady-state anisotropy (r^{SS}) values were also calculated using the life-time instrument in the steady-state photon-counting mode. These small values, in the range of 0.059-0.079, suggest that probes at either position were associated with fast segmental motion as seen in the flexible polypeptide adrenocorticotrophin, where $r^{SS} = 0.06$ (Ross et al., 1981b). By using sum and difference analysis, we found that these decays were best represented by two decay components. In all cases, a "fast"

Table 2. Time-resolved fluorescence intensity decay parametrs for various GAL4WV36-VP16 proteins.

proteins	τ_1(ns)	f_1	λ_1[a] max (nm)	τ_2 (ns)	f_2	λ_2 max (nm)	τ_3 (ns)	f_3	λ_3 max (nm)	$\langle\tau\rangle$ (ns)	χ^{2b}
GAL4WV36-VP16 FW442	0.92	12.9	340	3.05	50.5	350	5.97	36.6	350	3.77	1.25
GAL4WV36-VP16 FW473	0.94	17.5	340	2.89	55.2	350	5.80	27.3	350	3.35	1.27
GAL4WV36-VP16N FW442	0.86	12.3	340	3.01	50.9	355	5.99	36.8	350	3.89	1.30
GAL4WV36-VP16C FW473	0.81	14.7	340	2.73	49.1	350	5.96	36.2	345	3.95	1.28

[a] Approximate emission maximum of the spectrum associated with a specified decay lifetime.

[b] The reduced χ^2 for the global fit (χ^2=1 for an ideal fit).

Figure 6. Time-resolved anisotropy decay curves of various GAL4WV36-VP16 proteins. In panel A, the decay curve of GAL4WV36-VP16FW442 is denoted by the solid line and the decay curve of GAL4WV36-VP16FW473 is denoted by the dotted line. In panel B, the decay curve of GAL4WV36-VP16FW442 is denoted by the solid line and the decay curve of GAL4WV36-VP16N FW442 is denoted by the dotted line. Smoothed curves of the raw data are shown. A scaled lamp curve is given for reference (dashed line).

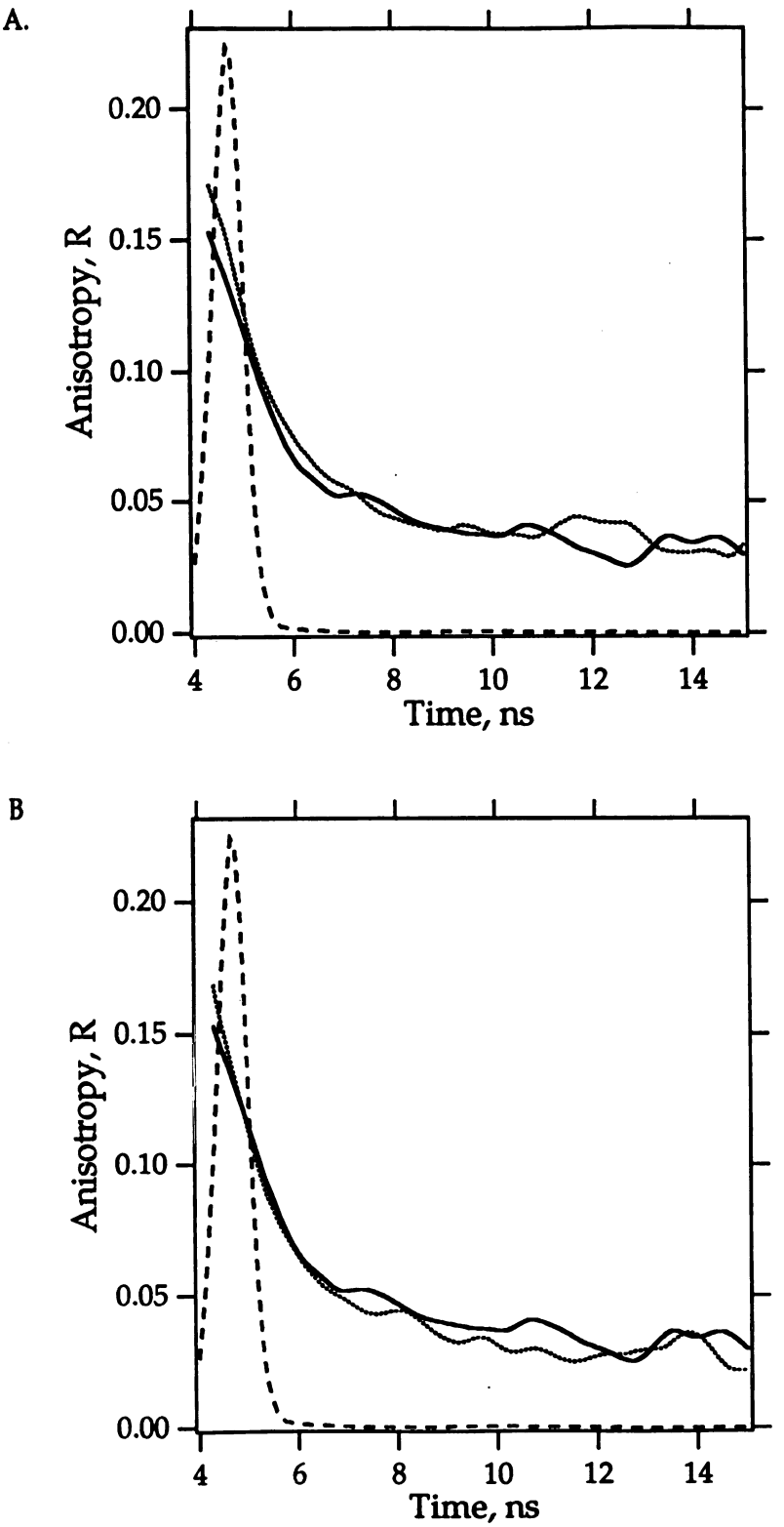
A.
0.20
0.15
0.10
0.05
0.00
Anisotropy, R
4
6
8
10
12
14
Time, ns
B
0.20
0.15
0.10
0.05
0.00
Anisotropy, R
4
6
8
10
12
14
Time, ns

Figure 6

Table 3. Fluorescence anisotropy decay parametrs for various GAL4WV36-VP16 proteins.

proteins	r^{ss}	β_1	ϕ_1 (ns)	β_2	ϕ_2 (ns)	$r_0(app)^a$	Θ^b	χ^{2c}
GAL4WV36-VP16 FW442	0.061	0.102	0.46	0.065	10	0.167	43.6	1.23
GAL4WV36-VP16 FW473	0.072	0.098	0.76	0.058	17	0.156	44.6	1.63
GAL4WV36-VP16N FW442	0.059	0.073	0.80	0.056	9.3	0.129	41.2	1.49
GAL4WV36-VP16C FW473	0.079	0.085	1.32	0.052	63	0.137	44.1	1.51

[a] The apparent limiting time zero anisotropy is defined as $\Sigma\beta_j$. This r_0 does not include β_j for motions faster than 300 ps.

[b] Use r_0(app) to calculate the cone semiangles.

[c] The reduced χ^2 for the fit.

rotation component with a subnanosecond rotational correlation time contributed 60% of the anisotropy decay while a "slow" component (associated with a rotational correlation time greater than 10 ns) accounted for about 40% of the depolarizing process. The longer correlation time has a magnitude roughly consistent with the rotation of the entire protein. The short correlation time reflects localized motion of a smaller protein segment including the Trp. If one assumes the localized motion of Trp is a wobbling of its transition moment within a cone, the extent of this motion can be described by the cone semiangle magnitude. The cone semiangles for these four proteins are large (in the range of 41° to 45°) and are comparable to those of known flexible polypeptides such as adrenocorticotrophin (41°) and glucagon (41°) (Eftink, 1991). These results indicate that the Trp at either position in the VP16 AAD is associated with a very flexible motion of a peptide segment averaging approximately 7-10 residues.

DISCUSSION

The fluorescence studies of the VP16 AAD described here showed that this domain was highly flexible and mobile, suggesting that it is poorly structured. The intrinsic probes placed at either of the two subdomains had very similar properties, suggesting that both subdomains are similarly unstructured. Each showed the characteristic "exposed" fluorescence spectrum with λ_{max} around 350 nm, consistent with highly exposed Trp. Rate constants for quenching by acrylamide for both probes are comparable to those of proteins with exposed Trp residues and little secondary structure. KI quenching for the two probes indicated that their microenvironments were negatively charged, consistent with the primary structures of these subdomains. Time-resolved intensity decay yielded similar lifetime species with similar contributions for

these two Trp residues. Anisotropy decay measurements suggested that both Trps were associated with highly flexible, disordered segments. Noteworthy is that each probe experienced the same environment whether in the full-length context or in truncated subdomains. We infer that deletion of either subdomain had no gross structural effect on the other subdomain. The fact that individual DAS components for each protein are not identical, but are distinguishable in these proteins shows that some structures persist, at least on nanosecond timescales (Green et al., 1990). On the other hand, the Trp multiexponentiality and anisotropy results point toward multiple conformers that intermix; no evidence for rapid (ns) exchange is seen, however. At this juncture, the most attractive view is one of a flexible but "lumpy" structure whose features switch and vary in microseconds. In summary, these fluorescence properties closely resemble those of the well characterized class of polypeptides such as adrenocorticotropin, bombesin and glucagon that have little persistent three-dimensional structure and behave nearly as flexible coils (Ross et al., 1981b; Tran and Beddard, 1985; Cockle and Szabo, 1981). Recent mutational analyses of this domain further suggested the importance of residues Phe-475 and Phe-479 (Triezenberg et al, unpublished data). Trp substitution mutants at these positions can be subjected to the same kinds of studies. We expect similar results will be obtained to illustrate the disordered structure of this AAD.

These results are consistent with results from the previous CD and NMR studies of the isolated VP16 AAD (O'Hare and Williams, 1992; Donaldson and Capone, 1992), in which no significant secondary structure was detected. In those studies, an isolated AAD peptide fragment was used. Structural analyses of the GAL4, GCN4 and glucocorticoid receptor AAD also employed peptide fragments (Van Hoy et al., 1993; Dahlman-Wright et al., 1995). In the present work, we used the chimeric GAL4-VP16 proteins and determined the

transcription activities of these proteins. The concordant results suggest that the presence of the GAL4 DNA binding domain does not induce or confer any specific structure in the VP16 AAD.

Our results indicate that the VP16 AAD is largely disordered in solution and the two aromatic amino acids at position 442 and 473 are solvent exposed. In the primary structure of the VP16 AAD, abundant acidic residues are found near these aromatic residues. These acidic residues may increase the solubility of this domain. The cations in solution balancing these negative charges may interact with the aromatic residues by cation-pi interactions (Dougherty and Stauffer, 1990; Kumpf and Dougherty, 1993; Pang and Kozikowski, 1994). This kind of interaction is thought to stabilize large exposed hydrophobic residues.

The disordered structure of the VP16 AAD may be fundamental to the nature of the activation process. Eukaryotic transcriptional activation is a tremendously complicated process involving a large number of protein-protein interactions. Biochemical and genetic studies have suggested multiple target proteins of activators (Ingles et al., 1991; Choy and Green, 1994; Xiao et al., 1994a; Goodrich et al., 1993; Berger et al., 1992) and many activators enhance transcription synergistically (Carey et al., 1990; Emami and Carey, 1992). To promote such complicated macromolecular associations in vivo, an unstructured polymeric domain may have many advantages over a specific structured domain (Pontius, 1993). For example, flexible, weakly interacting, relatively unstructured polymeric domains can promote the rapid renaturation of complementary DNA strands (Pontius and Berg, 1990; Pontius and Berg, 1991). In such weak interactions, charged groups and hydrophobic residues in an unstructured polymeric domain have been thought to provide a suitable interaction force in the promotion of macromolecular associations (Pontius, 1993). For many AADs, transcriptional activities generally correlate with the number of acidic residues

and are also dependent on the bulky hydrophobic residues (Cress and Triezenberg, 1991; Triezenberg, 1995). According to this model, these residues in the AAD are important to enhance the large number of macromolecular associations in many steps of the transcription process, mainly through non-specific interactions. Relatively unstructured domains in activators may permit interaction with any of several different target proteins and thus may function at several steps in transcription activation (Choy and Green, 1994).

Recent studies show that distinct regions of the large subunit of RNA polymerase II share features in common with either acidic activators or a proline-rich activator (Xiao et al., 1994b; Xiao et al., 1994c). On the basis of the present and other structural studies, we believe these shared domains are relatively unstructured. These domains in the polymerase may interact with the same target proteins as those of activators. A tether-and-competition model for activation has been proposed (Xiao et al., 1994b; Xiao et al., 1994c), in which the dynamic exchange of numerous protein-protein interactions allows the assembly and the disassembly of the transcription complex. Thus, these unstructured domains may facilitate the dynamic exchange interactions in the activation process.

The lack of structure of the VP16 AAD inferred from biophysical studies seems contradictory to the mutational analyses of the VP16 AAD, which showed that its activity is critically dependent on certain types of hydrophobic residues in certain positions. A hypothesis to explain this paradox is that whatever structural element is needed for this specificity is formed during interaction with in vivo targets, and that certain hydrophobic residues in the AAD are critical for this transition. The α-helix structure in VP16 AAD observed under more hydrophobic and low pH conditions and the β-sheet structure induced in AAD of GAL4 and GCN4 in acidic solution support this hypothesis. This hypothesis

can be further tested by studying the biophysical properties of the AAD in the presence of its putative target proteins. To this end, we have begun to examine the fluorescence properties of the VP16 AAD, labeled with Trp analogs as intrinsic probes, in the presence of various general transcription factors (Shen et al., 1995). We have seen evidence for "target induced structure" and we expect that important qualitative and quantitative insights will be gained from this approach. Thus, time-resolved fluorescence may cast new light on mechanisms of transcriptional activation.

ACKNOWLEDGMENT

We thank Shelley Berger for providing DNA template, primer and yeast nuclear extract for the in vitro transcription assay.

REFERENCES

Ando, T., & Asai, H. (1980) *J. Biochem. 88*, 255-264.

Badea, M. G., & Brand, L. (1979) *Methods Enzymol. 75*, 378-425.

Berger, S. L., Cress, W. D., Cress, A., Triezenberg, S. J., & Guarente, L. (1990) *Cell 61*, 1199-1208.

Berger, S. L., Pina, B., Silverman, N., Marcus, G. A., Agapite, J., Regier, J. L., Triezenberg, S. J., & Guarente, L. (1992) *Cell 70*, 251-265.

Carey, M., Lin, Y. S., Green, M., & Ptashne, M. (1990) *Nature 345*, 361-364.

Chasman, D. I., Leatherman, J., Carey, M., Ptashne, M., & Kornberg, R. D. (1989) *Mol. Cell. Biol. 9*, 4746-4749.

Choy, B., & Green, M. R. (1994) *Nature 366*, 531-536.

Cockle, S. A., & Szabo, A. G. (1981) *Photochem. Photobiol. 34*, 23-27.

Cousens, D. J., Greaves, R., Goding, C. R., & O'Hare, P. (1989) *EMBO. J. 8*, 2337-2342.

Cress, W. D., & Triezenberg, S. J. (1991) *Science 251*, 87-90.

Dahlman-Wright, K., Baumann, H., McEwan, I. J., Almlöf, T., Wright, A. P. H., Gustafsson, J-Å., & Härd, T. (1995) *Proc. Natl. Acad. Sci. USA 92* , 1699-1703.

Dale, R. E., Chen, L. A., & Brand, L. (1977) *J. Biol. Chem. 252*, 7500-7510.

Donaldson, L., & Capone, J. P. (1992) *J. Biol. Chem. 267*, 1411-1414.

Dougherty, D. A., & Stauffer, D. A. (1990) *Science 250*, 1558-1560.

Eftink, M. R., & Ghiron, C. A. (1981) *Anal. Biochem. 114*, 199-227.

Eftink, M. R. (1991) In *Protein Structure Determination*, Suelter, C. H. Eds., John Wiley & Sons, Inc., pp. 127-206.

Emami, E. H., & Carey, M. (1992) *EMBO J. 11*, 5005-5012.

Green, S. M., Knutson, J. R., & Hensley, P. (1990) *Biochemistry 29*, 9159-9168.

Gill, S. C., & von Hipple, P. H. (1989) *Anal. Biochem. 182*, 319-326.

Goodrich, J. A., Hoey, T., Thut, C. J., Admon, A., & Tjian, R. (1993) *Cell 75*, 519-530.

Hahn, S. (1993) *Cell 72*, 481-483.

Hayward, G. S. (1993) *Sem. Virol. 4*, 239-251.

Ingles, C. J., Shales, M., Cress, W. D., Triezenberg, S. J., & Greenblatt, J. (1991) *Nature 351*, 588-590.

Jiang, Y., Triezenberg, S. J., & Gralla, J. D. (1994) *J. Biol. Chem. 269*, 5505-5508.

Kinosta, K., Kawato, S., & Ikegami. (1977) *Biophys. J. 20*, 289-305.

Knutson, J. R., Walbridge, D. G., & Brand, L. (1982) *Biochemistry 21*, 4671-4679.

Knutson, J. R., Beechem, J. M., & Brand, L. (1983) *Chem. Phys. Lett. 102*, 501-507.

Kraulis, P. J., Raine, A. R. C., Gadhavi, P. L., & Laue, E. D. (1992) *Nature 356*, 448-450.

Kumpf, R. A., & Dougherty, D. A. (1993) *Science 261*, 1708-1710.

Kunkel, T. A. (1985) *Proc. Natl. Acad. Sci. USA 82* , 488-492.

Leuther, K. K., Salmeron, J. M., & Johnson, S. A. (1993) *Cell 72*, 575-585.

Lipari, G., & Szabo, A. (1980) *Biophys. J. 30*, 489-506.

Ma, J., & Ptashne, M. (1987) *Cell 48*, 847-853.

Narayan, S., Widen, S. G., Beard, W. A., & Wilson, S. H. (1994) *J. Biol. Chem. 269*, 12755-12763.

Nelson, H. (1995) *Curr. Opin. Genetics Dev. 5*, 180-189.

O'Hare, P. (1993) *Sem. Virol. 4*, 239-251.

O'Hare, P., & Williams, G. (1992) *Biochemistry 31*, 4150-4156.

Pan, T., & Coleman, J. E. (1989) *Proc. Natl. Acad. Sci. USA 86*, 3145-3149.

Pang, Y. P., & Kozikowski, A. P. (1994) *Comp-Aid. Mol. Des. 8*, 669-681.

Paranjape, S. M., Kamakaka, R. T., & Kadonaga, J. T. (1994) *Ann. Rev. Biochem. 63*, 265-297.

Pontius, B. W. (1993) *Trends in Biochem. Sci. 18*, 181-186.

Pontius, B. W., & Berg, P. (1990) *Proc. Natl. Acad. Sci. USA 87*, 8403-8407.

Pontius, B. W., & Berg, P. (1991) *Proc. Natl. Acad. Sci. USA 88*, 8237-8241.

Ptashne, M. (1988) *Nature 355*, 683-689.

Regier, J. L., Shen, F., & Triezenberg, S. J. (1993) *Proc. Natl. Acad. Sci. USA 90*, 883-887.

Ross, J. B. A., Schmidt, C. J., & Brand, L. (1981a) *Biochemistry 20*, 4369-4377.

Ross, J. B. A., Rousslang, K., & Brand, L. (1981b) *Biochemistry 20*, 4361-4369.

Sadowski, I., Ma, J., Triezenberg, S., & Ptashne, M. (1988) *Nature 335*, 563-564.

Shen, F., Triezenberg, S. J., Hensley, P., Porter, D., & Knutson, J. (1995) Manuscript in preparation.

Sigler, P. (1988) *Nature 333*, 210-212.

Tjian, R., & Maniatis, T. (1994) *Cell 72*, 5-8.

Tran, C. D., & Beddard, G. S. (1985) *Eur. J. Biochem. 13*, 59-64.

Triezenberg, S. J. (1995) *Curr. Opin. Genetics Dev. 5*, 190-196.

Triezenberg, S. J., LaMarco, K. L., & McKnight, S. L. (1988a) *Genes Dev. 2*, 730-742.

Triezenberg, S. J., Kingsbury, R. C., & McKnight, S. L. (1988b) *Genes Dev. 2*, 718-729.

Van Hoy, M., Leuther, K. K., Kodadek, T., & Johnson, A. J. (1993) *Cell 72*, 587-594.

Walker, S., Greaves, R., & O'Hare, P. (1993) *Mol. Cell. Biol. 13*, 5233-5244.

Walker, S., Hayes, S., & O'Hare, P. (1994) *Cell 79*, 841-852.

Wilson, A. C., LaMarco, K., Peterson, M. G., & Herr, W. (1993) *Cell 74*, 115-125.

Xiao, H., Pearson, A., Coulombe, B., Truat, R., Zhang, S., Regier, J. L., Triezenberg, S. J., Reinberg, D., Flores, O., Ingles, C. J., & Greenblatt, J. (1994a) *Mol. Cell. Biol. 14*, 7013-7024.

Xiao, H., Friesen, J. D., & Lis, J. T. (1994b) *Mol. Cell. Biol. 14*, 7507-7516.

Xiao, H., Lis, J. T., Xiao, H., Greenblatt, J., & Friesen, J. D. (1994c) *Nucleic Acids Res. 22*, 1966-1973.

Yankulov, K., Blau, H., Purton, T., Robert, S., & Bentley, D. L. (1994) *Cell 77*, 749-759.

Zawel, L. R., & Reinberg, D. (1995) *Ann. Rev. Biochem. 64*, 533-561.

CHAPTER IV

TRANSCRIPTIONAL ACTIVATION DOMAIN OF THE HERPESVIRUS PROTEIN VP16 BECOMES CONFORMATIONALLY CONSTRAINED UPON INTERACTION WITH BASAL TRANSCRIPTION FACTORS

INTRODUCTION

The herpes simplex type-1 virion protein VP16 is a potent transcriptional activator that specifically activates viral immediate (IE) gene expression (Hayward, 1993; O'Hare, 1993). As a transcriptional regulatory protein, it contains two functional domains. The amino-terminal portion of the protein, in association with host cellular proteins, binds to specific sequences upstream of the IE core promoter (Walker et al, 1994; Wilson et al., 1993). The transcriptional enhancement activity resides in the carboxyl-terminal 78 amino acids (Triezenberg et al., 1988; Cousens et al., 1989). This domain can strongly activate transcription in various systems when attached to the DNA-binding domain of a heterologous protein (Sadowski et al., 1989). The VP16 activation domain is rich in acidic residues and has been regarded as a prototype acidic activation domain (AAD) (Mitchell and Tjian, 1989). Extensive mutational studies of this domain have identified aromatic and hydrophobic amino acids critical for its activity, for example the Phe at position 442 (Cress & Triezenberg, 1990; Regier et al., 1993). These studies have further suggested that the VP16 AAD contains two independent subdomains: the N-subdomain (residues 413-456) and the C-subdomain (residues 453-490) (Regier et al., 1993; Walker et al., 1994; Goodrich et al., 1993).

The activation mechanisms of eukaryotic transcriptional activators have been the focus of many studies (Zawel and Reinberg, 1995; Triezenberg, 1995). In addition to alleviating chromatin-mediated inhibition (Paranjape et al., 1994), activators have been proposed to interact with components of the basal transcription apparatus to stimulate or stabilize the formation of the transcription initiation complex at the promoter. Biochemical approaches have identified several potential targets of activation domains, particularly for the AAD of VP16. TBP (TATA-box binding protein) was the first basal factor shown to directly bind to the VP16 AAD (Stringer et al., 1990). The specificity of this interaction was demonstrated by a correlation between binding of VP16 mutants to TBP and the transcription activity of these mutants (Ingles et al., 1991). Later, VP16 was shown to directly interact with another basal transcription factor, TFIIB (Lin et al., 1991), although there is some discrepancy about the specificity of this interaction (Roberts and Green, 1994; Walker et al., 1993; Goodrich et al., 1993). Recently, a specific interaction between VP16 and a subunit of TFIIH has been reported (Xiao et al., 1994a), as have interactions between VP16 and putative co-activator or adaptor proteins (Goodrich et al., 1993; Silverman et al., 1994). Direct interactions between various of these target proteins and many other activation domains have also been shown (Triezenberg, 1995). Although the physical interactions have been demonstrated, their relevance and role in transcriptional activation are still largely unknown.

Despite abundant functional studies of activation domains, little is known of their structures. No activation domain structure has yet been solved by X-ray crystallographic analyses or NMR. The limited biophysical studies of several AADs suggest that isolated AADs are unstructured (O'Hare and Williams, 1992; Donaldson and Capone, 1992; Van Hoy et al., 1993; Schmitz et al., 1994; Dahlman-Wright et al., 1995). We recently reported fluorescence analyses

employing chimeric proteins comprising the GAL4 DNA-binding domain (1-147) fused to the VP16 activation domain (Shen et al., 1995a). Trp residues were substituted for Phe at either 442 or 473 of VP16, thus providing unique fluorescence probes at two positions. Dynamic quenching, time-resolved fluorescence decay and time-dependent anisotropy decay studies showed that the Trp residues at either position are solvent exposed and highly mobile. Our results, in agreement with CD and NMR studies of this domain, reveal that the isolated VP16 AAD is poorly structured. Noteworthy is that many of the biophysical studies suggest that under certain conditions (low pH, hydrophobic solvent) these AADs can acquire specific conformations such as helix and β-sheet. These conditions might mimic the in vivo conditions under which the AAD interacts with its target proteins. The AADs therefore have been hypothesized to adopt a specific conformation in the presence of their target proteins. However, no structural characterizations of these AADs have yet been carried out in the presence of their target proteins.

One major difficulty in studying protein-protein interactions by various biophysical means is that the signals from different proteins overlap and make the interpretation ambiguous. Recently, several groups reported that Trp analogs (5-hydroxy-tryptophan or 7-aza-tryptophan) can be successfully incorporated into proteins by using Trp auxotrophic E. coli strains and supplementing the growth media with the relevant Trp analog (Ross et al., 1992; Hogue et al., 1992; Hogue and Szabo, 1993). The excitation spectra of these Trp analogs are shifted to longer wavelengths compared to Trp itself. Hence, fluorescence of proteins containing these Trp analogs can be selectively excited in the presence of other proteins containing natural Trp. Here we used this strategy to study the structural features of the VP16 AAD in the presence of two basal transcription factors TBP and TFIIB. Our results indicate that the structure of the

VP16 AAD becomes considerably constrained upon its interaction with these basal factors, particularly with TBP.

EXPERIMENTAL PROCEDURES

Chemicals And Reagents

L-tryptophan, L-5-hydroxytryptophan, and D, L-7-azatryptophan were purchased from Sigma. The E. coli tryptophan auxotrophic strain CY15077 (W3110ΔtrpEA2) and the $lacI^q$-bearing plasmid pMS421 were kindly provided by Dr. Charles Yanofsky. Plasmid pKA9 carrying the *S. cerevisiae* SPT 15 gene in a pET expression vector was a gift of Dr. Fred Winston. Plasmid phIIB expressing the human TFIIB in a pET vector was a gift of Dr. Danny Reinberg. Yeast nuclear extract and plasmid pCZ3GAL were gifts of Dr. Shelley Berger. HeLa cell nuclear extracts and plasmid pML were kindly provided by Chun-hsiang Chang and Dr. Zachary Burton.

Purification Of 5-OH-Trp or 7-aza-Trp Incorporated GAL4-VP16

Expression plasmids for GAL4-VP16 fusion proteins with unique Trp codons in the VP16 activation domain have been described (Shen et al., 1995a). E. coli strain CY15077 was transformed with pMS421 and with an expression plasmid for one of the various GAL4-VP16 fusion proteins. Cell growth and Trp analog incorporation procedures were followed as described (Ross et al., 1992) with some modifications. The cells were maintained under ampicillin (100 μg/ml) and streptomycin (20 μg/ml) selection. An overnight culture was diluted 1:100 into M9 medium supplemented with 0.1 mM $CaCl_2$, 1 mM $MgSO_4$, 0.5% glucose, 0.1% thiamine, 1% casamino acids and 0.25 mM L-tryptophan. The culture was grown at 37°C to an OD_{550} of 0.6. The cells were then collected by

centrifugation and resuspended in the original volume of M9 medium, except that 0.25 mM L-5-OH-Trp or 0.5 mM D, L-7-aza-Trp was added in place of L-Trp. After the culture was grown for additional 20 minutes, expression of GAL4-VP16 fusion proteins was induced by addition of IPTG to final concentration of 1 mM. The cells were harvested after 2hr of growth at 37°C, and the analog-labeled GAL4-VP16 proteins were purified using procedures described elsewhere (Shen et al., 1995a).

Purification of Recombinant TBP

TBP was purified using a procedure from M. Brenowitz (pers. communication) with minor modifications. E. coli BL21 (DE3) cells carrying the plasmids pLysS and pKA9 were grown at 37°C in LB medium containing 30 μg/ml chloramphenicol and 25 μg/ml ampicillin. TBP expression was induced by the addition of 1 mM IPTG when cell density reached an OD_{600} of 0.4. Cells were shifted to 30°C to grow for an additional 2 hr. Cells were harvested by centrifugation and resuspended in a buffer comprising 20 mM HEPES, pH 7.9, 1 mM EDTA, 1 mM EGTA, 10 mM 2-mercaptoethanol, 2 μg/ml pepstatin, 2 μg/ml leupeptin, 1 mM benzamidine and 0.8 mM PMSF, in a volume of 20 ml per liter of culture. After lysis by sonication, the cell debris was removed by centrifugation. Protamine sulfate was added to the supernatant to 0.3 mg/ml. The precipitate was removed by centrifugation and the supernatant was dialyzed against buffer D (20 mM HEPES, pH 7.9, 20% glycerol, 1 mM EDTA) plus 100 mM KCl. The crude protein fraction was loaded onto a Pharmacia Q-Sepharose Fast Flow column, from which TBP eluted mainly in the flow through. This Q-Sepharose Fast Flow chromatography step was repeated, and the flow through fraction was loaded onto a Pharmacia S-Sepharose Fast Flow column. The column was washed with buffer D plus 100 mM KCl, and then eluted with a

linear gradient from 100 mM KCl to 460 mM KCl in buffer D. Fractions containing TBP (at 95% purity or greater as analyzed by SDS-PAGE) were stored at -70°C.

Purification of Recombinant TFIIB

TFIIB was purified using modified published procedures (Barberis et al., 1993). E. coli BL21 cells containing phIIB were grown in LB media containing 100 µg/ml ampicillin at 37°C. TFIIB expression was induced by the addition of 0.4 mM IPTG when an OD_{600} of 0.6 was reached. Cells were harvested after a 2hr additional growth. The cell pellet were resuspended (50 ml/liter culture) in a buffer comprising 20 mM HEPES, pH 7.9, 25 mM EDTA, 10 mM 2-mercaptoethanol, 0.2 mM PMSF, 0.2 mM benzamidine, 2 µg/ml pepstatin and 100 mM KCl. The cells were broken by sonication and the lysate was cleared by centrifugation. Polyethyleneimine (pH 7.9) was added dropwise to the supernatant to 0.1% and the precipitate was removed by centrifugation. Ammonium sulfate was added to the supernatant to 45% saturation. The precipitated proteins were resuspended in the resuspension buffer and dialyzed against buffer B (20 mM HEPES, pH 7.9, 10% glycerol, 0.2 mM EDTA, 0.2 mM EGTA, 0.2 mM PMSF, 2 mM dithiothreitol) plus 100 mM KCl. The crude protein fraction was loaded onto a Whatman P-11 column. The column was washed with buffer B plus 100 mM KCl, and then washed with buffer B plus 300 mM KCl. The column was eluted with a linear gradient of 300 mM to 800 mM KCl in buffer B. Fraction containing TFIIB of highest purity (eluting between 620 - 670 mM KCl) were pooled and dialyzed against buffer B plus 100 mM KCl and loaded onto a pre-equilibrated DE-52 column. The flow through contained TFIIB at greater than 95% homogeneity. The protein was stored at -70°C.

GAL4-VP16 Activity Assay

Activities of the various GAL4-VP16 fusion proteins were tested in in vitro transcription reactions using yeast nuclear extracts as described (Berger et al., 1990; Shen et al., 1995a).

Recombinant TBP And TFIIB Activity Assay

In vitro transcription assays using HeLa nuclear extracts were performed as described (Chang et al., 1993). The template plasmid pML, containing the adenovirus major late promoter (AdMLP) was linearized with SmaI. The activity of purified recombinant TBP was tested using HeLa extracts pre-incubated at 47°C for 15 min. to inactivate endogenous TBP (Horikoshi et al., 1990). To test the activity of recombinant TFIIB , the HeLa nuclear extract was depleted of endogenous TFIIB as follows: 0.12 ml agarose- conjugated antibodies directed against TFIIB (Santa Cruz Biotechnology) was equilibrated with a buffer comprising 20 mM HEPES, pH 7.9, 20% glycerol, 1 mM EDTA, 0.2 mM EGTA, 0.5 mM dithiothreitol, 0.2 mM PMSF and 500 mM KCl. 5M NaCl and 2% Triton X-100 was added to 120 µl HeLa nuclear extract to bring the final NaCl concentration to 500 mM and the final Triton X-100 concentration to 0.02%. This extract was incubated with the equilibrated anti-hTFIIB agarose bead at room temperature for 40 min. and at 4°C for an additional 1.5 hr. The agarose beads were centrifuged at 2.5 krpm for 5 min. and the supernatant was used as the TFIIB depleted extract.

Spectroscopy

All proteins were dialyzed against PBS buffer (pH 7.4, 8.1 mM Na_2HPO_4, 1.4 mM KH_2PO_4, 137 mM NaCl and 2.7 mM KCl) containing 8% glycerol (v/v). Protein concentrations were estimated from 280 nm extinction coefficients based

on amino acid composition (Gill and von Hippel, 1989). The 280 nm extinction coefficients of 5-OH-Trp and 7-aza-Trp were used as described (Hogue and Szabo, 1993). Absorbance measurements were obtained using a Perkin-Elmer Lambda 4B UV/VIS spectrophotometer.

The steady-state fluorescence spectra were obtained with a SLM 8000 spectrofluorometer as described (Shen et al., 1995a). The excitation wavelength was 309 nm. The emission spectra titration experiments of 7-aza-Trp incorporated GAL4-VP16 were performed by recording the initial emission spectrum of the 4 μM 7-aza-Trp incorporated GAL4-VP16, and then adding small aliquots of concentrated TBP or TFIIB solution, and recording emission spectra until no further change could be detected. The same amounts of TBP or TFIIB were added to the buffer control and these blank emission spectra were also recorded. Final emission spectra were corrected for blank control and for dilution.

Steady-state fluorescence anisotropy was measured using a L-format detection configuration. The excitation bandpass was 4 nm and the emission bandpass was 8 nm. Excitation was at 309 nm and emission was at 360 nm. Every data point was measured at least 8 times. Data was fit to the equations (Lakowicz, 1983) describing formation of the 1:1 binary complex between GAL4-VP16 and TBP:

$$r = \frac{r_B f_B I_B + r_F (1 - f_B) I_F}{f_B I_B + (1 - f_B) I_F} \qquad (1)$$

where r is the measured anisotropy when the fluorophore are present in both the free form (5-OH-Trp incorporated GAL4-VP16) and the bound form (complex with TBP), r_B and r_F are the anisotropy of the free and bound fluorophores, f_B

and f_F refer to the fraction of the total fluorophore which is present in the bound and free forms, I_B and I_F are the fluorescence intensities of the fluorophore in bound or free forms.

and:

$$f_B = \frac{([V]+[T]+K_D)-\sqrt{([V])+[T]+K_D)^2-4[V][T]}}{2[V]} \qquad (2)$$

where [V] is the total concentration of the 5-OH-Trp incorporated GAL4-VP16 used in the study and [T] is the concentration of the added TBP. K_D is the dissociation constant for the association between GAL4-VP16 and TBP. K_D values were determined using least-squares regression (IGOR, Wavemetrix, Lake Oswego, OR).

Quenching experiments were performed at an excitation wavelength of 309 nm. Aliquots of 8M acrylamide were added to 0.4 ml 2 μM 5-OH-Trp incorporated GAL4-VP16 (or mixtures of 2 μM 5-OH-Trp incorporated GAL4-VP16 and 4 μM TBP or TFIIB) or 4 μM 7-aza-Trp incorporated GAL4-VP16 (or mixtures of 4 μM 7-aza-Trp incorporated GAL4-VP16 and 8 μM TBP or TFIIB) and to the appropriate solvent blank (0.4 ml buffer or 8 μM TBP or TFIIB). The values of fluorescence emission intensity at 338 nm (for 5-OH-Trp incorporated proteins) or at 396 nm (for 7-aza-Trp incorporated proteins) were corrected for dilution and for blank. Quenching data were analyzed by the classic Stern-Volmer equation for dynamic quenching:

$$F_0/F = 1+K_{sv}[Q] \qquad (3)$$

or by the single species dynamic-static quenching equation:

$$F_0/F = (1+K_{sv}[Q])\exp(V[Q]) \quad (4)$$

or by the two species quenching equation:

$$F_0/F = \frac{1+K_a[Q]}{1+K_a(1-f_a)[Q]} \quad (5)$$

where F_0 and F are the fluorescence intensity in the absence and presence of quencher, [Q] is the quencher concentration, K_{sv} is the Stern-Volmer dynamic quenching constant. V is the static quenching constant. f_a is the fractional contribution of the fluorophores which are accessible to the quencher and K_a is the Stern-Volmer constant for the accessible fraction. K_{sv}, V, f_a and K_a values were determined using least-squares regression (IGOR, Wavemetrix, Lake Oswego, OR).

Time-resolved fluorescence was measured on a single photon counting fluorometer (Green et al., 1990; Shen et al., 1995a). Anisotropy decay curves were obtained by alternatively recording emission oriented parallel and perpendicular to the plane of excitation. When the anisotropy decay curves for the mixture of 2 μM 5-OH-Trp incorporated GAL4-VP16 with 4 μM TBP or TFIIB were recorded, those of the appropriate blank (4 μM TBP or TFIIB) were also recorded at the same time. Excitation wavelength was at 309 nm and emission wavelength was at 360 nm. Time per channel was 90 ps and 512 channels were recorded. Time-resolved fluorescence data were analyzed by Denise Porter and Jay Knutson at National Institutes of Health.

RESULTS

Incorporation Of 5-OH-Trp And 7-aza-Trp Into GAL4WV36-VP16 Proteins

By using a Trp auxotrophic E. coli strain, 5-OH-Trp or 7-aza-Trp were biologically incorporated into various GAL4-VP16 proteins (Figure 1). These proteins were purified to more than 95% homogeneity and were functionally active when tested by in vitro transcription assays (data not shown). Therefore, the structural features revealed by these proteins should reflect those of the wild type VP16 AAD. Figure 2A shows the peak normalized absorbance spectra of GAL4-VP16 proteins with Trp or its analogs incorporated at position 442 of the VP16 AAD. The absorbance spectrum of the protein containing 5-OH-Trp demonstrated a characteristic shoulder between 290 nm and 320 nm, while that of the protein containing 7-aza-Trp showed extended low energy absorbance. The fluorescence excitation spectra of the same GAL4-VP16 fusion proteins (Figure 2B) demonstrate that the Trp analogs at position 442 can be selectively excited at 310 nm. Figure 2C shows the normalized emission spectra of these fusion proteins. GAL4-VP16 containing 5-OH-Trp had an emission maximum at 340 nm, the same maximum observed for the free amino acid analog. GAL4-VP16 containing 7-aza-Trp showed an emission maximum at 396 nm, close to that of 7-aza-Trp in aqueous solution (398 nm). Absorbance spectra, excitation spectra and emission spectra of GAL4-VP16 proteins with Trp analogs incorporated at position 473, or at position 442 in a truncated activation domain, all showed similar properties, indicating that both Trp analogs were successfully incorporated into all the proteins. Moreover, the concordance of the spectra of the labeled proteins with the spectra of free amino acid analogs supports our observation that these residues of the VP16 activation domain are largely solvent-exposed (Shen et al., 1995a).

Figure 1. Schematic representations of the various transactivators used in this study. All proteins contain the GAL4 DNA binding domain (aa. 1-147) with the valine substitution at position 36, designated as GV. All proteins also contain a 2 or 3 amino acid linker between GAL4 domain and VP16 domain. GV-5HW442 or GV-5HW473 are in-frame fussions of GV to the VP16 activation domain (aa. 413-490) with the incorporation of 5-hydroxy-tryptophan at position 442 or 473, respectively. N-5HW442 contains a truncated VP16 activation domain (aa. 411-456) with5-hydroxy-tryptophan at position 442. GV-7AW442 or GV-7AW473 contain the full-length VP16 activation domain (aa. 413-490) with the incorporation of 7-aza-tryptophan at position 442 or 473, respectively.

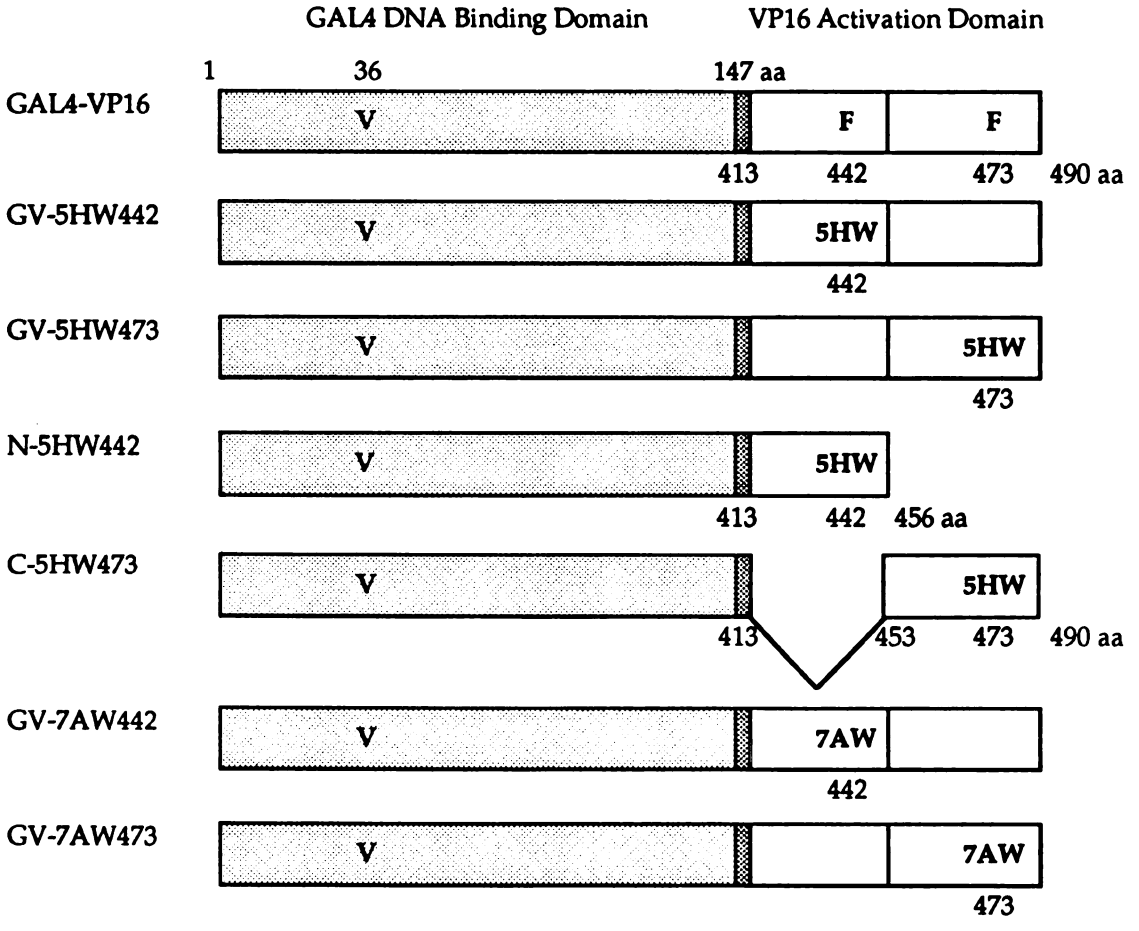
GAL4 DNA Binding Domain
VP16 Activation Domain
1
36
147 aa
GAL4-VP16
V
F
F
413
442
473
490 aa
GV-5HW442
V
5HW
442
GV-5HW473
V
5HW
473
N-5HW442
V
5HW
413
442
456 aa
C-5HW473
V
5HW
413
453
473
490 aa
GV-7AW442
V
7AW
442
GV-7AW473
V
7AW
473

Figure 1

Figure 2. Spectroscopic properties of GAL4-VP16 fusion proteins bearing Trp analogs at position 442 or 473. (A) Peak-normalized absorbance spectra. (B) Peak-normalized excitation spectra. Emission was observed at 360 nm for GV-FW442 and GV-5HW442, and at 380 nm for GV-7AW442. (C) Peak-normalized emission spectra with excitation at 310 nm. In all panels, solid line: native GV-FW442; dotted line: GV-5HW442; and dashed line: GV-7AW442.

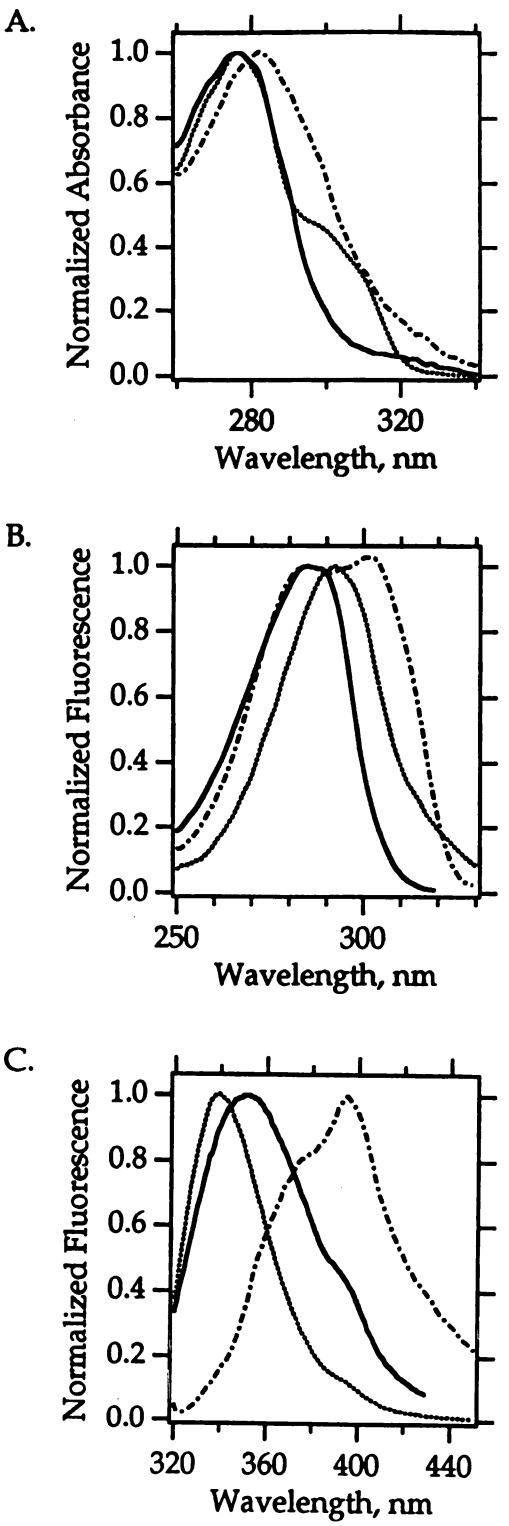
A.
Normalized Absorbance
1.0
0.8
0.6
0.4
0.2
0.0
280
320
Wavelength, nm
B.
Normalized Fluorescence
1.0
0.8
0.6
0.4
0.2
0.0
250
300
Wavelength, nm
C.
Normalized Fluorescence
1.0
0.8
0.6
0.4
0.2
0.0
320
360
400
440
Wavelength, nm

Figure 2

The presence of 5-OH-Trp or 7-aza-Trp in the GAL4-VP16 proteins enables the fluorescence of the fusion proteins to be selectively excited at 310 nm in the presence of other Trp-containing proteins. Recombinant basal transcription factors TBP and TFIIB were purified from E. coli, and their transcriptional activities were confirmed using specifically-depleted nuclear extracts (data not shown). As expected, these proteins were not efficiently excited using 310 nm light; the fluorescence observed for a two fold molar excess of TBP or TFIIB when excited at 310 nm amounted to less than 10% of the signal observed for GAL4-VP16 proteins bearing Trp analogs in the presence of a two fold molar excess of TBP or TFIIB.

Interaction Between TBP And VP16 AAD Changes The Polarity Of The Environments Surrounding 7AW-442 And 7AW-473

The emission spectra of 7-aza-Trp is very sensitive to the polarity of the environment (Hogue and Szabo, 1993). In aqueous solution, its emission maximum is near 400 nm, but in hydrophobic environments a maximum at 370 nm is observed. To test whether TBP or TFIIB could change the polarity around residues 442 and 473 in the VP16 AAD, increasing amounts of TBP or TFIIB were added to GV-7AW442 or GV-7AW473 and emission spectra were recorded. In the absence of either basal transcription factor, both GV-7AW442 and GV-7AW473 showed the characteristic 396 nm emission maximum of exposed 7-aza-Trp. With the addition of increasing amounts of TBP to either labeled protein, the relative intensity around 370 nm region increased gradually and eventually reached saturation (Figure 3A and Figure 3B). To quantitate the spectra shift, ratio of the emission intensities at the two wavelengths (F_{376} / F_{396}) was calculated at each concentration of TBP or TFIIB (Figure 3C and Figure 3D).

Figure 3. Effects of TBP and TFIIB on fluorescence emission spectra of GV-7AW442 (panel A) and GV-7AW473 (panel B) at 310 nm excitation. 2 μM of the activators were used in these experiments. Solid line: activator alone; dotted line: titration with 2 μM TBP; dashed line: titration with 4 μM TBP; and dash-dotted line: titration with 8 μM TBP. The ratio of emission intensity (F_{376} / F_{396}) of GV-7AW442 and GV-7AW473 in the presence of TBP (triangles) and TFIIB (squares) are shown in panel C and panel D, respectively.

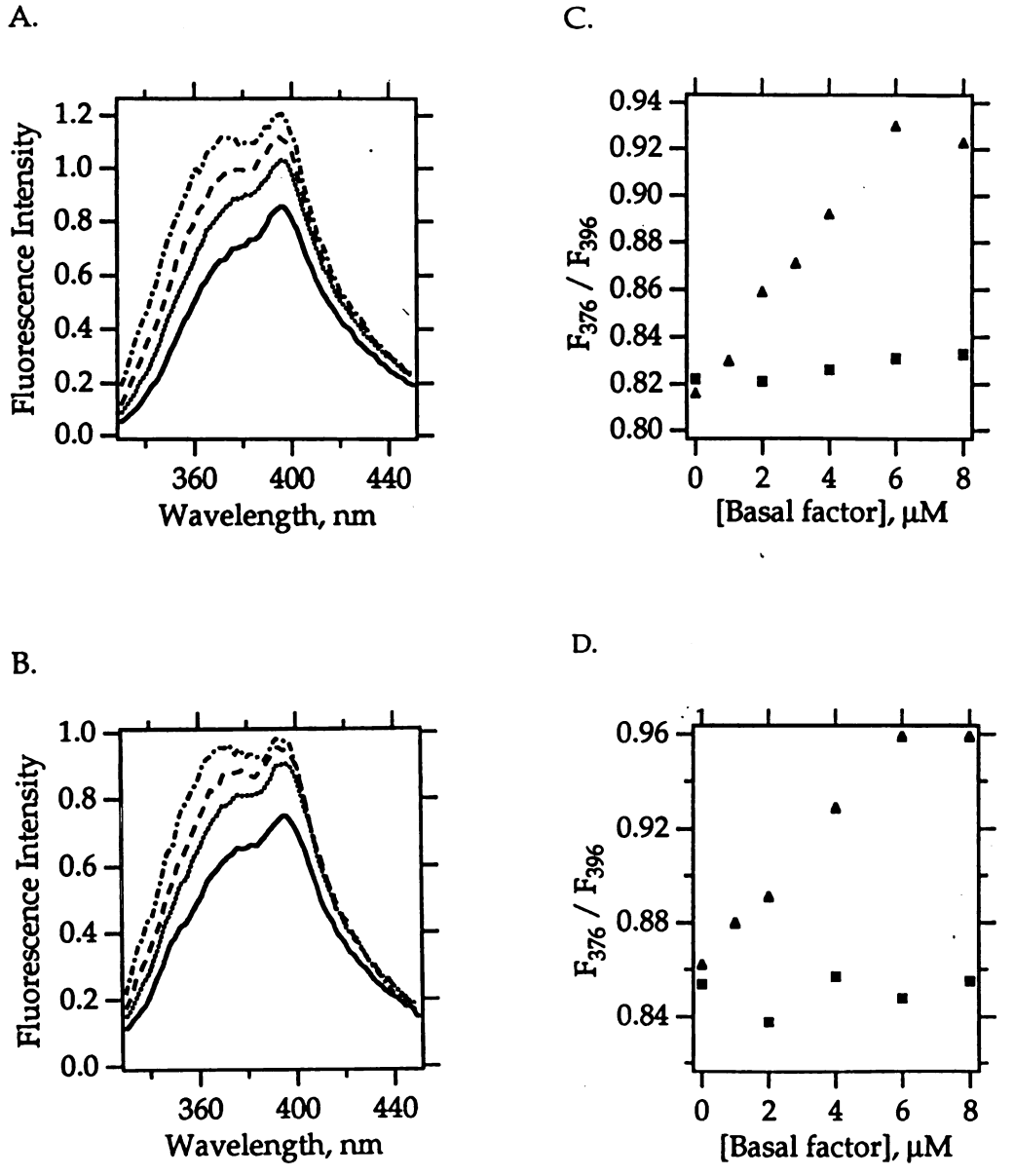
A.
C.
B.
D.
Fluorescence Intensity
Wavelength, nm
F_{376} / F_{396}
[Basal factor], μM

Figure 3

These ratios increased from 0.81 to 0.96 with the addition of TBP. Thus, residues at both positions are found in more hydrophobic environments in the presence of TBP. In contrast, addition of TFIIB did not increase the relative intensity around 370 nm region of these proteins. The F_{376} / F_{396} ratio was unchanged by the addition of increasing amounts of TFIIB (Figure 3C and Figure 3D), suggesting that even if TFIIB interacts with the activator, the polarity of the environments surrounding both 442 and 473 remain the same.

It should also be noted that the quantum efficiency of GV-7AW442 and GV-7AW473 increased modestly in the presence of TBP. The relative intensity around 370 nm region increased; however, the emission maximum is still at 396 nm. These fluorescence properties most closely match those of the model compound, 7-aza-indole, in alcohol, rather than those of 7-aza-indole in aprotic solvents such as acetonitrile (Chapman and Maroncelli, 1992). Hydroxyl groups in alcohols induce tautomerization of 7aza-indole, resulting in two populations of fluorescing molecules. The results of this study implies that the surroundings of both 7AW-442 and 7AW-473 become more hydrophobic; however, either the solvent is not totally excluded from these residues, or there are nearby polar residues which hydrogen bond to the 7AW to cause tautomerization.

Interaction Between Basal Factors And VP16 AAD Reduces The Solvent Accessibility Of Residues At Amino Acid Positions 442 And 473

Acrylamide quenching experiments were performed to test whether the presence of TBP or TFIIB affected the solvent accessibility of the fluorophores at residues 442 and 473. Activator proteins labeled with 5-OH-Trp were mixed with saturating amounts of TBP or equivalent amount of TFIIB in the presence of increasing concentrations of acrylamide. The Stern-Volmer plots of these quenching experiments are shown in Figure 4, and the best fit parameters are

Figure 4. Stern-Volmer plots for the quenching of the fluorescence of GV-5HW442 (panel A) and GV-5HW473 (panel B) by acrylamide. 2 μM of the activators and 4 μM of TBP or TFIIB were used in these experiments. Closed circles: activator alone; triangles: in the presence of TBP; and squares: in the presence of TFIIB. Each set of data were compared to the various quenching models described in the text. The solid line represents the quenching model to which the data are best fit.

A.

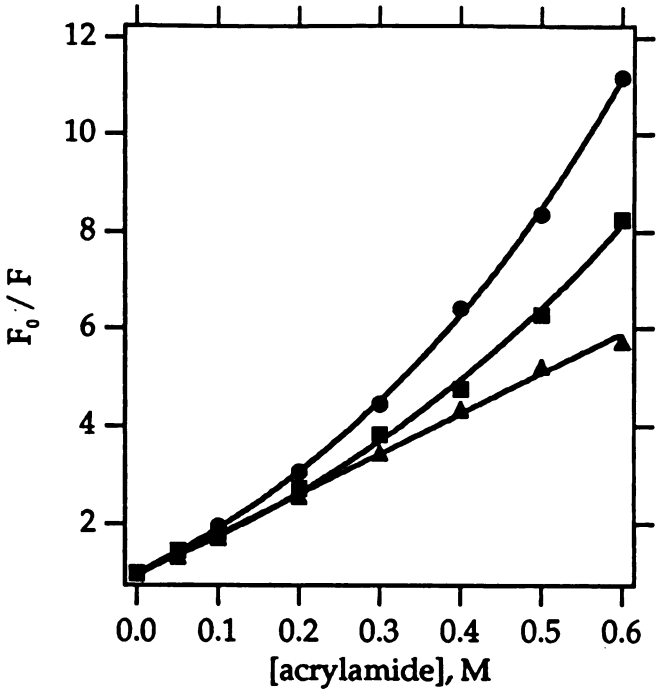
12
10
8
6
4
2
F_0 / F
0.0
0.1
0.2
0.3
0.4
0.5
0.6
[acrylamide], M

B.

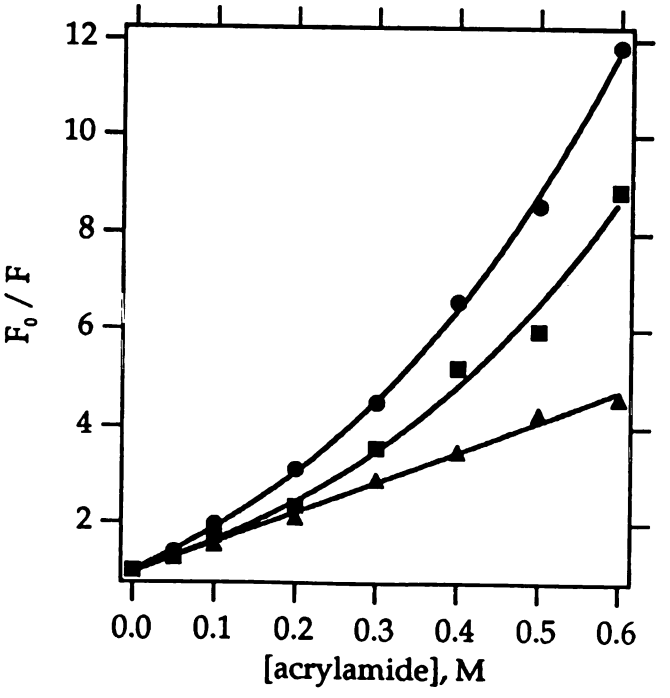
12
10
8
6
4
2
F_0 / F
0.0
0.1
0.2
0.3
0.4
0.5
0.6
[acrylamide], M

Figure 4

summarized in Table 1. In the absence of basal transcription factors, the Stern-Volmer plots of both GV-5HW442 (Figure 4A) and GV-5HW473 (Figure 4B) showed upward curvature. These data were best fit to a model invoking both dynamic and static quenching, yielding Stern-Volmer constants (K_{sv}) of 6.8 M^{-1} and 6.4 M^{-1} and static quenching constants (V) of 1.3 M^{-1} and 1.5 M^{-1} for the proteins labeled at 442 and 473, respectively. The dynamic quenching constants for GV-5HW442 and GV-5HW473 were both 2.6 $M^{-1}ns^{-1}$. The Stern-Volmer plot of the free amino acid analog 5-OH-Trp also showed upward curvature, with K_{sv} of 22.8 M^{-1} and V of 1.5 M^{-1} (data not shown), yielding a dynamic quenching constant of 6.3 $M^{-1}ns^{-1}$. Dynamic quenching constants for both GV-5HW442 and GV-5HW473 are thus in the same order of magnitude as that for free 5-OH-Trp. Consistent with the quenching study of GAL4-VP16 containing natural Trp (Shen et al., 1995a), these results suggest that residues 442 and 473 are solvent exposed.

In the presence of saturating amount of TBP, both GV-5HW442 and GV-5HW473 became less accessible to solvent. The Stern-Volmer plots of both proteins were linear and the data were best fit to the purely dynamic quenching model, with K_{sv} of 8.2 M^{-1} and 6.3 M^{-1}, respectively. In this case, the dynamic quenching rate constant was 2.6 $M^{-1}ns^{-1}$ for GV-5HW442 and 2.2 $M^{-1}ns^{-1}$ for GV-5HW473. In the presence of similar amount of TFIIB, the Stern-Volmer plots of both proteins showed upward curvature, as observed for those of the labeled fusion proteins alone. The analysis gave a K_{sv} of 5.7 M^{-1} and 3.9 M^{-1}, and a static quenching constant V of 1.0 M^{-1} and 1.6 M^{-1}, respectively. The dynamic quenching rate constant was 2.2 $M^{-1}ns^{-1}$ for GV-5HW442 and 1.5 $M^{-1}ns^{-1}$ for GV-5HW473. Although both TBP and TFIIB made both probes less accessible to the quencher, the nature of the effect is very different in the two cases. The presence of TBP eliminated the static quenching process, whereas it did not change the dynamic quenching process significantly. In contrast, in the presence of TFIIB

Table 1. Analysis of acrylamide quenching data for 5HW incorporated GAL4-VP16 proteins.

proteins	data best fit to dynamic model	data best fit to dynamic & static model			
	K_{sv} (M^{-1})	K_{sv} (M^{-1})	V (M^{-1})	$<\tau>$ (ns)[a]	k_q ($M^{-1}ns^{-1}$)
GV- 5HW442		6.8	1.3	2.60	2.6
GV- 5HW442 + TBP	8.2			3.21	2.6
GV- 5HW442 + TFIIB		5.7	1.0	2.66	2.2
GV- 5HW473		6.4	1.5	2.43	2.6
GV- 5HW473+ TBP	6.3			2.82	2.2
GV- 5HW473+ TFIIB		3.9	1.6	2.66	1.5

[a] Mean lifetimes are calculated from DAS measurements.

both static and dynamic quenching remain, albeit somewhat reduced. Moreover, the addition of TBP to the truncated activator N-5HW442 reduced quenching rate by acrylamide as it did to the full-length AAD, whereas the addition of TFIIB had no effect on accessibility (data not shown). Thus, if there is any interaction between TFIIB and the activators, the effect of that interaction on the structure of the VP16 AAD is apparently different from that seen with TBP.

The 7-aza-incorporated activator proteins were also tested in acrylamide quenching assays (Figure 5A and Figure 5B). Stern-Volmer plots of acrylamide quenching of GV-7AW442 and GV-7AW473 were linear, yielding K_{sv} of 2.3 M^{-1} and 3.3 M^{-1} respectively (Table 2). Acrylamide was a less efficient quencher for 7-aza-Trp than for Trp or 5-OH-Trp. The presence of TBP reduced the solvent accessibility of both residue 442 and 473. The downward curve of the Stern-Volmer plots were best fit to a two-species model, with approximately 40% of the probe molecules being inaccessible to acrylamide (assumed K_{sv} of zero) and an accessible fraction of approximately 60% having K_{sv} of 4.0 M^{-1} or 7.0 M^{-1} for GV-7AW442 and GV-7AW473 respectively. In contrast, the presence of TFIIB with GV-7AW442 did not change the quenching mechanism nor did it change significantly K_{sv}. However, TFIIB did reduce the solvent accessibility of GV-7AW473. Its Stern-Volmer plot was downward curved; in a two-species model, approximately 30% of the probe was inaccessible and the accessible fraction had a K_{sv} of 4.9 M^{-1}. In this case, TFIIB caused a change similar to that seen with TBP.

Steady-State Anisotropy Analysis And Dissociation Constants For Binding Of TBP And VP16 AAD

The steady-state fluorescence anisotropy of the 5-OH-Trp-labeled GAL4-VP16 proteins was measured at 360 nm in the presence of TBP or TFIIB (Figure 6). Addition of TBP to GV-5HW442 resulted in a large saturable increment in its

Figure 5. Stern-Volmer plots for the quenching of the fluorescence of GV-7AW442 (panel A) and GV-7AW473 (panel B) by acrylamide. 4 μM of the activators and 8 μM of TBP or TFIIB were used in these experiments. Closed circles: activator alone; triangles: in the presence of TBP; and squares: in the presence of TFIIB. Each set of data were compared to the various quenching models described in the text. The solid line represents the quenching model to which the data are best fit.

A.

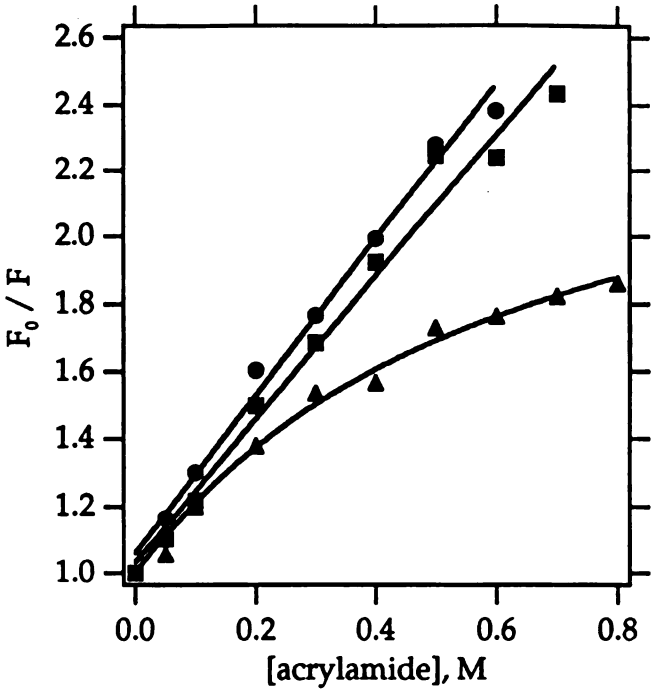
2.6
2.4
2.2
2.0
1.8
1.6
1.4
1.2
1.0
F_0 / F
0.0
0.2
0.4
0.6
0.8
[acrylamide], M

B.

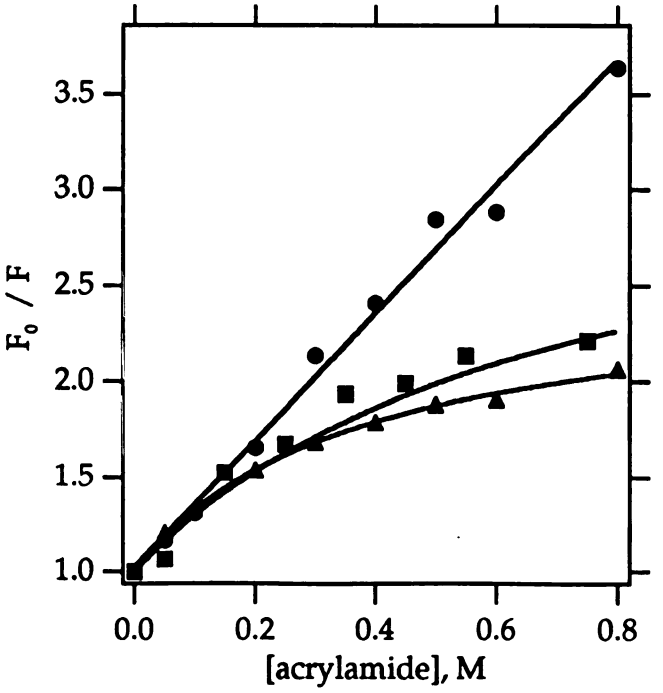
3.5
3.0
2.5
2.0
1.5
1.0
F_0 / F
0.0
0.2
0.4
0.6
0.8
[acrylamide], M

Figure 5

Table 2. Analysis of acrylamide quenching data for 7AW incorporated GAL4-VP16 proteins.

proteins	data best fit to single species model	data best fit to multiple species model	
	K_{sv} (M^{-1})	F_a	K_a(M^{-1})
GV-7AW442	2.3		
GV-7AW442 + TBP		0.61	4.0
GV-7AW442 + TFIIB	2.1		
GV-7AW473	3.3		
GV-7AW473 + TBP		0.60	7.0
GV-7AW473 + TFIIB		0.70	4.9

Figure 6. Steady-state anisotropy analysis of GV-5HW442 (Panel A), N-5HW442 (Panel B) and GV-5HW473 (Panel C) in the presence of TBP or TFIIB. 2 μM of the activators were used in these experiments. Triangles, titration of the activator with TBP; squares, titration of the activator with TFIIB. Solid line represents the best fit of the data to the equation describing formation of the 1:1 binary complex of activator and TBP. The calculated dissociation constants for GV-5HW442:TBP, N-5HW442:TBP and GV-5HW473:TBP interaction are 3.3 (± 1.7) x 10^{-7} M, 3.8 (± 1.4) x 10^{-7} M and 2.8 (± 0.6) x 10^{-8} M, respectively.

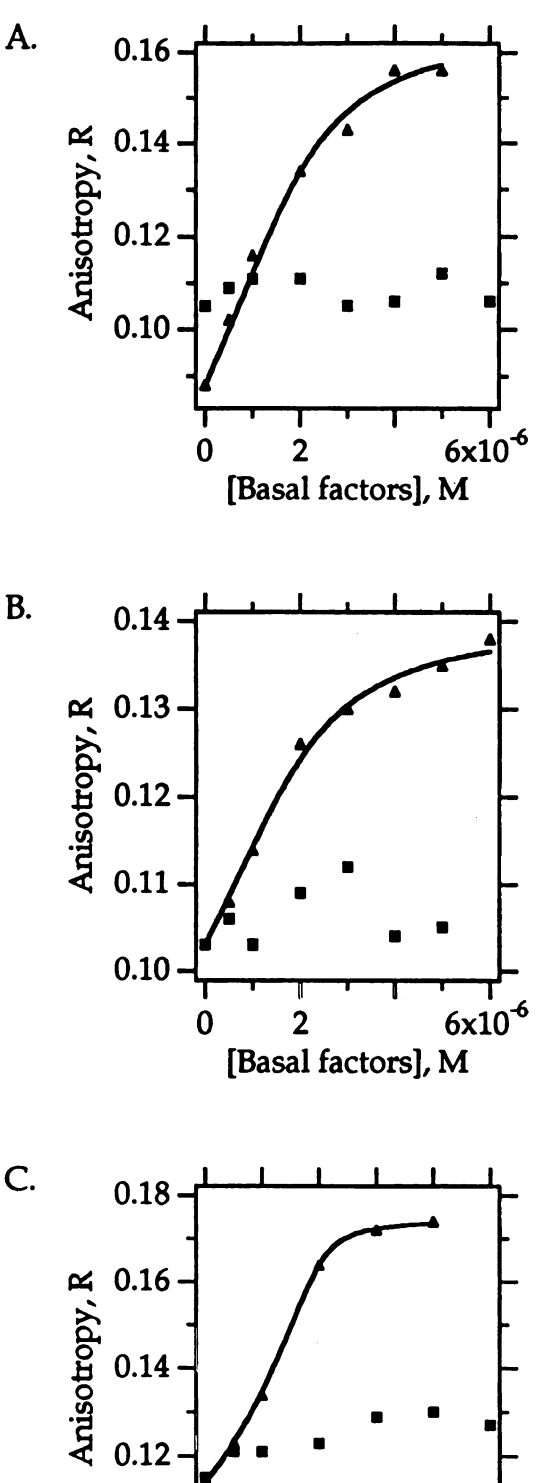
A.
0.16
0.14
0.12
0.10
Anisotropy, R
0
2
6x10-6
[Basal factors], M
B.
0.14
0.13
0.12
0.11
0.10
Anisotropy, R
0
2
6x10-6
[Basal factors], M
C.
0.18
0.16
0.14
0.12
0.10
Anisotropy, R
0
1
2
3
5x10-6
[Basal factors], M

Figure 6

anisotropy (Figure 6A), indicating a large decrease in the mobility of the 5-OH-Trp fluorophore. Assuming a 1:1 stoichiometry for the GAL4-VP16:TBP complex, the dissociation constant for the interaction was calculated to be 3.3 (±1.7) x 10^{-7} M. The magnitude of the anisotropy change can not be attributed solely to the increase in mass of the complex, which would be expected to cause an anisotropy increase of approximately 10% (given the molecular weights of each component and assuming both proteins as a single sphere when estimating the anisotropy change using the Perrin equation). Therefore the large (70%) increase in anisotropy in the presence of TBP suggests that the local motion of the fluorophore is significantly reduced upon interaction with TBP.

In contrast, the addition of TFIIB to GV-5HW442 had little or no effect on anisotropy (Figure 6A). We infer either that GV-5HW442 did not form a complex with TFIIB, or that even if a complex formed, TFIIB did not change the segmental motion of the fluorophore in the GV-5HW442. Similar effects of TBP and TFIIB were observed for the truncated fusion protein bearing 5-OH-Trp at position 442 of N-5HW442 (Figure 6B). When the analog was incorporated at position 473 of the full-length activation domain (GV-5HW473), the anisotropy also increased rapidly as TBP was added to the system, and the anisotropy reached a limiting value (Figure 6C). The calculated dissociation constant for this interaction is 2.6 (± 0.6) x 10^{-8} M. Again, addition of TFIIB to the same protein caused no significant anisotropy change.

Interaction Between TBP And VP16 Restricts The Segmental Motion In the AAD

The findings from steady-state anisotropy analysis were further confirmed by time-resolved anisotropy decay measurements. The anisotropy decay curves are shown in Figure 7 and the fitted parameters are summarized in Table 3. The

Figure 7. Time-resolved anisotropy decay curves of GV-5HW442 (Panel A), N-5HW442 (Panel B) and GV-5HW473 (Panel C) in the absence or presence of TBP or TFIIB. 2 μM of the activators and 4 μM of TBP or TFIIB were used in these experiments. Smoothed curves of the raw data are shown. Solid line: activator alone; dotted line: in the presence of TBP; and dash-dotted line: in the presence of TFIIB. A scaled lamp curve is given for reference (dashed line).

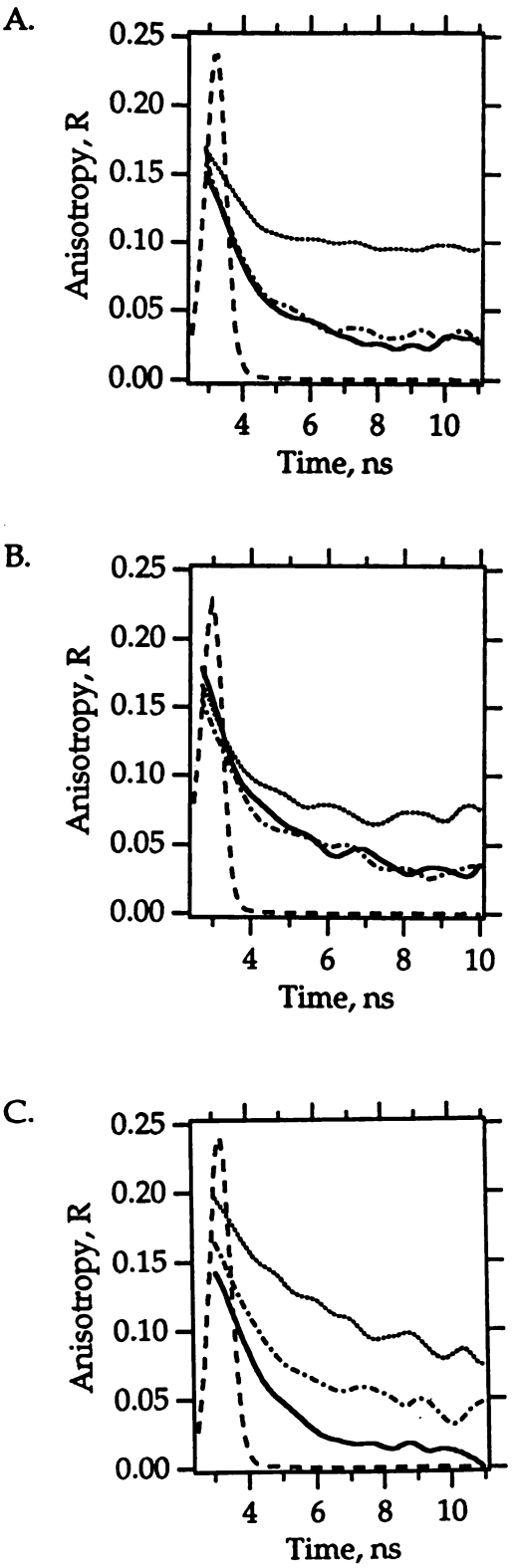
A.
0.25
0.20
0.15
0.10
0.05
0.00
Anisotropy, R
4
6
8
10
Time, ns
B.
0.25
0.20
0.15
0.10
0.05
0.00
Anisotropy, R
4
6
8
10
Time, ns
C.
0.25
0.20
0.15
0.10
0.05
0.00
Anisotropy, R
4
6
8
10
Time, ns

Figure 7

Table 3. Fluorescence anisotropy decay parametrs of 5HW incorporate GAL4-VP16 in the absence or presence of basal transcription factors.

proteins	β_1	ϕ_1 (ns)	β_2	ϕ_2 (ns)	r_0(app)[a]	Θ[b]	χ^{2c}
GV-5HW442	0.169	0.37	0.054	5.37	0.223	52.3	1.36
GV-5HW442 + TBP	0.086	0.39	0.108	39	0.194	34.9	1.29
GV-5HW442 + TFIIB	0.175	0.30	0.075	4.86	0.25	48.7	1.68
GV-5HW473	0.224	0.14	0.110	1.96	0.334	47.0	1.02
GV-5HW473 + TBP	0.073	1.24	0.128	16.1	0.201	30.8	1.83
GV-5HW473 + TFIIB	0.115	0.65	0.079	10.5	0.194	42.6	1.60
N-5HW442	0.206	0.20	0.108	4.34	0.314	46.1	1.48
N-5HW442 + TBP	0.111	0.54	0.083	37	0.194	41.5	1.28
N-5HW442 + TFIIB	0.137	0.39	0.079	6.01	0.216	44.9	1.98

[a] The apparent limiting time zero anisotropy is defined as $\Sigma\beta_j$. This r_0 does not include β_j for motions faster than 300 ps.
[b] Use r_0(app) to calculate the cone semiangles.
[c] The reduced χ^2 for the fit.

anisotropy decay of all the proteins were best fit to two components: a subnanosecond fast decay component representing segmental motion around the 5-OH-Trp fluorophore and the slower decay component in the range of 2-6 ns. In all of these proteins, the segmental motion contributed at least 60% of the anisotropy decay. The extent of these segmental motions were comparable with those of the known most flexible proteins (Eftink, 1991). These results are consistent with our previous results using GAL4-VP16 bearing natural Trp (Shen et al., submitted) and taken together suggest that both VP16 subdomains are very mobile. The rotational correlation times (ϕ_2) for the slower decay components reflect a molecular size smaller than that predicted for a globular GAL4-VP16 protein, and presumably represent the size of the activation domain itself tethered to the GAL4 DNA binding domain by a highly flexible linker.

The anisotropy decay of these proteins were then measured in the presence of a two-fold molar excess of TBP or TFIIB. Under these conditions, binding between GAL4-VP16 and TBP reached saturation as indicated by steady state anisotropy titration experiments. In the presence of TBP, anisotropy decay of GV-5HW442 is greatly slowed (Figure 7A). As for the activator fusion protein alone, data was also best fitted to two decay components. However, the contribution of the segmental motion (β_1) was dramatically reduced from 75% to 40% of the total, and the slow component dominated this decay process (Table 3). If one assumes segmental motion can be reconciled with the "wobble in cone" model (i.e., the localized motion of Trp is a wobbling of its transition moment within a cone), the extent of this motion can be described by the cone semiangle magnitude (Kinosita et al., 1977; Lipari and Szabo, 1980). The cone semiangle for the GV-5HW442 alone (52°) is larger than or comparable to those of many known flexible polypeptides such as apocytochrome C with a reported semiangle of 47° (Eftink, 1991). However, the presence of TBP reduced the calculated cone

semiangle to 35°. This result indicates that the segmental motion around residue 442 in the VP16 AAD is restricted in the presence of TBP. Moreover, the rotational correlation time of the slow component (ϕ_2) increased, reflecting the change in molecular mass from the activation domain alone to a complex containing GAL4-VP16 and TBP together. In contrast, TFIIB did not cause any change in the anisotropy decay of GV-5HW442 (Figure 7A). The lack of any effect on ϕ_2 suggests that TFIIB did not interact with the VP16 AAD, or that if any interaction does exist, the mode of association has no effect on the overall rotation of the AAD.

The anisotropy decay curves of the chimeric protein containing the VP16 AAD N-subdomain in the presence of TBP and TFIIB are shown in Figure 7B. TBP formed a complex with N-5HW442, evidenced by the increase in the rotational correlation time (ϕ_2) of the slow decay component (Table 3). TBP also reduced the amplitude (β_1) of the segmental motion around residue 442, although the magnitude of the effect is less than that seen for the full-length protein (GV-5HW442). In contrast, TFIIB had much less an effect on the anisotropy decay of N-5HW442, consistent with the results seen for TFIIB with the full- length protein labeled at 442.

The anisotropy decay curves of GAL4-VP16 labeled at position 473 of the full-length activation domain (GV-5HW473) in the presence of TBP or TFIIB are shown in Figure 7C. As observed with the probe at aa 442, TBP greatly restricted the segmental motion around residue 473 (β_1, Table 3). In addition, the apparent size of the segment associated with this fluorophore at 473 became larger, as shown by the increment of the rotational correlation time of the fast decay component (ϕ_1). The rotational correlation time of the slow component (ϕ_2) also increased, albeit not to the extent seen with the probe at 442. In this case, the slow component may represent the "freezing" of a subdomain surrounding 473,

rather than the size of the entire GAL4-VP16:TBP complex. This result suggests that binding of TBP may have a different effects on the flexibility of the two subdomains of the VP16 AAD.

In this experiment, the presence of TFIIB also affected the anisotropy decay, reflected in an increase in the rotational correlation time of the slow component (ϕ_2). The magnitude of this parameter was smaller than that expected for the TFIIB:GV-5HW473 complex, and thus probably represents only a subdomain of that complex. TFIIB also moderately restricted the motion surrounding residue 473 (β_1). The extent of restriction was much smaller than that caused by TBP; TBP reduced the cone semiangle of local motion from 47° to 31°, whereas TFIIB only reduced it to 43°.

DISCUSSION

Previous structural characterization of the AADs of VP16, GAL4, GCN4, NF-κB p65 and glucocorticoid receptor by CD and NMR studies revealed that these domains were unstructured in aqueous solution under neutral pH (O'Hare and Williams, 1992; Donaldson and Capone, 1992; Van Hoy et al., 1993; Schmitz et al., 1994; Dahlman-Wright et al., 1995). However, the AADs of VP16, NF-κB p65 and glucocorticoid receptor all form an α-helix conformation in less polar solvent (O'Hare and Williams, 1992; Donaldson and Capone, 1992; Schmitz et al., 1994; Dahlman-Wright et al., 1995). The AADs of GAL4 and GCN4 form β-sheet in lower pH solution or in a hydrophobic solvent (Van Hoy et al., 1993). Authors of these reports all speculate that in the process of transcriptional activation, the AADs adopt higher-order structure upon contacting their target molecules by an "induced fit" mechanism. The present report provides biophysical evidence to support that speculation, in that the local structure surrounding key residues of

the VP16 AAD was significantly constrained upon interaction with TBP, and to a less extent, with TFIIB. The induced conformations in transcription factors have been previously shown only in the DNA binding basic region of Leucine zipper proteins (Weiss et al., 1990; Patel et al., 1991) and the arginine-rich RNA binding domain of HIV Tat proteins (Calnan et al., 1991). The finding of the induced ordered structure in the VP16 activation domain will likely lead to a more refined analysis of the specific secondary and tertiary structures induced by its target proteins.

In this study, Trp analogs with unique fluorescent properties were incorporated at key positions of the VP16 transcriptional activation domain. These spectrally enhanced proteins were used to study the interactions between this activation domain and the basal transcription factors TBP and TFIIB. In the absence of these factors, studies of the VP16 AAD containing 5-OH-Trp or 7-aza-Trp at positions 442 or 473 showed that both residues are solvent exposed and are associated with highly mobile protein segments, consistent with our previous fluorescence analyses of the VP16 AAD containing natural Trp at these positions. The presence of TBP induced a significant change in the VP16 AAD, with a more ordered or constrained structure becoming apparent using fluorescent probes at either position. In contrast, effects of TFIIB interaction were observed only for probes at position 473 of the VP16 AAD, and those effects were weaker than those induced by TBP. Probes placed at positions 442 and 473 showed similar changes in the presence of basal transcription factor TBP. Probes at position 442 either in the full-length AAD or in the truncated subdomain also showed similar changes upon interaction with TBP.

Interaction Of The VP16 AAD With TBP

In the presence of basal transcription factor TBP, 7-aza-Trp residues at either position 442 or 473 of the VP16 AAD showed an increased fluorescence emission at 376 nm, indicating that these residues were present in a more hydrophobic environment than in unbound VP16. Acrylamide quenching results for VP16 AADs labeled with either 5-OH-Trp or 7-aza-Trp are consistent with the spectral shift results. In the presence of TBP, fluorophores at both position 442 and 473 became less accessible to quenching by acrylamide. More importantly, the mechanism of the quenching process seems to be qualitatively different, suggesting that the microenvironments of these two residues are distinct from those in the absence of TBP. For example, with 5-OH-Trp at either position in the VP16 AAD, the presence of TBP apparently eliminated the static quenching, presumably by blocking formation of the ground state complex between the quencher and the fluorophore. Moreover, qualitative changes in quenching mechanism were also seen using AADs labeled with 7-aza-Trp. In this case, the presence of TBP resulted in quenching curves that best fit a two-species model, with a sizable fraction of the probe being inaccessible to the quenching agent. Together, these results suggest that when the VP16 AAD interacts with TBP, both residues 442 and 473 become more shielded from solvent. Whether these residues became buried within a folded VP16 domain or became embedded as part of the binding interface with TBP is not revealed by these experiments. However, TBP does not completely block access to either residue 442 or 473. Further, the spectra of AADs containing 7-aza-Trp was not completely blue shifted to the 370 nm region, nor was the quenching rate by acrylamide reduced to that typical of completely buried residues.

The steady-state anisotropy of GV-5HW442, N-5HW442 and GV-5HW473 increased substantially in the presence of TBP. Dissociation constants were

calculated from these analyses. Dissociation constants between TBP and GV-5HW442 or N-5HW442 were both in the range of 3×10^{-7} M, while that between TBP and GV-5HW473 was in the range of 3×10^{-8} M. The differences in these dissociation constants may correspond to differences in transcriptional activities as a result of the Phe -> Trp mutations at position 442 and 473. The substitution mutant FW442 retains 70% activity as a full length AAD, whereas the FW473 mutation had negligible effect on activity (Regier et al., 1993). An affinity capture method had previously yielded an apparent dissociation constant of 2×10^{-7} M between the VP16 AAD and ^{35}S-labeled yeast TBP (Ingels et al., 1991). The ten fold difference in the results may be due to inherent differences between spectroscopic and capture-type assays, or to differences in the fusion protein constructs used in these experiments.

Time-resolved anisotropy decay measurements demonstrate that the mobility of protein segments surrounding positions 442 and 473 is markedly reduced in the presence of TBP (Figure 7 and Table 3). When the VP16 AAD was labeled with 5-OH-Trp at either position, the fraction of the anisotropy associated with fast decay (β_1) was reduced by roughly 50% by binding to TBP, while the fraction associated with slow decay (β_2) was increased. Assuming that segmental motion can be correlated with the fluorophore wobbling within a cone (Kinosita et al., 1977; Lipari and Szabo, 1980), the calculated cone semiangle (Θ) is reduced from approximately 50° to approximately 30°, representing a considerable constraint on the segmental motion. Moreover, the increase in the rotational correlation time for the slow decay component (ϕ_2) in the presence of TBP indicates that this component is moving with a much greater mass. For the probe at position 442, this mass may approach that of the GAL4-VP16:TBP complex altogether, whereas for the probe at position 473 the increase is less dramatic and likely represents a somewhat smaller subdomain of the complex. The rotational

correlation time for the fast decay component (ϕ_1) also increased for the probe at position 473 (but not for the probe at position 442), which may indicate that the fast decay component results from a larger peptide segment surrounding 473 being induced by the binding of TBP. Curiously, a subtle difference can be observed when the probe at position 442 is examined in the full-length and truncated versions of the AAD. TBP apparently caused a greater restriction of the segmental motion in the full-length AAD than in the N-subdomain (compare calculated cone semiangles (Θ) for the two AADs in the absence and presence of TBP). Nonetheless, the rotational correlation times for the slow decay component (ϕ_2) of the truncated AAD increased, suggesting binding between VP16 N- subdomain and TBP. Together, these results suggest that the N-subdomain (surrounding Phe-442) is the major targeting site of TBP, but the C-subdomain still has some impact on this TBP-activator interaction, either by providing a second, weaker binding site or by modulating the TBP:N-subdomain interaction.

Interaction Of The VP16 AAD With TFIIB

The effects of a second basal transcription factor, TFIIB, on the fluorescence of the VP16 AAD were both qualitatively and quantitatively different than those induced by TBP. Most notably, the presence of TFIIB had little or no effect on the fluorescence of Trp analogs incorporated at position 442 in the N-subdomain. No change was seen in the emission spectrum of GV-7AW442 (Figure 3), nor in the type of acrylamide quenching observed for GV-7AW442. TFIIB did not change the steady-state anisotropy of GV-5HW442 and N-5HW442 (Figure 6) nor did it change any aspect of time-resolved anisotropy decay of GV-5HW442 and N-5HW442 (Figure 7). Altogether, there is no evidence of any structural change in the N-subdomain caused by TFIIB.

In contrast to the lack of effect on the N-subdomain, TFIIB did induce some changes in the fluorescence of the VP16 AAD with probes in the C-subdomain (position 473). TFIIB altered the quenching of GV-7AW473 by acrylamide (Figure 5B), such that the quenching curves are best fit to a two-species model similar to that proposed for the effect of TBP. However, no shift in the emission spectrum of GV-7AW473 was observed in the presence of TFIIB (Figure 3). TFIIB also partially protected both GV-5HW442 and GV-5HW473 from acrylamide quenching (Figure 4), although the quenching mechanisms apparently retain both static and dynamic components, in contrast to the effect of TBP. This protection was C-subdomain-dependent, as it disappeared for N-5HW442 (data not shown). These differences in acrylamide quenching results for AAD proteins bearing 5-OH-Trp and 7-aza-Trp may be due to intrinsic differences in the quenching characteristics of these analogs. In sum, these results suggest that TFIIB may only sterically reduce the accessibility of the quenching reagent without net changes in the polarity of the environment around residue 473 and thus no change in the emission spectrum of GV-7AW473 is induced.

TFIIB caused a modest change in the anisotropy decay of GV-5HW473 (Figure 7C and Table 3), although the effects were less striking than those seen for TBP and no noticeable effect was observed on the anisotropy decay of GV-5HW442. In particular, cone semiangle (Θ) reduction caused by TFIIB is much smaller than that caused by TBP. The magnitude of the effect on the rotational correlation times for both the fast and slow decay components was approximately half that observed with TBP, implying that the sizes of the domains responsible for these components were not dramatically altered. The lack of any significant change in steady-state anisotropy in the presence of TFIIB (Figure 6C) might further suggest that the VP16:TFIIB interaction is weak.

Taken together, these results indicate that the interaction of the VP16 AAD with TBP is very different from its interaction with TFIIB. The two basal factors affect the structure of different subdomains of VP16, such that TBP altered the fluorescence of probes at both 442 and 473 whereas TFIIB affected only probes at 473. The magnitude of the effects induced by TBP was also consistently greater than those induced by TFIIB. Furthermore, TBP reduced the polarity of the microenvironments surrounding both probes, whereas TFIIB did not, and TBP had a more striking qualitative effect on the acrylamide quenching characteristics than did TFIIB. TBP restricted the segmental motion in the VP16 AAD more profoundly than TFIIB, and altered the steady-state anisotropy sufficiently to permit the calculation of dissociation constants. While these results do not rule out the ability of TFIIB to interact with the VP16 AAD entirely, it is striking that few if any effects are observed on the properties of amino acids at or near positions critical to the transcriptional function of the VP16 AAD.

Comparisons To other Model Systems

The disordered structure of acidic activation domains of transcriptional activators and their structural transitions in the presence of target binding proteins have precedents in other biological systems. One example is seen in the structure of tubulin. Tubulin is the major subunit protein of microtubules, polymeric structures that are major components of the cytoskeleton (Sackett, 1995). The sequences of the carboxyl terminal region of many isotypes of tubulin are highly variable, but are always very acidic. A large number of proteins interact with the surface of microtubules through the carboxyl-terminal region of tubulin. Secondary predictions indicate this region is likely to fold with a high content of α-helix. However, most experimental results suggest that these regions are extended and unstructured. Interestingly, α-helical structure was

observed in the presence of hydrophobic solvent (trifluoroethanol, methanol) or on lowering the pH. A second analogy can be seen in the trypsin-trypsinogen system (Huber and Bennett, 1983). The dissociation constant between the trypsinogen (with a flexible and disordered binding domain) and the basic pancreatic trypsin inhibitor (PTI) is 10^{-5} M, whereas that between the trypsin (with a rigid and ordered binding domain) and PTI is 10^{-13} M. Trypsinogen in the trypsinogen-PTI complex acquires a trypsin-like conformation (i.e., with rigidly structured binding domain) revealed by X-ray crystallographic analyses. The reduced affinity of trypsinogen for PTI is a consequence of the energy required to order the binding domain. Thermodynamic studies and structural comparisons have demonstrated a large negative heat capacity change associated with the known protein-ligand or protein-protein complexation in which local or more extensive folding occurs in the protein or ligand accompanies binding (Spolar and Record, 1994). In these systems, binding energy from protein-ligand or protein-protein interaction creates part or all of the binding sites or even drives folding beyond the interface.

The biological functions of these systems are drastically different; however, the common requirement to promote complicated macromolecular association in vivo may have evolved using similar strategies. Binding to a flexible segment such as VP16 AAD requires the reduction of its conformational entropy at the expense of association energy. Therefore, this kind of interaction, in which the flexible segment must be stabilized before it can provide optimal noncovalent interaction, is weaker than interaction with a rigid, stereochemically complementary surface. Nonetheless, an unstructured polymeric domain may have many advantages over a specific structured domain (Pontius, 1993). At neutral pH in aqueous solution, charge repulsion between the many ionized residues in these domains may inhibit formation of specific structure. These

domains are therefore flexible and extend away from the proteins. The flexible and extended nature of these domains increases the possibility of encountering the target proteins, and the charged amino acid side chains may provide a suitable force for promoting macromolecule association. The presence of target proteins may provide appropriately arranged basic charges to neutralize the acidic residues and therefore the acidic domains could adopt specific conformation in the complex.

In addition to the charged or strongly polar amino acids commonly found in transcriptional activation domains, hydrophobic (and particularly aromatic) residues are often critical for the function of transcriptional activators. Aromatic residues have been shown in several case to provide the binding docking force for protein-ligand interaction. The examples include binding between acetylcholine receptor and acetylcholine (Dougherty and Stauffer, 1990), between acetylcholine esterase and its selective inhibitor huperzine A (Pang and Kozikowski, 1994) and between FK506-binding proteins (FKBP) and the immunosuppressant FK506 (Braun et al., 1995). Aromatic residues have also been shown to be directly involved in protein-protein interactions. For example, a specific Phe of one subunit of bacteriophage λ cro protein is embedded into a receptor pocket on its dimer partner (Mossing and Sauer, 1990). For another example, the acidic tail of the anticoagulant hirudin binds to the exosite of thrombin and possesses a critical Phe which insert itself into a hydrophobic cleft of the thrombin molecule upon binding (Rydel et al., 1990). Aromatic amino acids are also the most common residues found in the antibody binding sites in known antibody-antigen complexes as well as the postulated combining sites in free Fab fragments (Mian et al., 1991). We speculate that the critical aromatic residues in the VP16 AAD participate directly in the binding of target proteins, providing some degree of binding stability and specificity.

VP16 is an unusually strong transcriptional activator. Its unusual potency has been attributed to a greater range of targets in the transcriptional apparatus (Tansey et al., 1994) which may allow VP16 to act during multiple steps of preinitiation complex assembly (Choy and Green, 1993). In addition to the basal transcription factors (TBP, TFIIB and TFIIH), two transcriptional coactivators ($dTAF_{II}$ 40 and yeast ADA2) have also been shown to interact with VP16 AAD directly (Goodrich et al., 1993; Silverman et al., 1994). The results of this report do not contradict the multiple targets model. Although our results demonstrate most clearly a specific interaction between TBP and VP16 AAD, a weaker and more limited interaction with TFIIB was also observed. Interestingly, a TBP mutant deficient in interacting with TFIIB was shown to be deficient in GAL4-VP16 activated transcription (Kim et al., 1994). This result suggests that in addition to interacting with TBP directly, the AAD interacts with the TBP-TFIIB-promoter complex (Hahn, 1993). Thus, the weak intrinsic interaction between VP16 AAD and TFIIB may be strengthened in the presence of TBP. Future experiments employing other putative target proteins or combinations of target proteins may be useful in addressing this and similar questions.

Transcriptional activation is likely not to result from simple static interactions of activators with basal transcription factors but rather may involve the dynamic exchange of interactions between activation domains, basal factors and coactivators. Recent studies show that distinct regions of the large subunit of RNA polymerase II share features in common with either acidic or proline-rich activators (Xiao et al., 1994b; Xiao et al., 1994c). By analogy to activation domains, these RNA pol II domains may also be relatively unstructured. The activation domains and the RNA pol II domains may interact with the same basal transcription factors or coactivators, and the balance of these interactions may

lead to the pre-initiation complex assembly or to initiation and elongation. If these interactions were to occur between rigid, stereochemically complementary protein surfaces, the binding might be so strong that exchange of such tight interactions would be difficult. In contrast, interaction of a target protein with flexible segments is weaker since association energy must be spent to compensate for the reduction of the conformational entropy. Thus, the transitions between ordered and disordered structures in activation domains (and their cognates in RNA pol II) may be a means to facilitate the dynamic interaction exchanges and hence to regulate the activation process.

ACKNOWLEDGMENTS

We thank Dr. Charles Yanofsky for providing the E. coli tryptophan auxotrophic strain CY15077 (W3110ΔtrpEA2) and the lacI^q-bearing plasmid pMS421. We thank Dr. Fred Winston for providing the plasmid pKA9 carrying the *S. cerevisiae* SPT 15 gene. We thank Dr. Danny Reinberg for providing the plasmid phIIB expressing the human TFIIB and for providing the procedure of making TFIIB depleted HeLa nuclear extract. We thank Dr. Shelley Berger for providing DNA template, primer and yeast nuclear extract for testing the activity of GAL4-VP16. We thank Chun-hsiang Chang and Dr. Zachary Burton for providing the HeLa cell nuclear extracts and plasmid pML for testing the activity of TBP and TFIIB. We thank Dr. Michael Brenowitz for providing procedures for TBP purification.

REFERENCES

Barberis, A., Müller, C. W., Harrison, S. C., & Ptashne, M. (1993) *Proc. Natl. Acad. Sci. USA 90*, 5628-5632.

Badea, M. G., & Brand, L. (1979) *Methods Enzymol. 75*, 378-425.

Braun, W., Kallen, J., Mikol, V., Walkinshaw, M. D., & Wüthrich, K. (1995) *FASEB J. 9*, 63-72.

Chang, C. H., Kostrub, C. F., & Burton, Z. F. (1993) *J. Biol. Chem. 268*, 20482-20489.

Chapman, C. F., & Maroncelli, M. (1992) *J. Phys. Chem. 96*, 8430

Choy, B., & Green, M. R. (1993) *Nature 366*, 531-536.

Cousens, D. J., Greaves, R., Goding, C. R., & O'Hare, P. (1989) *EMBO J. 8*, 2337-2342.

Cress, W. D., & Triezenberg, S. J. (1991) *Science 251*, 87-90.

Dahlman-Wright, K., Baumann, H., McEwan, I. J., Almlof, T., Wright, A. P. H., Gustafsson, J., & Hard, T. (1995) *Proc. Natl. Acad. Sci. USA 92*, 1699-1703.

Dougherty, D. A. & Stauffer, D. A. (1990) *Science 250*, 1558-1560.

Donaldson, L., & Capone, J. P. (1992) *J. Biol. Chem. 267*, 1411-1414.

Eftink, M. R. (1991) In *Protein Structure Determination*, Suelter, C. H. Eds., John Wiley & Sons, Inc., pp. 127-206.

Gill, S. C., & von Hipple, P. H. (1989) *Anal. Biochem. 182*, 319-326.

Goodrich, J. A., Hoey, T., Thut, C. J., Admon, A., & Tjian, R. (1993) *Cell 75*, 519-530.

Hahn, S. (1993) *Nature 363*, 672-673.

Hayward, G. S. (1993) *Sem. Virol. 4* , 239-251.

Hogue, C. W. V., Rasquinha, I., Szabo, A. G., & MacManus, J. P. (1992) *FEBS Lett. 310*, 269-272.

Hogue, C. W. V., & Szabo, A. G. (1993) *Biophys. Chem. 48*, 159-169.

Horikoshi, M., Yamamoto, T., Ohkuma, Y., Weil, P. A., & Roeder, R. G. (1990) *Cell 61*, 1171-1178.

Huber, R., & Bennett, W. S. (1983) *Biopolymer 22,*, 261-279.

Ingles, C. J., Shales, M., Cress, M. D., Triezenberg, S. J., & Greenblatt, J. (1991) *Nature 351*, 588-590.

Kim, T. K., Hashimoto, S., Kelleher, R. J., Flanagan, P. M., Kornberg, R. D., Horikoshi, M., & Roder, R. G. (1994) *Nature 369*, 252-255.

Knutson, J. R., Davenport, L., & Brand, L. (1986) *Biochemistry 25*, 1805-1810.

Lakowicz, J. R. (1983) In *Principles of Fluorescence Spectroscopy*, Plenum Press, pp 145-150.

Lipari, G., & Szabo, A. (1980) *Biophys. J. 30*, 489-506.

Lin, Y. S., Ha, I., Maldonado, E., Reinberg, D., & Green, M. R. (1991) *Nature 353*, 569-571.

Mitchell, P. J., & R. Tjian. (1989) *Science 245*, 371-378.

Mian, S., Bradwell, A. R., & Olson, A. J. (1991) *J. Mol. Biol. 217*, 133-151.

Mossing, M. C., & Sauer, R. T. (1990) *Science 250*, 1712.

O'Hare, P. (1993) *Sem. Virol. 4*, 239-251.

O'Hare, P., & Williams, G. (1992) *Biochemistry 31*, 4150-4156.

Pang, Y. P. & Kozikowski, A. P. (1994) *Comp-Aid. Mol. Des. 8*, 669-681.

Patel, L., Abate, C., & Curran, T. (1990) *Nature 347*, 572-574.

Paranjape, S.M., Kamakaka, R. T., & Kadonaga, J. T. (1994) *Ann. Rev. Biochem. 63*, 265-297.

Pontius, B. W. (1993) *Trends in Biochem. Sci. 18*, 181-186.

Regier, J. L., Shen, F., & Triezenberg, S. J. (1993) *Proc. Natl. Acad. Sci. USA 90*, 883-887.

Roberts, S. G. E., & Green, M. R. (1994) *Nature 371*, 717-720.

Ross, J. B. A., Senear, D. F., Waxman, E., Kombo, B. B., Rusinova, E., Huang, Y. T., Laws, W. R., & Hasselbacher, C. (1992) *Proc. Natl. Acad. Sci. USA 89*, 12023-12027.

Rydel, T. J., Ravichandran, K. G., Tulinski, A., Bode, W., Huber, R., Roistsch, C. & Fenton II, J. W. (1990) *Science 249*, 277-280.

Sackett, D. (1995) In *subcellular Biochemistry 24*, Biswas, B. B., & Roy, S. Eds., Plenum Press, New York, pp. 255-302.

Schmitz, M. L., Silva, M. A. D. S., Altman, H., Czisch, M., Holak, T. A., & Baeuerle, P. A. (1994) *J. Biol. Chem. 269*, 25613-25620.

Silverman, N., Agapite, J., & Guarente, L. (1994) *Proc. Natl. Acad. Sci. USA 91*, 11665-11668.

Spolar, R. S. & Record, M. T. Jr. (1994) *Science 263*, 777-784.

Stringer, K. F., Ingles, C. J., & Greenblatt, J. (1990) *Nature 345*, 783-786.

Tansey, W. P., Ruppert, S., Tjian, R., & Herr. W. (1994a) *Genes Dev. 8*, 2756-2769.

Triezenberg, S. J., LaMarco, K. L., & McKnight, S. L. (1988) *Genes Dev. 2*, 730-742.

Triezenberg, S. J. (1995) *Curr. Opin. Genetics Dev. 5*, 190-196.

Van Hoy, M., Leuther, K. K., Kodadek, T., & Johnson, A. J. (1993) *Cell 72*, 587-594.

Walker, S., Greaves, R., & O'Hare, P. (1993) *Mol. Cell. Biol. 13*, 5233-5244.

Walker, S., Hayes, S., & O'Hare, P. (1994) *Cell 79*, 841-852.

Weiss, M. A., Ellenberger, T., Wobbe, C. R., Lee, J. P., Harrison, S. C., & Struhl, K. (1990) *Nature 347*, 575-578.

Wilson, A. C., LaMarco, K., Peterson, M. G., & Herr, W. (1993) *Cell 74*, 115-125.

Xiao, H., Pearson, A., Coulombe, B., Truat, R., Zhang, S., Regier, J. L., Triezenberg, S. J., Reinberg, D., Flores, O., Ingles, C. J., & Greenblatt, J. (1994) *Mol. Cell. Biol. 14*, 7013-7024.

Xiao, H., Friesen J. D., & Lis, J. T. (1994b) *Mol. Cell. Biol. 14*, 7507-7516.

Xiao, H., Lis, J. T., Xiao, H., Greenblatt, J., & Friesen J. D. (1994c) *Nucleic Acids Res. 22*, 1966-1973.

Zawel, L., & Reinberg, D. (1995) *Ann. Rev. Biochem. 64*, 533-561.

CHAPTER V

SUMMARY AND FUTURE STUDY

SUMMARY

In the course of this thesis study, I applied both molecular biology and biophysical approaches to study two important questions in the field of transcriptional activation, i.e., the structural features of the activation domains and the mechanisms of transcriptional activation. Using oligonucleotide-directed mutagenesis, I substituted eleven amino acids for the critical position 442 of the VP16 AAD. This study, in combination of previous mutagenesis analyses of this domain, suggest that the most abundant amino acids of an activation domain are not sufficient for its function. Instead, aromatic or hydrophobic amino acids are equally or more important (Cress and Triezenberg, 1991; Regier et al., 1993; Triezenberg, 1995). Our observations and hypothesis have stimulated numerous subsequent mutational studies of various activation domains, focusing on evaluating the importance of the most abundant and hydrophobic amino acids. Results from all these studies support the hypothesis originally raised from the study of the VP16 AAD, which emerges as a common theme of diverse activation domains (Almlöf et al., 1995; Moriuchi et al., 1995; Hardwick et al., 1992; Blair et al., 1994a; Leuther et al., 1993; Drysdale et al., 1995; Lin et al., 1994; Blair et al., 1994b; Schmitz et al., 1994).

Mutational analyses have suggested that particular amino acids are critical for the function of activation domains. However, direct structural studies require biophysical approaches. To obtain high purity activator proteins for biophysical

studies, I largely modified a previously reported purification protocol of the recombinant chimeric protein GAL4-VP16 which was chosen to be used in our studies (Chasman et al., 1989). This newly developed purification procedure significantly improved the purity of GAL4-VP16 to greater than 95% homogeneity. It not only benefited my thesis work, but also contributed to the crystallization project being attempted in our lab.

In contrast to the accumulated knowledge from mutational analyses of various activation domains, only limited biophysical studies have been reported. No three dimensional structure of any activation domain has yet been solved by crystallographic analysis or NMR spectroscopy, partly due to the practical limitations of these high-resolution techniques. For example, crystallographic studies require high-quality single crystals which are not readily available. Nonetheless, other biophysical approaches can provide different insights into protein structure without providing the total three-dimensional structure. These techniques include fluorescence spectroscopy, circular dichroism (CD), and vibrational [Raman and infrared (IR)] spectroscopy.

Fluorescence spectroscopy is a powerful tool for studying the structure, dynamics, and interactions of proteins in solution (Lakowicz, 1983; Eftink, 1991). It can reveal a variety of molecular details of proteins and is highly sensitive and responsive to various molecular processes. Aromatic amino acids are the residues which fluoresce. Of these, tryptophan is the most valuable probe. Fortunately, mutational analyses highlighted the importance of aromatic amino acids for the function of various activation domains, suggesting great potential for study by fluorescence spectroscopy.

In this thesis study, we applied steady- state and time-resolved fluorescence approaches to study the eukaryotic activation domain for the first time. Unique intrinsic fluorescent probes were obtained by replacing

phenylalanine residues with tryptophan at positions 442 or 473 of VP16 AAD. As revealed by emission spectra, decay associated spectra, fluorescence quenching analysis and time-resolved anisotropy decay measurements, the two residues at key positions of VP16 AAD are very solvent exposed and associated with substantial flexibility (segmental motion). These results suggest that this isolated acidic activation domain is unstructured in solution, consistent with previous CD and NMR studies of this domain (O'Hare and Williams, 1992; Donaldson and Capone, 1992). Recent biophysical studies of other acidic activation domains including those of GAL4, GCN4, glucocorticoid receptor and NF-κB also suggest their unstructured nature (Van Hoy et al., 1993; Schmitz et al., 1994; Dahlman-Wright et al., 1995). Our study is unique in that we have used an activation domain which was known to be transcriptionally competent. In contrast, previous studies employed peptides of unknown transcriptional activity. Our demonstrated functional relevance is particularly important as it excluded the possibilities that the peptides used in other studies might not assume the functional conformations of activation domains or the proteins were denatured during sample preparation. Further, the solvent exposed property of the critical residues in VP16 AAD (such as the Phe-442) indicated by this fluorescence study enable us to understand the roles of these aromatic and hydrophobic residues better. Exposed critical residues in the activation domains are more likely directly involved in interactions with other proteins than maintaining the structures of these domains.

After structural characterization of the VP16 AAD by fluorescence spectroscopy, we set out to study the mechanisms of activation, specifically, the interactions between VP16 AAD and two basal transcription factors, TBP and TFIIB. Two aspects of previous studies made these interactions very attractive subjects for further exploration by biophysical approaches. On one hand,

biochemical analyses have shown that the VP16 activation domain can bind to various components of the basal transcriptional machinery, such as TBP and TFIIB, to activate transcription (Zawel and Reinberg, 1995). However, not much information other than the fact that they physically associate can be extracted from these studies. On the other hand, although no secondary structures were identified in several AADs by CD and NMR spectroscopy, these domains were found to assume specific secondary structures under certain solution conditions (such as low pH or high concentration of hydrophobic solvent). The speculation has been that these unstructured domains acquire "target induced structure" upon interaction with their target proteins, and the low pH or high concentration of hydrophobic solution conditions happen to mimic the in vivo environment of these AADs when they interact with target proteins (O'Hare andWilliams, 1992; Donaldson and Capone, 1992; Van Hoy et al., 1993; Schmitz et al., 1994; Dahlman-Wright et al., 1995; Shen et al., 1995a). However, there was no direct physical evidence for this hypothesis, partly due to the anticipated ambiguity in interpreting the mixed signals from complex protein-protein interaction system.

A new development in fluorescence spectroscopy, i.e., utilization of Trp analogs as intrinsic probes in proteins, enabled us to directly characterize any structural change in the VP16 AAD in the presence of basal transcription factors and examine the interactions between this activation domain and basal transcription factors. In this study, we successfully incorporated either 5-OH-Trp or 7-aza-Trp into critical positions of VP16 AAD. Using these spectrally enhanced proteins, we observed that the conformation of VP16 AAD became constrained in the presence of TBP, thus for the first time providing direct experimental evidence for the "target induced structure" hypothesis. We also determined the binding affinity between TBP and VP16 AAD. The calculated binding affinity is relatively modest, suggesting that the interactions in the

process of transcriptional activation are transient and dynamic. Our results also support models of TBP as a target protein for transcriptional activators.

In summary, the combined molecular biology and biophysical studies have advanced our understanding of two important questions in eukaryotic transcriptional activation. Further, these studies have suggested new hypotheses to test and indicated the potential usefulness of these techniques in future research.

FUTURE STUDY

Suggested by my thesis work, the following aspects can be considered for future studies:

Structure Of Activation Domains

Various fluorescence techniques have been successfully applied to study the VP16 AAD. I used GAL4-VP16 proteins possessing unique Trp at position 442 or 473 of the VP16 AAD. Our results indicated that these two positions are solvent exposed and associated with segmental motion. We inferred from these results that this isolated domain is unstructured. To confirm this conclusion, we can use these techniques to study GAL4-VP16 proteins bearing Trp at other positions. In principle, we can substitute any residue with Trp in the AAD, although we prefer to probe the functionally critical positions. After the oligonucleotide -directed mutagenesis analyses of the VP16 AAD, fellow students in our laboratory, Jeff Regier, Peter Horn and Susan Sullivan, undertook chemical mutagenesis, error-prone PCR mutagenesis and alanine scanning mutagenesis approaches to gain further insights into structural features of the VP16 AAD. From their studies, other critical amino acids are suggested, such as

the Phe-475 and Phe-479. These positions are also highly dependent on the aromatic character of Phe and therefore Trp substitutions should not be deleterious to their activities. Thus, this set of activator proteins can be readily studied.

Another class of proteins of great interest to study is the set of VP16 AADs harboring double or multiple mutations, one of which is a Trp substitution while the others are detrimental substitutions. For example, comparison studies of FW442 protein and FW442/LS444 protein, or FW473 protein and FW473/FA479 could reveal any structural perturbation cause by the detrimental substitutions. Many different combinations could be studied, together might providing a more clear picture of the structure of this AAD.

Activator-Target Protein Interaction

Using Trp-analog incorporated proteins, we have learned much from VP16 AAD-TBP and VP16 AAD-TFIIB interactions by fluorescence spectroscopy techniques. These approaches can be applied to further study activator-target protein interactions. First, VP16 AADs labeled at other positions can be used to confirm our observations. The above described VP16 AADs harboring double mutations will be useful to correlate the effects of the detrimental substitutions on transcrrptional activity and on the interactions with basal factors. Second, various TBP or TFIIB mutants can be used, such as the TBP C-terminal core protein, the truncated TFIIB mutants, and the basal transcription-competent but activation-deficient TBP or TFIIB mutants (Tansey et al., 1994; Kim et al., 1994; Roberts et al., 1993). Functional domains in the basal factors which are important for interactions with the VP16 AAD could be suggested from these studies. The correlation between the roles of the basal factors in transcriptional activation and their interactions with the VP16 AAD could also be evaluated. Third,

interactions of VP16 AAD with other potential target proteins such as $TAF_{II}40$, TFIIH p62 subunit, holo-TFIID and adaptor proteins can be explored. Moreover, interactions can be studied using combinations of potential target proteins. For example, activators have been suggested to interact with TBP-TFIIB-promoter complex by functional studies, thus studying the interaction in the presence of both TBP and TFIIB might be informative (Kim et al., 1994).

In the complex with DNA, basal factors and activator proteins may exist in different oligomerization states or have different conformations when compared to their free forms (Coleman et al., 1995). Therefore, the interactions between activation domains and basal factors may be different when they are bound to DNA. Fortunately, the Trp analog incorporated proteins not only serve as valuable reagents for protein-protein interaction studies, but also for protein/DNA systems as excitation at 310 nm exclusively excite Trp-analog incorporated proteins where DNA absorption is also negligible (Laue et al., 1993). Thus we can add DNA fragments bearing TATA sequence, or GAL4 binding sites, or both sequences into the above described activator-target protein interaction systems to investigate these interactions in the presence of DNA.

These fluorescence approaches have general applications in studying structural features of other activation proteins or activator-target protein interactions. Since many activators have critical aromatic residues, they can be readily studied by these methods which we have used for the study of VP16 AAD.

"Target-Induced Structure" In Activation Domains

Different spectroscopy techniques are complementary each other for probing protein structures. Although our fluorescence studies suggest that an ordered structure is induced in the VP16 AAD, these approaches can not resolve

the induced structure. Instead, the isotope edited FTIR (Fourier transform infrared) spectroscopy might be a promising means to identify the secondary structure induced in the VP16 AAD (Harris et al., 1992; Zhang et al., 1994).

In IR spectra, the amide bands that arise from the vibration of the peptide groups provide information on the secondary structure of proteins. The amide I band is the most widely used amide mode in studies of protein secondary structure. The amide I band originates mainly from the C=O stretch and a good correlation between the amide I band frequency and the type of secondary structure has been established (Surewicz and Mantsch, 1988; Surewicz et al., 1993). Amide I bands centered between 1650 and 1658 cm^{-1} are assigned to α-helical structure, between 1620 and 1640 cm^{-1} are assigned to β-strands, and between 1640 and 1648 cm^{-1} are assigned to non-ordered conformation.

In recent studies, carbon-13 isotope has been substituted into the carbonyl group of proteins (Harris et al., 1992; Zhang and Vogel, 1994; Zhang et al., 1994). The uniform labeling of proteins with ^{13}C caused the amide I band of these proteins to shift 35-55 cm^{-1} to lower frequency, leaving a clear window in the IR spectrum to observe the amide I band of another unlabeled peptide or protein. This technique has been successfully used to study the interactions of calmodulin and its target peptides (Zhang et al., 1994). In that study, amide I band of ^{13}C-labeled calmodulin shifted 55 cm^{-1} to lower frequency, enabling the amide I band of its target peptides be exclusively measured after mixing with it. A position change of the amide I bands of these target peptides was observed after mixing with ^{13}C-labeled calmodulin, indicating that these target peptides underwent a conformation change from random coil to induced α-helical structure upon complex formation.

We will apply this approach to try to identify any TBP-induced secondary structure in the VP16 AAD. TBP will be uniformly labeled with carbon-13 by

expressing in M9 minimal medium using $^{13}C_6$-glucose as the carbon source. A preliminary experiment has demonstrated that TBP can be adequately expressed in M9 minimal medium. This ^{13}C-labeled TBP is expected to exhibit its amide I band at lower frequency, leaving the clear window to observe the amide I band of VP16 AAD. A peptide corresponding to the 421-449 aa of VP16 AAD has been synthesized. The amide I band of this peptide alone is expected be in the range assigned to non-ordered conformation. FTIR spectrum of VP16 AAD peptide will also be recorded in the presence of ^{13}C-labeled TBP. We expect to observe its amide I band position shift upon its interaction with TBP reflecting the induced structure in VP16 AAD. The position of its amide I band in the presence of TBP might allow us to assign the induced secondary structure.

Our observations that an ordered structure in VP16 AAD is induced upon its interaction with TBP have suggested cocrystallization experiment of VP16 and TBP which is being pursued by our collaboration with crystallographer Paul Sigler . Due to the lack of ordered structure in isolated VP16 AAD, the VP16 AAD crystals may only be acquired in its complex with TBP. Hence, this cocrystallization experiment is another attempt to resolve the induced structure in VP16 AAD. NMR isotope-editing procedures may also be useful for determination of the induced structure in VP16 AAD (Otting et al., 1986; Fesik et al., 1990). In this case, VP16 AAD will be isotopically labeled with ^{13}C or ^{15}N and their complex with TBP will be examined. In this way, NOEs (the nuclear overhauser effect, most of the structural information for proteins in solution comes from evaluation of NOEs) involving VP16 AAD protons directly attached to ^{13}C or ^{15}N can be selectively detected.

The combined power of applying molecular biology, biochemical and biophysical approaches to study the structures of activators and the mechanisms

of activation will undoubtedly advance our understanding of transcriptional regulation.

REFERENCES

Almlöf, T., Wright, A. P. H., & Gustafsson, J-Å. (1995) *J. Biol. Chem. 270,* 17535-17540.

Blair, W. S., Bogerd, H., & Cullen, B, R. (1994a) *J. Virol. 68,* 3803-3808.

Blair, W. S., Bogerd, H. P., Madore, S. J., & Cullen, B, R. (1994b) *Mol. Cell. Biol. 14,* 7226-7234.

Chasman, D. I., Leatherman, J., Carey, M., Ptashne, M., & Kornberg, R. D. (1989) *Mol. Cell. Biol. 9,* 4746-4749.

Coleman, R. A., Taggart, A. K., Benjamin, L. R., & Pugh, B. F. (1995) *J. Biol. Chem. 270,* 13842-13849.

Donaldson, L., & Capone, J. P. (1992) *J. Biol. Chem. 267,* 1411-1414.

Drysdale, C. M., Dueñas, E., Jackson, B. M., Reusser, U., Braus, G. H., & Hinnebusch, A. G. (1995) *Mol. Cell. Biol. 15,* 1220-1233.

Eftink, M. R. (1991) In *Protein Structure Determination,* Suelter, C. H. Eds., John Wiley & Sons, Inc., pp. 127-206.

Fesik, S. W., Zuiderweg, E. P. R., Olejniczak, E. T., & Gampe, R. T. (1990) *Biochem. Pharmacol. 40,* 161.

Gill, G., Pascal, E., Tseng, Z. H., & Tjian, R. (1994) *Proc. Natl. Acad. Sci. USA 91,* 192-196.

Hardwick, J. M., Tse, L., Applegren, N., Nicholas, J., & Veliuona, M. A. (1992) *J. Virol. 66,* 5500-5508.

Harris, P. I., Robillard, G. T., van Dijk, A. A., & Chapman, D. (1992) *Biochemistry 31,* 6279-6284.

Kim, T. K., Hashimoto, S., Kelleher, R. J., Flanagan, P. M., Kornberg, R. D., Horikoshi, M., & Roder, R. G. (1994) *Nature 369*, 252-255.

Lakowicz, J. R. (1983) In *Principles of Fluorescence Spectroscopy*, Plenum Press, pp 145-150.

Laue, T. M., Snear, D. F., & Ross, J. B. A. (1993) *Biochemistry 32*, 2469-2472.

Leuther, K. K., Salmeron, J. M., & Johnston, S. A. (1993) *Cell 72*, 575-585.

Lin, J., Chen, J., Elenbaaas, B., & Levine, A. J. (1994) *Genes Dev 8*, 1235-1246.

Moriuchi, H., Moriuchi, M., Pichiyangkura, R., Triezenberg, S. J., Straus, S. E., & Cohen, J. I. (1995) *Proc. Natl. Acad. Sci. USA 92*, in press.

O'Hare, P., & Williams, G. (1992) *Biochemistry 31*, 4150-4156.

Otting, G., Senn, H., Wagner, G., & Wütherch. (1986) *J. Magn. Reson. 70*, 500.

Regier, J. L., Shen, F., & Triezenberg, S. J. (1993) *Proc. Natl. Acad. Sci. USA 90*, 883-887.

Roberts, S. G. E., Ha, I., Maldonado, E., Reinberg, D., & Green, M. R. (1993) *Nature 363*, 741-744.

Schmitz, M. L., Silva, M. A. D. S., Altman, H., Czisch, M., Holak, T. A., & Baeuerle, P. A. (1994) *J. Biol. Chem. 269*, 25613-25620.

Shen, F., Triezenberg, S. J., Hensley, P., Porter, D., & Knutson, J. (1995) Manuscript in preparation.

Surewicz, W. K., & Mantsch, H. H. (1988) *Biochimica et Biophysica Acta 952*, 115-130.

Surewicz, W. K., Mantsch, H. H., & Chapman, D. (1993) *Biochemistry 32*, 389-394.

Tansey, W. P., Ruppert, S., Tjian. R., & Herr, W. (1994) *Genes Dev. 8*, 2756-2769.

Triezenberg, S. J. (1995) *Curr. Opin. Genetics Dev. 5*, 190-196.

Zawel, L. R., Kumar, K. P., & Reinberg, D. (1995) *Genes Dev. 9*, 1479-1490.

Zhang, M-J., & Vogel, H. J. (1994) *Biochemistry 33*, 1163-1171.

Zhang, M-J., Fabian, H., Mantsch, H. H., & Vogel, H. J. (1994) *Biochemistry 33*, 10883-10888.